Université de Montréal

Therapeutic potential of endothelin receptor type A and bradykinin receptor B1 dual antagonism in osteoarthritis treatment

par
Gabriel Nathan Kaufman

Département de Sciences Biomédicales
Faculté de médecine

Mémoire présenté à la Faculté des études supérieures
en vue de l'obtention du grade de Maître ès sciences (M.Sc.)
en Sciences Biomédicales, option musculo-squelettique

Novembre, 2010

Université de Montréal
Faculté des études supérieures

Ce mémoire intitulé:

Therapeutic potential of endothelin receptor type A and bradykinin receptor B1 dual antagonism in osteoarthritis treatment

présenté par:

Gabriel Nathan Kaufman

a été évalué par un jury composé des personnes suivantes:

Daniel Lajeunesse Ph.D.,	président-rapporteur
Florina Moldovan M.D. Ph.D.,	directrice de recherche
Pierre Moffatt Ph.D.,	membre du jury

Mémoire accepté le: .....

RÉSUMÉ

Nous avons préalablement démontré que l'endothéline-1 (ET-1), un peptide vasoconstricteur de 21 acides aminés, joue un rôle central dans le métabolisme des tissus articulaires et a des fonctions cataboliques sur le cartilage articulaire dans l'ostéoarthrose, en liant son récepteur de type A (ETA). Suite à la relâche du nonapeptide vasodilatateur bradykinine (BK), et l'augmentation d'expression du récepteur B1 des kinines (BKB1), ces médiateurs engendrent un cycle d'inflammation, une destruction du cartilage, et une douleur articulaire. Lors de cette étude, l'efficacité thérapeutique des antagonistes spécifiques du ETA et/ou BKB1 dans un modèle animal d'ostéoarthrose a été testée. Notre hypothèse est que l'antagonisme va diminuer la progression de la pathologie et de la douleur articulaire.

L'ostéoarthrose a été induite chez des rats par rupture chirurgicale du ligament croisé antérieur. Les animaux ont été traités par injections intra articulaire hebdomadaires des antagonistes peptidiques spécifiques du ETA et/ou BKB1. La douleur articulaire a été évaluée par le test d'incapacitance statique durant les deux mois postopératoires ; la morphologie articulaire a été examinée *post mortem* par radiologie et histologie.

On constate que le traitement a diminué la douleur et a préservé la morphologie articulaire ; la double inhibition a été plus efficace que la simple inhibition. En conclusion, l'antagonisme double d'ETA et BKB1 améliore la douleur chronique et prévient la dégradation articulaire dans l'ostéoarthrose, ce qui suggère que ces récepteurs peuvent être des cibles thérapeutiques potentiels pour le traitement de

cette pathologie.

Mots clés : ostéoarthrose, inflammation, douleur, endothéline, bradykinine, modèle animal, antagoniste peptidique

ABSTRACT

The author's laboratory has previously shown that endothelin-1 (ET-1), a 21-residue vasoconstrictive peptide, plays a central role in joint tissue metabolism, and has a catabolic function in matrix collagen degradation in osteoarthritis. These effects occur primarily through ligation of the endothelin-1 receptor A subtype (ETA). The subsequent release of the nonapeptide vasodilator bradykinin (BK) in the joint microenvironment, and up-regulation of bradykinin receptor B1 (BKB1) expression, engenders a vicious cycle of synovial membrane inflammation, articular cartilage destruction, and joint pain. In the present work, we describe a preclinical study of the efficacy of treatment of surgically induced osteoarthritis with ETA and/or BKB1 specific peptide antagonists. We hypothesize that antagonism will diminish osteoarthritis progress and articular pain.

Osteoarthritis was surgically induced in rats by transection of the anterior cruciate ligament. Animals were subsequently treated with weekly intra-articular injections of specific peptide antagonists of ETA and BKB1. Hind limb pain was measured by the static weight bearing test for two months post-operatively. Post-mortem, knee joints were analyzed radiologically and histologically.

Local antagonist treatment diminished overall limb pain, and accelerated post-operative recovery, after disease induction. Treatment also protected joint radiomorphology and histomorphology, with dual antagonism being slightly more protective.

ETA and BKB1 dual antagonism improves chronic pain and prevents joint

degradation in osteoarthritis. They therefore represent a novel therapeutic target: specific receptor dual antagonism may prove beneficial in disease management.

Key words: osteoarthritis, inflammation, pain, endothelin, bradykinin, animal model, peptide antagonist

CONTENTS

LIST OF TABLES

LIST OF FIGURES

LIST OF ABBREVIATIONS

ACLT	anterior cruciate ligament transection
ADAMTS	A Disintegrin-like And Metalloprotease domain (reprolysin-type) with ThromboSpondin type I motif
AKT/PKB	protein kinase B
ANOVA	analysis of variance
AP-1	activating protein-1
BK	bradykinin
BKB1	bradykinin receptor B1
BKB2	bradykinin receptor B2
CATIA	Computer Aided Three-dimensional Interactive Application
CD	cluster of differentiation
COMP	cartilage oligomeric matrix protein
COX-2	cyclooxygenase-2
CREB	c-AMP response element-binding
c-REL	v-rel reticuloendotheliosis viral oncogene homolog (avian)

DC	Doctor of Chiropractic
DMOAD	disease-modifying osteoarthritis drug
DNA	deoxyribonucleic acid
DX	digital micro-X-ray
ECM	extracellular matrix
ELISA	enzyme-linked immunosorbent assay
ERK	extracellular signal-regulated kinase
ET-1	endothelin-1
ETA	endothelin receptor type A
ETB	endothelin receptor type B
ETL	echo train length
EULAR	European League Against Rheumatism
DVM	Doctor of Veterinary Medicine
GPCR	G-protein-coupled receptor
ICE	interleukin-1β converting enzyme
IκB	inhibitor of NF-κB
IKK	inhibitor of NF-κB kinase
IL	interleukin
IL1RN	interleukin-1 receptor antagonist
iNOS	inducible nitric oxide synthase

JNK	c-jun NH_2-terminal kinase
kDa	kilo-Daltons
MAPK	mitogen-activated protein kinase
MDCM	*Medicinae Doctorem et Chirurgiae Magistrum*
MEK	mitogen-activated protein kinase kinase
MEKK	mitogen-activated protein kinase kinase kinase
MMP	matrix metalloproteinase
MR	magnetic resonance
MSME	multislice multiecho
MT-MMP	membrane type matrix metalloproteinase
NF-κB	nuclear factor kappa-light-chain-enhancer of activated B cells
NO	nitric oxide
NOS1	nitric oxide synthase 2, induced
NSAID	non-steroidal anti-inflammatory drug
OA	osteoarthritis
OARSI	Osteoarthritis Research Society International
PAI	plasminogen activator inhibitor
PGE_2	prostaglandin E2
PhD	*Philosophiae Doctorem*

PI3-K	phosphatidylinositol 3-kinase
PLA_2	phospholipase A2
PLC	phospholipase C
PKC	protein kinase C
PTGS2	prostaglandin-endoperoxide synthase 2
RA	rheumatoid arthritis
RARE	rapid acquisition with relaxation enhancement
RELA	v-rel reticuloendotheliosis viral oncogene homolog A, NF-κB3, p65 (avian)
RELB	v-rel reticuloendotheliosis viral oncogene homolog B
RF	radio frequency
ROI	region of interest
RT-qPCR	reverse transcription-quantitative real-time polymerase chain reaction
TE	echo time
TGF	transforming growth factor
TIMP	tissue inhibitor of metalloproteinases
TLR	Toll-like receptor
TNF	tumour necrosis factor

TR	repetition time
u-PA	urokinase-type plasminogen activator
u-PAR	urokinase-type plasminogen activator receptor
USB	universal serial bus

ACKNOWLEDGMENTS

They helped every one his neighbour; and every one said to his brother,

Be of good courage.

-Isaiah 41:6

If I have seen further it is by standing on ye sholders of Giants.

-Isaac Newton, letter to Robert Hooke, 5 February 1675/6

No scientific research occurs alone, without help and support. The author wishes to acknowledge and thank all those that have aided, abetted, and otherwise contributed to his work over the last two years in the Orthopaedic Molecular Biology Laboratory. First, he thanks Charlotte Zaouter, the research assistant who assisted with the surgeries and histological studies. He also wishes to thank the purchasing agent and senior research associate Irène Londoño for her patience, guidance, and moral support, as well as for begrudgingly indulging the author's shopping fetish as it extends to high-end laboratory equipment. Their excellent technical assistance permits the laboratory to function at the highest level.

Archana Sangole, late of École Polytéchnique de Montréal, contributed her considerable expertise to select a measurement technology for the static weight bearing apparatus and to help with initial design conception. Barthélemy Valteau of the Paediatric Mechanobiology Laboratory reverse-engineered the actual design and drafted plans for the static weight bearing apparatus; he also assisted with the equations for calculation of the static weight bearing data. Their contributions allowed us to measure perceived pain in our animals, which had been a major

obstacle for our laboratory.

Pierre Sirois, of IPS Thérapeutique Inc., contributed the bradykinin receptor B1 antagonist R-954 which was used in the study; Michelle Dion, a fellow Master's student in the author's lab, deserves credit for making the match between her former professor and us. Gordon Ng, of Amgen Inc., suggested the rat surgical model as an experimental approach. The author thanks Saadallah Bouhanik of the Viscogliosi Laboratory for Molecular Genetics of Musculoskeletal Disorders for providing access to and help with the Faxitron micro-X-ray system, as well as Jason Cakiroglu (MR engineer) and Barry J. Bedell (director) of the Small Animal Imaging Lab at McGill University, for providing access to the 7 Tesla MR scanner. The author acknowledges the kind assistance of the veterinarians Stéphane Faubert and Serge Nadeau for their surgical instruction, as well as Denise Carrier (director) and the staff of the Sainte-Justine Hospital Research Centre animal facility for their technical assistance. He also acknowledges the insightful comments and helpful suggestions of Kessen Patten (post-doctoral fellow) on his article manuscript. Finally, he thanks his principal investigator, Florina Moldovan, for providing a lab for a Master's internship which has proved to be an environment that has encouraged significant professional growth.

This work was supported by operating grants from the The Arthritis Society (RG05/084) and the Canadian Institutes of Health Research (IMH-94011). Salarial support for the author was provided by a Sainte-Justine Hospital Foundation/Foundation of Stars bursary.

CHAPTER 1

INTRODUCTION

Osteoarthritis (OA), a disorder also known as degenerative joint disease or degenerative arthritis, is the most frequent joint disease in seniors. It is the most common form of arthritis, affecting more than 10% of adult Canadians [39]. Most often involving the hands and the large weight-bearing joints (hips, knees, back), OA is clinically characterized by the progressive destruction of articular cartilage, subchondral bone remodelling, osteophyte formation, and synovial membrane inflammation; the pathophysiological mechanisms responsible for these changes are not yet completely understood [79]. This leads to joint pain, which in turn leads to reduced physical activity and thereby raises the risk of other diseases. In severe cases, joint replacement surgery is necessary, which represents a major health-care burden: this approach has significant morbidity and is extremely expensive. Current treatment only alleviates symptoms, and does not attack the basic biological causes of the disease. It is therefore of paramount importance to understand the molecular and cellular causes of OA pathogenesis, in order to establish specific therapies.

The author's laboratory has previously demonstrated that the vasoconstrictor peptide endothelin-1 (ET-1) plays a central role in joint tissue metabolism, and has a catabolic function in matrix collagen degradation in osteoarthritis [109, 132, 187]. These effects occur primarily through ligation of the endothelin-1 receptor

A subtype (ETA) [110, 124, 144]. The subsequent release of the nonapeptide vasodilator bradykinin (BK) in the joint microenvironment, and up-regulation of bradykinin receptor B1 (BKB1) expression, engender a cycle of synovial membrane inflammation, articular cartilage destruction, and joint pain [142, 189, 206]. We hypothesize that blocking these receptors with specific antagonists will ameliorate disease state and slow OA pathogenesis. This thesis deals with the therapeutic potential of such an approach.

In the literature review, we provide a basic overview of OA, a summary of classic inflammatory processes, and a discussion of the role of endothelial molecules in the context of joint inflammation and pain. We then discuss current experimental approaches to model OA in laboratory animals, with a focus on assessing joint pain. The experimental work described is a preclinical study, in the form of a submitted article manuscript (with an expanded methods section as a separate chapter), where surgically induced OA was treated by local injections of ETA and/or BKB1 specific peptide antagonists. We then discuss our results in light of current work in the field, along with limitations of our study and suggested experimental work. We conclude with a general interpretation of our results and suggest two avenues for further research.

CHAPTER 2

LITERATURE REVIEW

2.1 Osteoarthritis

2.1.1 Disease overview

Osteoarthritis (OA) is a joint pathology defined as the progressive destruction of articular cartilage, accompanied by subchondral bone remodelling, osteophyte formation, and synovial membrane inflammation [79]. Clinically, this disease progresses slowly and principally affects the hands and large weight-bearing joints. Functional limitations ensue and cause significant morbidity: symptomatic OA reduces quality of life [150] and can contribute to emotional distress. Patients end up engaging in adaptive behaviours [80], such as avoiding exercise, which negatively impact overall health.

OA also engenders a significant economic burden with direct patient-based costs, such as medication, hospitalization, and surgery, along with indirect costs from loss of productivity [4]. In a large US meta-analysis of health care costs, [114], out-of-pocket expenditures increased by $1 379 (women) and $694 (men) *per annum* for OA patients. Aggregated expenditures over the study period were $185.5 billion *per annum* (2007 US dollars), two-thirds of which are due to women's OA; the reported female-to-male disease ratio varies between 1.5 and 4 [10].

2.1.2 Prevalence and incidence

Prevalence, defined as the proportion of diseased individuals in a given population at a particular time point, and incidence, defined as the rate of new cases per time period in a given population, are two epidemiological measures of disease penetrance [120]. According to Arden and Nevitt [10], "OA is the most common joint disorder in the world." Jordan *et al.* [104] report a UK prevalence rate of knee OA at 18.1% over a 55-year study period. Hip and hand OA are much less common, with prevalence estimates ranging from 0.7-4.4% for the hip and roughly 2.5% for the hand. Oliveria *et al.* [161] report an age- and sex-standardized incidence of 240 cases of knee OA, 88 cases of hip OA, and 100 cases of hand OA, all per 100 000 person-years; new cases tended to plateau at around 80 years for both men and women. Both these measures track *symptomatic* OA: almost all humans will develop detectable "radiographic" OA [18, 33] or have cartilage damage on autopsy [10] as part of natural aging, but only some patients require treatment for joint pain. The reasons for this disparity are still poorly understood.

2.1.3 Risk factors

OA has several characterized risk factors that contribute in concert to pathogenesis. Increasing age is the risk factor most strongly correlated with OA. On a biomechanical level, this may arise from proprioceptive changes, decreased muscle tone, and altered gait. On a cellular level, chondrocytes may become less able to repair the tissue, due to decreased ability to synthesize cartilage components, decreased responsiveness to growth factors, and increased apoptosis [2].

Obesity is also strongly correlated with OA: a higher body mass index stresses the joints beyond healthy biomechanical limits, which results in altered loading and joint degeneration [97]. Joint overuse can have similar effects: elite athletes have increased rates of hip, knee, and ankle OA, relative to the general population [115]. High-level sports can also predispose athletes to OA due to injury: to cite a personal example, this author had both anterior cruciate ligaments reconstructed with associated medial meniscectomies due to basketball injuries. This intervention carries with it an increased risk of knee problems (Ronald A. Dimentberg MDCM, patient consultation): meniscus and ligament injuries can predispose patients to knee OA [108, 140]. As noted above in subsection 2.1.2, women, especially over the age of 50, report 1.5 to 4 times as much OA as men [10]. The reasons for this difference in disease ratio are poorly understood: it has been ascribed to oestrogen deficiency [223], since oestrogen can up-regulate proteoglycan synthesis [178]. Nonetheless, the evidence is currently inconsistent, with no prospective randomized clinical trials [2, 157].

OA has a strong genetic component: Zhai *et al.* [233] have reported 50-65% disease concordance between identical twins. While specific genes responsible have been difficult to identify due to the different manifestations of the disease, several candidate genes have been identified that most likely have additive effects [209]. Point mutations in types II, IV, V, and VI collagens, as well as cartilage oligomeric matrix protein (*COMP*) [145, 176] have been correlated with early-onset OA. Genome-wide linkage analyses have identified several pro-inflammatory genes that correlate with knee OA, such as the interleukin-1 (IL-1) genes IL-1

alpha (*IL1A*), IL-1 beta (*IL1B*), and IL-1 receptor antagonist (*IL1RN*) [125], along with a cyclooxygenase-2 (*PTGS2*) variant [210].

2.1.4 Symptomatology

OA is characterized by low-grade joint pain, which is the major criterion in the American College of Rheumatology disease classification [5]. This pain leads to functional limitation (as discussed above in section 2.1.1), and is the main complaint motivating patient presentation [60, 65]. Its aetiology is multifactorial: subchondral bone can have microfractures or symptomatic medullary hypertension, osteophytes can cause stretching of periosteal nerve endings, ligaments may be stretched, the joint capsule can be inflamed or distended, the synovium may be inflamed, and muscles may spasm [137]. Furthermore, neoinnervation of joint tissue concurrent with angiogenesis [13, 28] may contribute to deep joint pain. Articular degeneration in OA is progressive in nature: early cartilage roughening and subchondral bone sclerosis is followed by deepening cartilage fissuring and bone remodelling in the intermediate stage of degeneration. End-stage joint degeneration involves complete loss of articular cartilage, osteophyte formation, and subchondral cysts. These are accompanied by synovitis, which can be primary and/or reactive. Severe osteophytes are palpable and/or visible upon physical examination of the joint, along with crepitus [164].

2.1.5 Diagnosis

Diagnosis of OA follows established criteria, with minor differences for each joint system being assessed. Common themes are joint pain, restricted movement, bony enlargement, and reduced function. To take the example of knee OA: the most recent set of guidelines to be published are the 2010 EULAR (European League Against Rheumatism) recommendations [235]. They require three symptoms, namely persistent knee pain, limited morning stiffness, and reduced function, along with three signs: crepitus, restricted movement, and bony enlargement. These criteria have a sensitivity of 99% when all six are present. They are similar to the 1986 American College of Rheumatology criteria [5], which require three of the following six criteria: patient over 50 years old, morning joint stiffness, crepitus, bony tenderness, enlargement, and absence of palpable warmth.

Radiological evidence of joint degradation is often sought by X-ray, to measure joint space narrowing, and to visualize subchondral bone remodelling and osteophyte formation. Magnetic resonance (MR) imaging can be used to assess soft-tissue damage: cartilage lesions, muscle deficiencies, ligament tears, and meniscal problems in the case of the knee. This information can confirm diagnostic findings as established by evidence-based criteria. However, as we discuss above in subsection 2.1.2, such radiological evidence, especially X-ray findings, are sometimes a sign of normal aging, rather than of joint disease: symptomatic or painful OA is the condition that necessitates intervention.

Pain assessment of OA patients is primarily performed via self-administered

questionnaires such as the McGill Pain Questionnaire [143] or the Western Ontario and McMaster Universities Osteoarthritis Index [19, 139], which score perceived pain and functional limitations. These questionnaires must be statistically validated to be used in clinical practice [166]. A visual analogue scale or a simple pain rating ("On a scale of 1 to 10...") may provide the patient and clinician with a relatively simple and intuitive manner to communicate perceived pain: logging such scores over time may yield patterns of pain sensation.

Biomechanical functional tests, both qualitative and quantitative, are employed as well. Mechanical sensitivity of the joint can be assessed: OA patients have lower thresholds for cutaneous pain than healthy controls [93]. Range of motion and gait can be analyzed and quantified with an anatomical protractor, or by using external markers attached to anatomical reference points [211]. OA patients have reduced range of motion in affected joints [103] due to deep joint pain. Static weight bearing can be measured using a force platform which provides a map of foot pressure; this can be used to discern weight bearing changes in OA patients as they shift weight off the affected joint(s) [116].

The gold standard for biomechanical assessment is computerized motion analysis [78], where external markers are placed on anatomical reference points to track the limbs, and force sensor arrays quantify the force applied by the feet on the ground, or by the hands on the wall, depending on the test paradigm. In knee OA patients, walking speed, stride cadence and length are all reduced, along with knee flexion and swing phases. Peak applied forces are also lower. Stride time and overall stance phase are lengthened. All these alterations indicate that the

patients are engaging in adaptive behaviours due to their joint pain.

2.1.6 Treatment

Current OA treatments are almost all symptomatically based [6], since there is no known cure. That being the case, OA is medically managed with three main treatment modalities: non-pharmacologic, pharmacologic, and surgical. The algorithm for applying each of these strategies is based on successive recourse to more and more invasive treatments as necessary (Figure 2.1). Obesity and joint mechanics are the risk factors for OA that are most amenable to non-invasive intervention [97]. Weight loss programs, coupled with patient education and support, are the first lines of defence against OA functional limitations. Epidemiological research has shown that monthly telephone contact with trained social services personnel can improve patient well-being and functioning without significant cost increases [220]. Physical therapy can strengthen periarticular muscles and joint range of motion, thereby improving joint function. Occupational therapy can ensure proper joint protection, energy conservation, and effective adaptive strategies, such as cane or crutch use. Adherence to a program of both aerobic and strength training exercise has been directly correlated to improvements in joint pain and overall functioning [63]. Such non-pharmacologic measures "are the cornerstone of OA management" [6] and are continued even if other treatment modalities are subsequently adopted.

Current pharmacologic approaches for OA patients are essentially pain management strategies. While a disease-modifying OA drug (DMOAD) [170, 221] is

the *ne plus ultra* of OA pharmacologic research, the as of yet incomplete understanding of OA pathogenesis makes this goal difficult to attain. There is a need for a novel pharmacological approach to OA treatment: further understanding of the molecular mechanisms behind OA pathogenesis and progression should provide avenues towards targeted disease-modifying or -slowing treatments [3, 133]. Treatments in current clinical use for OA pain are the same as for any other chronic pain condition: analgesics (including NSAIDs and COX-2 inhibitors), corticosteroids, and so forth. These treatments are not without significant side-effect profiles: much of the task of the rheumatologist is to manage sequelae, such as steroid tolerance and/or gastrointestinal effects [234]. Opioids are discouraged due to the high possibility for dependence, unless the pain is severe and intractable with other agents [4, 6]. Oral supplements of cartilage matrix components such as glucosamine sulphate and chondroitin sulphate have been prescribed for pain relief in moderate OA [234], but a recent network meta-analysis of 10 clinical trials (3803 patients in total) by Wandel *et al.* [215] calculated that there was no clinically relevant effect of such treatment on perceived joint pain or on joint space narrowing. Viscosupplementation by intra-articular injection with hyaluronic acid is offered by some clinicians, but there is debate about its efficacy. In Quebec, the *Agence d'évaluation des technologies et des modes d'intervention en santé* does not currently recommend that it be covered by Medicare, due to the lack of conclusive evidence [50].

Surgical interventions for OA are considered treatments of last recourse, due to their high degree of invasiveness and increased cost, relative to non-surgical

modalities. They are quite effective: patients report significant improvements in function and reduction in joint pain within the year after surgery [234]. There are three main surgical options: osteotomy, partial or total joint replacement, and joint fusion [128, 234]. Osteotomy, defined as the surgical cutting of bone, is performed in OA in order to realign the affected joint such that the weight load is redistributed on unaffected joint compartments [48, 100]. While this does not cure the disease, it can delay total joint replacement, and is therefore recommended for young active patients who are not (yet) suitable for total joint replacement [128]. Joint arthroplasty involves removing the affected joint or joint compartment(s) and replacing them with prosthetic implants, usually made of polyethylene and cobalt-chrome-molybdenum alloy [55]. This treatment removes the diseased tissue: as such, it is quite effective at restoring function and alleviating joint pain [158]. The main drawback to joint replacement is that the implants only last 10-15 years, which can necessitate multiple surgeries, especially in patients younger than 50 years at the time of initial joint replacement [95]: this may be due to the increased joint use of younger patients. Joint arthrodesis or fusion, the treatment of choice before joint replacement became technically feasible, is only performed presently when joint replacement has failed and the joint is surgically unreconstructable. This usually occurs when a joint arthroplasty site becomes infected [47].

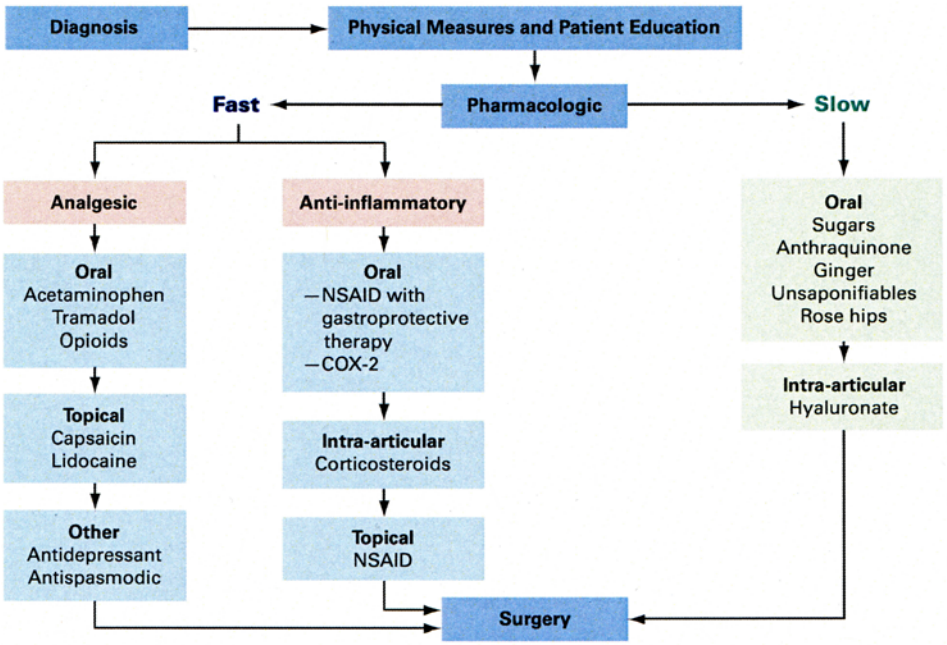

Figure 2.1: Flow chart depicting current therapeutic options for osteoarthritis. Once a diagnosis of OA is confirmed, non-pharmacologic interventions are started, as described above in subsection 2.1.6. If not effective at reducing pain, pharmacologic options, most often multimodal, are initiated. Joint arthroplasty is used as a last resort. Adapted from Altman [4].

2.1.7 Pathobiology

In early OA, extracellular matrix (ECM) components are structurally compromised. Chondrocytes and synoviocytes (synovial fibroblast-like cells) play a key role in this process, mainly by producing abnormally high levels of proteolytic enzymes. In advanced OA, this results in the complete loss of articular cartilage and in the formation of large lesions with bone exposure, along with subchondral bone remodelling. The associated gross and histological findings are well characterized, with cartilage fissures, loss of proteoglycans, osteophyte formation, and fibrosis [168]. This destruction is a hallmark of the failure of articular chondrocytes to maintain a homeostatic balance between ECM synthesis and degradation [54, 137]. Various factors, released from both cartilage and synovial mem-

brane, are involved in this process: aggrecanases, specifically ADAMTS-4 and ADAMTS-5; matrix metalloproteinases (MMPs), specifically MMP-1 (interstitial collagenase) and MMP-13 (collagenase 3); pro-inflammatory cytokines, such as IL-1β and TNF-α; growth factors, such as TGF-β-1; and nitric oxide (NO) [54, 135, 159, 175]. Among these, MMPs appear to play a critical role, as they are capable of degrading cartilage ECM components such as type II collagen and proteoglycans [24, 175]. The degradation products of articular collagen are type II collagen neoepitopes, which act as specific markers of joint disease, since they are found in the synovial fluid and urine of OA patients [44, 71]. Regulation of MMP gene expression and protein production involves several factors, including cytokines and growth factors [148, 175]: IL-1β stimulates the synthesis and secretion of MMPs and urokinase-type plasminogen activator (u-PA) [76]. Enzyme inhibitors such as tissue inhibitor of metalloproteinases (TIMP) and plasminogen activator inhibitor (PAI) regulate the balance of latent and active degradative enzymes; these inhibitors are controlled by TGF-β1 [2].

Aggrecanases are extracellular proteases that degrade aggrecan by cleaving at the glutamine^{373}-alanine^{374} site; they are part of a protein family known as the A Disintegrin-like And Metalloprotease domain (reprolysin-type) with ThromboSpondin type I motif (ADAMTS) [203]. ADAMTS-4 and ADAMTS-5 (also known as aggrecanases 1 and 2) are implicated in cartilage destruction in OA [12]. ADAMTS-4 is specifically up-regulated in OA synovium, and is induced by TGF-β1. ADAMTS-5 is constitutively expressed by synoviocytes, but is found in a truncated form (53-kDa instead of the normal 70-kDa form) in arthritic synovial

tissue: this may be due to alternative post-translational processing that is only active in a chronically inflamed joint [225].

Subchondral bone sclerosis is a sign of advanced OA. This may occur due to neoangiogenesis in the basal layers of degenerating cartilage, or as a result of abnormal healing of microfractures [75]. TGF-β1 is expressed in osteophytes [207], and may potentiate abnormal bone growth in OA. Subchondral bone can also have bone marrow lesions, as detected on MR [66]. While the implications for OA pathogenesis are unclear, it has been suggested that other tissue abnormalities such as cysts and avascular necrosis lead to the lesions seen on MR [2].

Classically, synovial inflammation was viewed as secondary or incidental to cartilage destruction in OA. However, recent findings have highlighted the role of primary synovial inflammation in OA pathogenesis [14]. Synovial hypertrophy and hyperplasia can occur asymptomatically early in OA, along with lymphocytic infiltration [22]. Pro-inflammatory mediator release from articular chondrocytes, along with cartilage breakdown products, can result in degradative enzyme release from the synovial membrane, thus aggravating the disease [181]. Most importantly, the synovial membrane produces IL-1β and TNF-α, which contribute to the pro-inflammatory and degradative processes in OA [2]. In sum, the release of pro-inflammatory and degradative mediators in the joint microenvironment contribute to tissue catabolism and inflammation (Figure 2.2), which then causes the joint pain characteristic of the disease (as discussed in subsection 2.1.4).

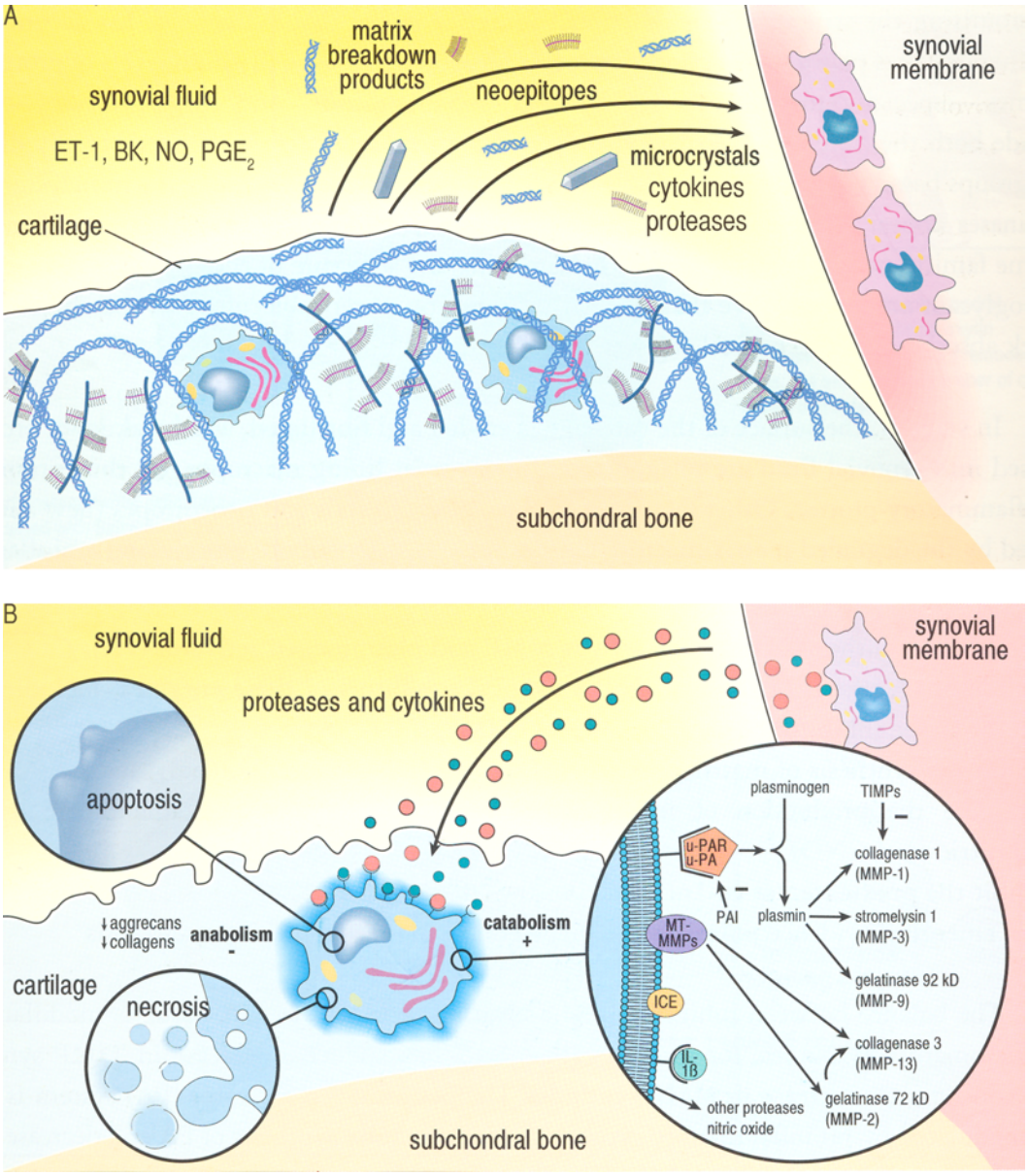

Figure 2.2: Biochemical basis of OA. Schematic overview of degradative mediators in joint microenvironment (A) and details of catabolic pathways (B). Adapted from Martel-Pelletier and Pelletier [136].

2.2 Inflammatory pain in OA

Arthritis is literally translated from the Latin as "inflammation of a joint" [164]. Inflammation in OA is now viewed as a central disease process [14]. It is the first step in a vicious cycle of joint pain, tissue damage, and further inflammation: as discussed above in subsection 2.1.7, synovial inflammation can be primary and/or reactive in OA, with multifactorial aetiology. As such, it can be examined in the context of inflammatory responses, which have common mechanisms in a wide variety of conditions. We briefly discuss generalities of inflammation, and focus on the pro-inflammatory roles of endothelial molecules in joint tissue.

2.2.1 Inflammation

Inflammation is the set of physiological responses of tissue to harmful stimuli, such as infection and tissue injury [117, 131]. Designed to remove the stimulus and initiate repair, inflammation is most likely an adaptive response to restore tissue homeostasis. There are four main components of an inflammatory pathway: inducers, sensors, mediators, and effectors; each acts in turn. Inducers are the initial cause of an inflammatory response, and sensors are those receptors or circulating factors that respond to the inducers. Mediators are the factors, produced downstream to sensor activation, that affect the tissues and systems in the inflammatory environment, and effectors are the cells and tissues that are specifically affected by the inflammatory response [141].

The inflammatory response is best understood in the context of immune re-

sponses to exogenous pathogens, where innate immune receptors on tissue macrophages and mast cells are triggered by pathogen-associated molecular patterns [17]. Ligation of these receptors leads to the production of chemokines, cytokines, vasoactive amines, eicosanoids, and other inflammatory mediators. These mediators affect vascular wall permeability, allowing plasma proteins and leukocytes to access the inflammation site. Elimination of the pathogen is followed by a repair phase, where macrophages secrete anti-inflammatory mediators and growth factors [194, 195]. If this acute response fails to clear the infection, the adaptive immune system, in the form of macrophages and T cells, is recruited and activated. Chronic inflammation results when pathogen clearance is unsuccessful, and often leads to tissue destruction [61].

According to Medzhitov [141], while other types of inflammation share many of the characteristics of infection-induced inflammation, the mechanisms that regulate such inflammation, along with their physiological roles, are unclear. In particular, they do not appear to fit the stereotypical patterns of acute-to-chronic progression as described above. Nonetheless, examination of the nature of endogenously-induced inflammation can shed light on many pathophysiological responses. (We do not discuss non-microbial exogenously induced inflammation, such as allergic inflammation, since it is beyond the scope of this work.)

Endogenous inducers of inflammation can take many forms, but all are signalling molecules produced by malfunctioning tissue. Many of these inducers are substances that are only produced upon tissue breakdown, or are only present in a given tissue compartment that is normally sequestered from the vascular system.

For example, hyaluronante, an ECM component that is normally a high-molecular-weight polymer, breaks down into fragments that are pro-inflammatory. These fragments provoke tissue repair in a reactive-oxygen-species-dependent manner [101, 102]. Another classic example is that of collagen (inducer), an ECM component that is normally sequestered from plasma, activates coagulation factor XII (sensor) upon rupture of the endothelial wall. Activated factor XII initiates, among others, the kallikrein-kinin system, which produces the vasodilator bradykinin (BK) (mediator), which acts on the vasculature and smooth muscle cells (effectors), as well as stimulating pain sensation [141]. (We discuss BK in the context of joint tissue below in subsection 2.2.8.) Chronic inflammation occurs in the same manner as with exogenous inducers, in that the acute inflammatory response fails to clear the noxious stimulus.

Clinically, inflammation is described by the four cardinal signs of Celcus (1st century AD): *rubor et tumor cum calore et dolore* (redness and swelling with heat and pain) [20, 179]. These signs are not exclusive: to quote Stedman's Medical Dictionary [58], "all the above signs may be observed in specific instances, but no single sign must, as a matter of course, be present." Moreover, an inflammatory process may be clinically undetectable, yet may be causing some of the cellular processes responsible for the cardinal signs, and tissue may be affected by pro-inflammatory mediators in the absence of inflammatory cell infiltration. Thus, many authors currently argue for a multi-modal and complex view of inflammation, in that it is not a single process but a collection of responses to trauma or infection, and that it is not binary (on-off) in nature, being influenced by a

multitude of extrinsic and intrinsic factors [20, 141, 192].

2.2.2 Pro-inflammatory signalling

Inflammation can effect signal transduction by an immense variety of pathways, both directly and indirectly induced. In the interests of clarity (as well as to remain within the scope of this work), we focus here on one of the main signalling cascades that has been implicated in OA pathogenesis (see subsections 2.2.5 and 2.2.8), along with many other inflammatory disease processes: the NF-κB (nuclear factor kappa-light-chain-enhancer of activated B cells) classical pathway. NF-κB refers to a family of five transcription factors that exist in almost all cell types and operate on pro-inflammatory and survival gene targets [105]. Three of the transcription factors, RELA (or p65), c-REL, and RELB, are transcriptionally active in their native state. The other two, NF-κB1 (or p105) and NF-κB2 (or p100) exist as inactive precursors [106].

NF-κB is activated via two separate pathways: the classical and the alternate. The classical pathway is activated by phosphorylation of IκB by the IKK complex, which triggers the ubiquitination and degradation of IκB. This allows the active subunit(s) to be phosphorylated and translocated to the nucleus, where they bind to their target DNA binding sites [59, 224]. This pathway is often activated by injury and/or inflammation, which causes the release of two first-response cytokines: IL-1β and TNF-α. These mediators bind to their receptors, which activate the IKK complex via second messenger signalling (Figure 2.3). With regard to OA pathogenesis, downstream genes activated by NF-κB include *PTGS2*, inducible

nitric oxide synthase (*NOS2*), and *MMP1* [183]. The alternate pathway involves inducible processing of p100. Activation of NIK and the IKK complex lead to p100 phosphorylation and eventual cleavage to p52. RELB and p52 form heterodimers which then translocate to the nucleus [105, 106, 224].

Parenthetically, the NF-κB system has been a target for much drug development [106]. However, since it has an important physiological role in immune system activation, indiscriminate inhibition could lead to undesired results [121]. Xu *et al.* [224] argue that a more complete understanding of the molecular mechanisms of the specific inhibitors will lead to more targeted therapies. This author would add that local therapy, as opposed to systemic treatment, should be considered as well, in order to avoid undesired side effects. (We argue for this approach below in section 5.2 with regard to our treatment strategy.)

2.2.3 Endothelial molecules in OA inflammation and pain

Endothelial mediators allow inflammation to occur, by vasoactivation and permeabilization of the vascular wall. As discussed above, one of the cardinal signs of inflammation is pain sensation, which occurs due to nociceptor activation by inflammatory mediators [112, 123]. Specific to OA, endothelial mediators can influence angiogenesis, which is a disease-modifying process. Pro-inflammatory cytokine release and inflammatory cell recruitment stimulate angiogenesis in synovial membrane, cartilage, and bone, thereby contributing to structural changes. This is accompanied by neoinnervation, which leads to joint nociceptor sensitization and deep joint pain [13, 28].

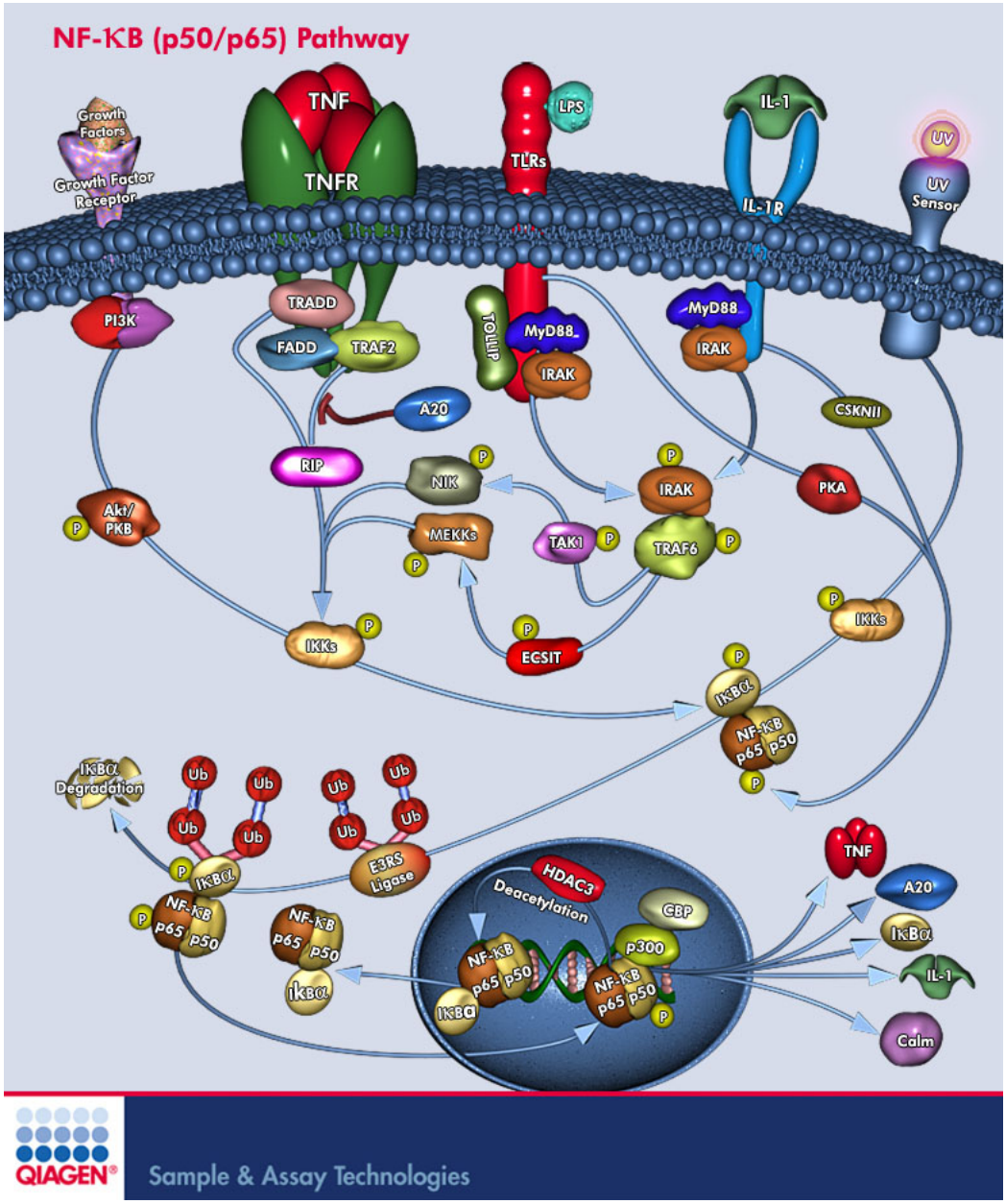

Figure 2.3: Classical NF-κB (p50/p65) pathways. From the GeneGlobe Pathway Atlas [169]. ©2010 Qiagen, all rights reserved.

We discuss two endothelial mediators of interest, which represent two vascular regulation systems: endothelin, in the renin-angiotensin-aldosterone system [185]; and bradykinin, in the kallikrein-kinin system [177]. These systems may cross-talk [196], which gives rise to our hypothesis (section 2.4 below) that endothelin and bradykinin receptors may be relevant therapeutic targets in OA.

2.2.4 Endothelin-1

Endothelin-1 (ET-1) is a 21-amino-acid potent vasoconstrictor peptide, mainly known for its role in maintaining vascular homeostasis. First isolated and characterized in 1988 [227], ET-1 has been implicated in a wide variety of pathologies, ranging from cardiovascular disorders to lung disease; most often, ET-1 acts in a pro-inflammatory role. In joint tissues, it is synthesized and released by endothelial cells, synoviocytes, and chondrocytes [146, 230]. It is of interest that ET-1 production can be induced by shearing force, which occurs in an OA joint with abnormal biomechanical loading.

The author's laboratory has previously shown that ET-1 plays a major role in OA pathogenesis. It reduces cartilage anabolism by inhibiting collagen type II and proteoglycan synthesis via NO mediation in a concentration-dependent manner [109]: chondrocytes treated with ET-1 and an iNOS inhibitor synthesized more proteoglycans and collagen than cells treated with ET-1 alone. This effect was reversed on both gene and protein levels by treatment with a NO donor. ET-1 is up-regulated in OA tissues, where it promotes MMP-1 and MMP-13 synthesis and activation, along with an increase in type II collagen neoepitopes and a decrease

in TIMP activity [187]. These effects occur via activation of the MAPK and AKT/PKB pathways, as detected by increased kinase phosphorylation. ET-1 also causes excessive production of NO, which is generated as the result of an increase in iNOS levels [132]. These effects occur mainly via endothelin receptor type A (ETA) [110].

2.2.5 Endothelin receptors

ET-1 has two receptor subtypes, A (ETA) and B (ETB). Both G-protein-coupled receptors (GPCRs), they are differentially expressed in various tissue types. The classical distribution of ET receptors is as follows: ETA is found in vascular smooth muscle, where it mediates ET-induced vasoconstriction; ETB is expressed predominantly in endothelial cells, where it mediates vasodilatation by the generation of prostaglandins and nitric oxide (NO) [53]. ETB may act as a clearance receptor for ET-1, thereby minimizing ETA activation, since ETB binds and remove ET-1 from circulation [26]. Both receptor subtypes are also found in the central nervous system, where they play a neuromodulatory role [40]. ETA is expressed in articular tissue by chondrocytes, synoviocytes, and endothelial cells, where it plays a significant role in cartilage and bone metabolism [124, 144]. ETA also potentiates inflammatory joint pain induced by ET-1 [52, 111].

ETA signals through $G_{q/11}$ and $G_{12/13}$, activating the PLC, PKC, and PI3-K pathways (Figure 2.4) [42, 49, 77, 134, 191]. It also activates MAPK pathways via intracellular calcium release, and AKT/PKB, downstream of PI3-K activation [29]. ETB activates G_i and $G_{q/11}$ in smooth muscle and endothelium

[49, 77, 134, 191]. Chen *et al.* [42] note that since ET-1 ligates both receptor subtypes, downstream signalling may cross-talk in both normal and pathological conditions; however, little is known about this. Similar to the downstream events of bradykinin receptor ligation (described in subsection 2.2.8), the downstream signalling pathways activated by ETA can influence early OA pathogenesis by causing chondocyte hypertrophy, MMP synthesis, and NF-κB activation.

2.2.6 ET-1 and inflammation in OA

ET-1 plays a pro-inflammatory role in articular cartilage catabolism in OA. It has been detected in the synovial fluid and plasma of both OA and rheumatoid arthritis (RA) patients at levels at least twice as high as healthy controls (on the order of 20 pg/mL for OA patients versus 1-10 pg/mL for controls) [152, 230]. ET-1 is also implicated in pain and hyperalgesia [90]. It functions as a nociceptive sensitizer: intradermal injection of ET-1 induces hyperalgesia in the human forearm [69] and rat hindpaw [89]. It can also cause overt pain: intra-articular injection of ET-1 induced knee joint inflammation in an animal model [52]. In this study, selective ETA antagonist treatment reduced nociception and joint inflammation caused by ET-1, carrageenan, or bacterial lipopolysaccharide. Conversely, treatment with an antagonist selective for ETB or a mixed ETA/ETB antagonist did not reduce ET-1-induced inflammation, but did reduce carrageenan-induced inflammation. Thus, ET-1/ETA signalling is implicated in articular nociception.

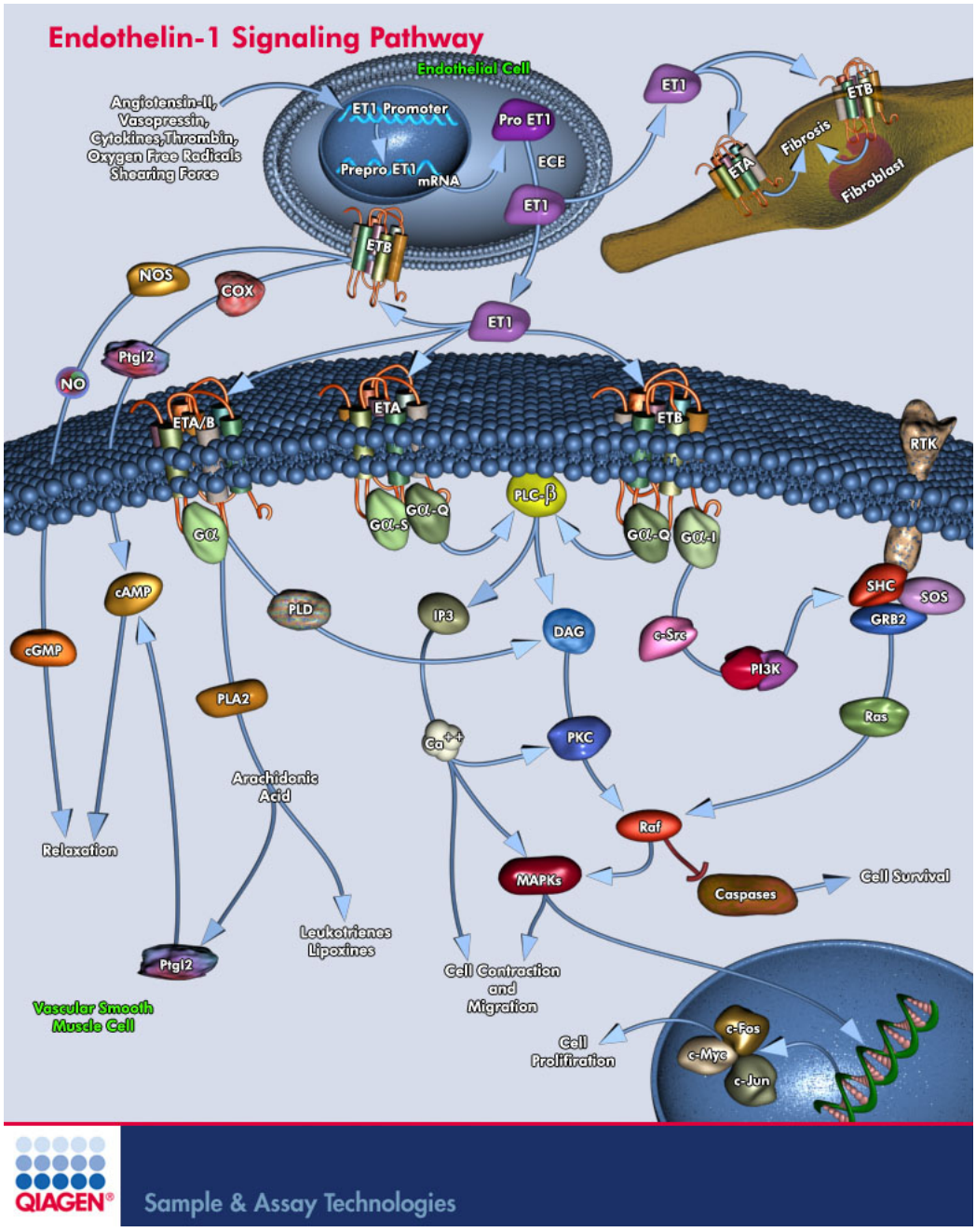

Figure 2.4: ET receptor signalling pathways. From the GeneGlobe Pathway Atlas [169]. ©2010 Qiagen, all rights reserved.

2.2.7 Bradykinin

Bradykinin (BK), a nonapeptide, is one of the most potent endogenous vasodilators known. It was identified in 1949 as being released from plasma globulin upon treatment with snake venoms and trypsin [180]. This release is due to the proteolytic cleavage of high-molecular-weight kininogen by kallikrein in a positive-feedback manner [177]. The main physiological roles of the kallikrein-kinin system, apart from its pro-inflammatory functions, are to regulate blood pressure and sodium homeostasis by influencing vascular tone [51, 107, 228]. The kallikrein-kinin system also helps to assemble clotting factors in the contact activation or intrinsic pathway of coagulation [37]. BK also has roles in inflammation and nociception: it has been identified as a pro-algesic factor in human inflammatory exudates [11]. BK is generated in all inflamed tissue [204], where it induces pain through nociceptor sensitization and activation [147]. As we discuss below (subsection 2.2.9), BK receptors are essential for this process: gene knockout models deficient for either BK receptor B1 (BKB1) or BK receptor B2 (BKB2) have reduced nociceptive ability [165, 188]. Specific to OA, BK is generated in OA synovial membrane and fluid; it also is released due to the increased vascular pressure in subchondral bone [142].

2.2.8 Bradykinin receptors

Bradykinin ligates two receptors, bradykinin receptor B1 and bradykinin receptor B2. Both GPCRs, they are expressed in many tissue types, but differ in expression levels based upon the tissue state. BKB2 is expressed constitutively

to a large extent in healthy tissue, and is primarily involved in the acute phase of inflammation [85, 149]. Conversely, BKB1 is only expressed in inflamed tissue: it is synthesized *de novo* following tissue injury [204]. BKB1 is also up-regulated in chronic inflammatory conditions (Figure 2.5), its expression often induced secondary to inflammatory mediator release [34, 35, 85]. The author's laboratory has detected BKB1 expression in human OA synovial membrane and cartilage by immunohistochemistry (Charlotte Zaouter, unpublished results).

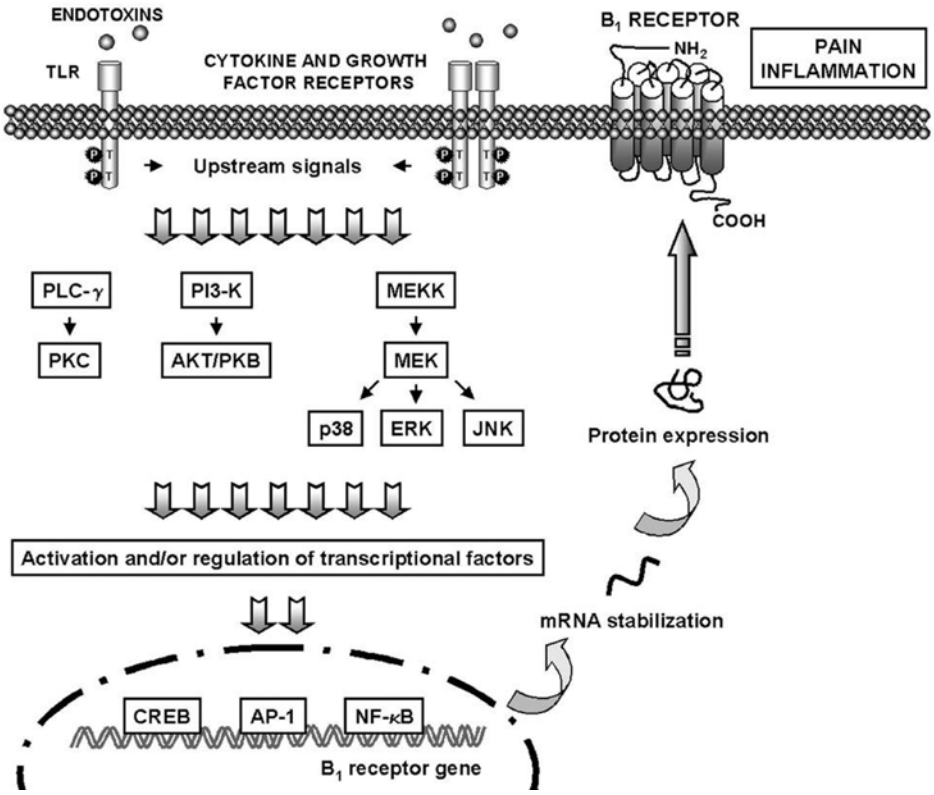

Figure 2.5: Upstream signalling molecules that may lead to BKB1 up-regulation include MAPKs, PKC, and PI3-K, which modulate transcriptional factors such as NF-κB, AP-1, and CREB that are involved in BKB1 gene expression. From Calixto *et al.* [35].

BK receptors generally signal through G_q [81, 118], though they also interact with G_s [122] and G_i [64, 226] (Figure 2.6). $G_{q/11}$ coupling eventually activates the PI3-K and PKC pathways. As well, G_i coupling leads to PLA_2 activation, which

results in prostaglandin production [226]. With regard to early OA pathogenesis, the PI3-K pathway activation can cause chondrocyte hypertrophy via AKT/PKB [208]. The PKC pathway activates downstream catabolic factors such as MMPs [94, 205, 214, 229] in OA chondrocytes; LaVallie *et al.* [119] suggest that atypical PKCζ potentiates NF-κB activation in OA chondrocytes via TNF-α and IL-1β.

2.2.9 BKB1, inflammation, and nociception in OA

It has been suggested that BK, via BKB1 signalling, plays a role in local tissue injury, pro-inflammatory reactions [23], and nociception [68]. Sainz *et al.* [189] have shown that, in an animal model of induced inflammatory arthritis, BK influences chronic inflammation through ligation of both BKB1 and BKB2. BKB2 appeared to be principally involved in the acute phase of inflammation by facilitating leukocyte activation (CD11b), homing (CD44), and transmigration (CD54). Treatment with a BKB2 antagonist did not affect disease evolution. In chronic RA, excessive release of kinins in the synovial fluid can produce oedema, pain, and loss of joint function due to activation of both BKB1 and BKB2 [36]. BKB1 also potentiates the effects of other pro-inflammatory mediators such as cytokines (IL-β, TNF-α), prostaglandins (PGE_2), and transcription factors (NF-κB). In OA, these mediators are capable of inducing bone and cartilage damage, synovial tissue hypertrophy, angiogenesis, and inflammatory cell infiltration [22]. BKB2, though it has been implicated in nociceptor sensitization in OA [142, 206], may be less relevant as a therapeutic target in the context of a chronic inflammatory response.

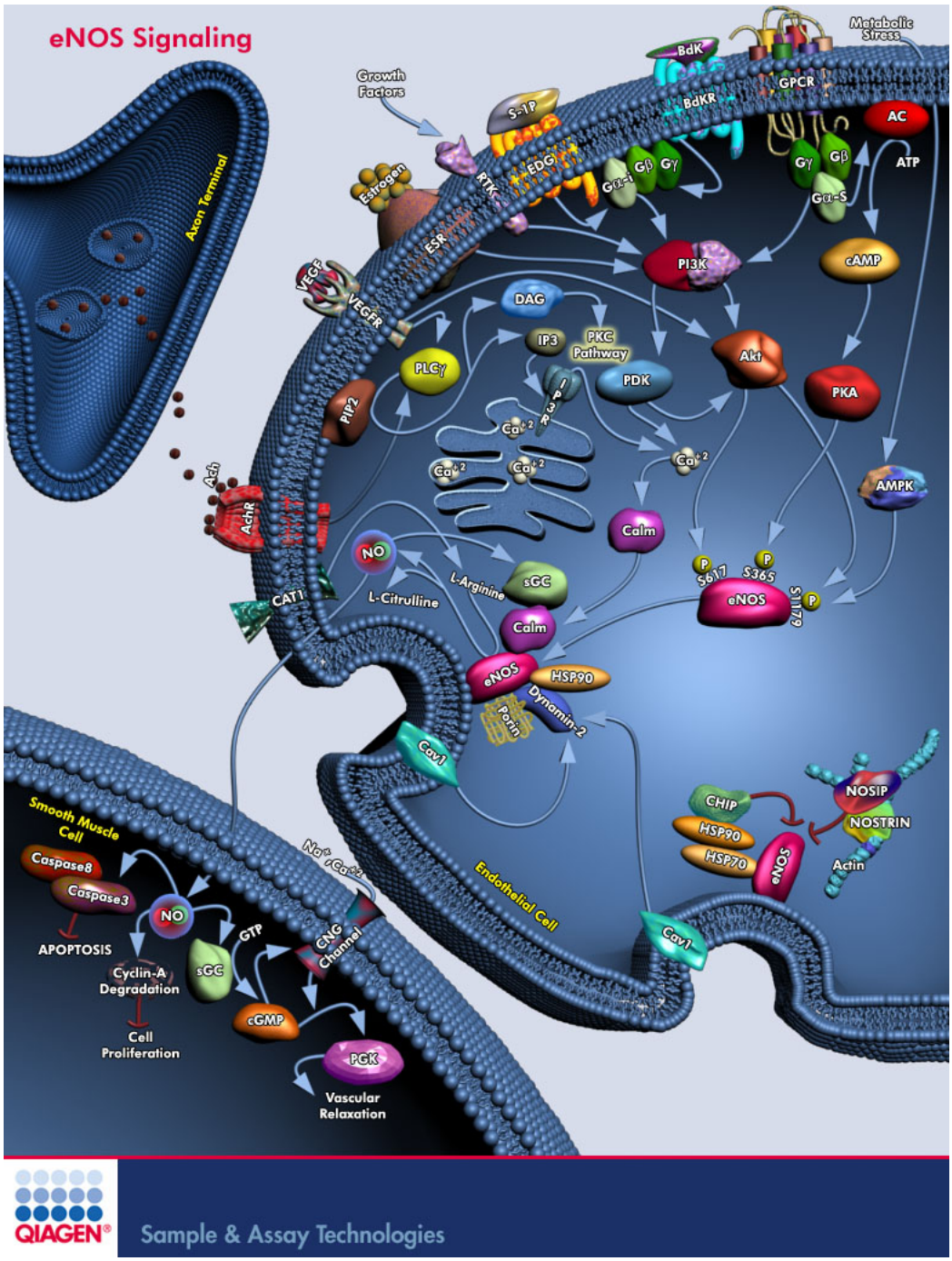

Figure 2.6: BK receptor signalling pathways. From the GeneGlobe Pathway Atlas [169]. ©2010 Qiagen, all rights reserved.

2.3 Animal models of osteoarthritis

Since we used a surgically induced rat model of OA to test our hypothesis (see section 2.4), we provide an overview of animal models of OA, and focus on joint pain assessment techniques.

2.3.1 Overview

Animal models of OA fall into three main categories: spontaneous, chemically induced, or mechanically induced [8, 33]. All these approaches share the goal of inducing articular degradation in the targeted joint, such that the final outcome is OA histopathology as examined by serial sectioning [138]. This is commonly evaluated by scoring using a histopathology assessment system which rates the severity of histological disease progression and the extent of joint tissue involvement. One such score that is now in common use is the OARSI (Osteoarthritis Research Society International) histopathology assessment system [168]. Animal models have elucidated many aspects of OA [212], but one must be careful not to over-interpret results, since (most) people are not animals: joint biomechanics and metabolism, as well as musculoskeletal growth patterns, differ significantly [33]. However, they remain the gold standard for preclinical studies.

Spontaneous OA models are species- and strain-specific. Often arising from a genetic disposition towards OA, such as type II or type IX collagen mutations in mice [72, 153], these models are highly variable in terms of their kinetics and prevalence. To take the example of a model that the author had initially consid-

ered using in his thesis project, 85% of STR/ort male mice will develop medial tibial plateau OA between 8 and 30 weeks of age [138]. These models are valuable to study the genetic and developmental factors involved in OA, since the kinetics of pathogenesis are probably closest to the human disease. The main advantages to these models are that the aetiology of OA is known, and that disease severity and incidence can be controlled to a certain extent [231].

Chemically induced OA models cause joint degradation by intra-articular injection of pro-inflammatory or degradative substances. Pathogenesis is often rapid, with significant articular changes and associated pathophysiology detectable within 3-7 days after injection, to take the case of monoiodoacetate injection into the rat knee [31]. Other common approaches include injections of papain, collagenase, and hypertonic saline. This class of model can be reproduced in essentially all of the species commonly used in musculoskeletal research: rodents, rabbits, dogs, guinea pigs, and so on [33].

Mechanically induced OA models cause OA by physically destabilizing the target joint. The most common approaches are surgical anterior cruciate transection and/or meniscectomy in the knee, due to its surgical accessibility and well characterized biomechanics. Joint immobilization [86] or denervation [129] are used less frequently. Initially reported in large-animal models such as dogs [75], this class of models has been adapted to small-animal studies more recently [9]. The disease kinetics are rapid and consistent, and reproduce post-traumatic OA [21, 219]. The main critique of this approach is that the pathology produced is actually more severe, and thus not directly comparable, to human OA, which is focal for the

most part; nonetheless, this varies enormously depending on the specific model. As described below in section 3.1, we chose a surgically induced OA model for our study upon expert recommendation (Gordon Ng PhD, personal communication).

2.3.2 Pain assessment in animal OA models

Classically, animal models of OA have focused on cartilage degradation, histopathological changes, and molecular aetiology. More recently, researchers have become increasingly interested in joint pain and functional limitations of OA as reproduced in animals. There are relatively few reports of pain assessment in OA animal models, given their established role in OA research (perhaps because pain specialists and orthopaedists do not communicate enough!), but the musculoskeletal research community is becoming more cognizant of the potential benefits of functional pain measurement.

Most pain assessment methods focus on OA induced in an animal knee, since it is an easily accessible joint with well-characterized biomechanics in both laboratory animals and humans; current methodological approaches are comprehensively reviewed by Neugebauer *et al.* [155]. Pain measurement can be divided into two modalities: direct assessment, which measures actual joint pain; and indirect assessment, which measures behaviours affected by joint pain. Most classic modalities are indirect, since they are somewhat easier to implement. As well, they may be more informative than direct modalities, since the functional limitations of OA motivate most patient complaints.

2.3.2.1 Indirect assessment

Common indirect assessments include weight bearing, posture and gait analysis, and spontaneous mobility. Weight bearing can be subdivided into two categories: static weight bearing (our modality of choice: see section 3.3.3), where the animal is stationary, and dynamic weight bearing, where the animal is moving. Both investigate the weight distribution of the animal by quantifying the force applied by the limbs; a healthy animal will bear weight roughly equivalently on their limbs, an animal experiencing limb pain will shift their weight to their other limb(s). This postural imbalance can be quantified in terms of percent weight [167], or difference in weight distribution change between treatment and experimental groups [31], to name two of the most popular approaches. Static weight bearing in rodents is often restricted to the hind limbs for practical reasons: it is easier to force a rat to rear in a restraint than to restrain it horizontally without allowing motion. However, since the animal is confined in a stationary artificial posture, static weight bearing has come under criticism, since animals rarely naturally adopt such a position for long periods of time. Furthermore, it does not take the shift of weight distribution to the forelimbs into account. Dynamic weight bearing, as the name suggests, occurs in an open-field environment which allows the animal to move freely [46]. One critique of this method is that since animals are required to move, the results can be influenced by the animal's motivation.

Posture and gait analysis are related to weight bearing assays, in that they attempt to quantify standing and walking behaviour using subjective rating scales

in order to calculate an integrated pain score [163]. Behaviours such as foot pad touch, limping, guarding, eversion, and avoiding contact with the affected limb, are all assessed and rated by direct observation. Hind paw elevation time and paw contact time can also be objectively measured by forced ambulation: rodents are placed on a rotating drum with sensor arrays wrapped around the surface, and limb use is monitored electronically [91]. The main advantage to such techniques is that they are used in clinical practice; it is thus easy to "compare" results obtained with animals to human functional tests (as well, it is simpler for clinicians to understand researchers' results using these techniques!).

Open-field activity monitoring, first described as simple observation of an animal's motion, velocity, rearing, and so on, in an open field [83, 84], has undergone a technological revolution in recent years. In-cage activity monitoring, now *de rigueur*, involves placing the animal's home cage in a frame that can either receive signals from an implanted radio transmitter, or can track motion via infrared photo-beams [74, 155]. The resulting data, from either high- or low-technology instrumentation, can be related to pain behaviour in terms of level of activity: animals in pain will move less and rest more.

Mechanical sensitivity of the distal paw represents a widespread and classic set of modalities to assess limb hyperalgesia. The distal paw is stimulated with increasing pressure stimuli, applied either with von Frey filaments (thin nylon monofilaments of increasing stiffness) to the plantar surface [30, 67] or a Randall-Selitto algesiometer (a wedge-shaped compressive probe) to the dorsal surface [172], and paw withdrawal thresholds are measured. Heat stimulus can also be

applied by infrared apparatus, hot plate, or hot water [96, 198, 199]. Animals with hyperalgesia will have lower pain thresholds and will withdraw their paw faster than healthy animals, given the same painful stimulus. These methods, while valuable in the context of diffuse neuropathic pain models, are rather unrelated, in our opinion, to knee joint OA. This is concurrent with expert advice (Geoffrey Bove DC PhD, personal communication), since OA pain is deep joint pain, and these tests measure secondary hyperalgesia, which is uncommon in human patients [167]. Furthermore, von Frey filaments, while widely accepted in the pain research field, have been recently criticized for the inconsistency and experimenter bias inherent in the method. As well, doubts have arisen as to whether von Frey filaments are testing a pain modality or an itch modality, especially with lower filament stiffnesses [30].

2.3.2.2 Direct assessment

More recent reports of joint pain assessment in animals use direct modalities that measure actual joint pain. While these tests are often more difficult to perform, and interpretation of results more subjective in nature, relative to indirect modalities, the data obtained is directly related to perception of OA deep joint pain. This information can prove valuable in assessing the effects of potential treatments. Perhaps the most intuitive of these methods is direct compression of an arthritic knee joint, which measures mechanical sensitivity. The joint is squeezed on the medio-lateral axis, and the force required to elicit a hind limb withdrawal reflex and/or vocalization is measured qualitatively (i.e.

light squeeze, medium squeeze, high pressure) [73] or quantitatively by calibrated forceps equipped with strain gauges that measure applied force at the tips and provide a digital read-out [127, 197, 232]. Animals with joint pain will have lower withdrawal thresholds; they will withdraw their paw in response to lower compressive forces than healthy animals. This technique, using calibrated forceps, was initially considered by this investigator, but was discarded in favour of static weight bearing upon expert advice (Stéphane Faubert DVM, personal communication) due to its high degree of invasiveness and subjective nature: the animal must remain in a very uncomfortable manual restraint for the test, and scoring a positive pain response is highly subjective.

Mechanical sensitivity has also been assessed by measuring the struggle threshold angle or range of motion, which is decreased in an arthritic joint [193, 232]. While the femur is maintained motionless, the tibia is extended until the animal struggles. The extension distance that the heel travels during movement is measured, and is used to calculate the extension angle by trigonometry. By defining the length of the tibia as the two sides of a triangle which are adjacent to the angle, and the distance travelled by the heel as the third side, which is opposite the angle, the cosine law is applied to solve for the angle. (This author would be concerned about measurement errors, due to the relatively small dimensions involved!).

Han and Neugebauer [87, 88] have developed an apparatus with a recording chamber connected to a computerized analysis system to measure and quantify the painful vocalizations evoked by joint compression. Rodent vocalizations in the

audible range represent a defence mechanism, and ultrasonic vocalizations in the 22 kHz range reflect an emotional response. Upon knee joint compression (using the calibrated forceps described above), both the vocalizations evoked during the stimulation, and those that outlast the stimulation, are recorded and analyzed. In rats with arthritic knee joints, the rate and duration of vocalizations are increased, and the compressive threshold required to elicit vocalizations is decreased, as compared to healthy controls. Neugebaueur *et al.* [155] suggest an interesting line of future research: since vocalization during stimulation and vocalization after stimulation are generated by different neural mechanisms, analyzing which stimuli cause which set of vocalization responses could help decipher the neural components of arthritic pain perception.

2.4 Hypothesis and objectives

The author's laboratory has previously shown (as described above in subsection 2.2.4) that ET-1 plays a central role in joint tissue metabolism, and has a catabolic function in matrix degradation in OA. These effects occur primarily through ligation of ETA. We hypothesize that ET-1 signalling, via ETA, up-regulates BKB1 expression and BK release in OA tissues, and that this engenders a vicious cycle of synovial membrane inflammation, articular cartilage destruction, and joint pain. Therefore, we view these receptors, taken together, as novel therapeutic targets in OA. We propose that antagonism of these receptors (treatment with specific peptide antagonists of ETA and/or BKB1) may represent a novel therapeutic option to alleviate, and perhaps prevent or reverse, the pain,

inflammation, and tissue damage that occur as OA progresses from an acute to a chronic state. We hypothesize that ETA and BKB1 antagonism will diminish OA progress and joint pain, with dual antagonism acting in an additive manner.

There were three main objectives of the author's Master's research project. Since the laboratory had no previous experience with OA animal models, nor with pain measurement, he was tasked to develop and optimize an animal model of OA, and to design and validate an *in vivo* pain measurement modality. His project culminated with a preclinical animal study to test the efficacy of ETA and BKB1 antagonism at reducing OA joint pain, radiological indices of disease, and histopathology.

CHAPTER 3

MATERIALS AND METHODS

3.1 Animal model of osteoarthritis

Originally, we had planned to use the STR/ort spontaneous mouse model of OA [138] (a kind offer from Alain Moreau PhD, director of the Viscogliosi Laboratory for Molecular Genetics of Musculoskeletal Disorders, at Sainte-Justine Hospital Research Centre), but severe strain reproduction problems, as well as confusion about the precise method of pain assessment to be used that would be appropriate for mice, given their small physique, led us to choose a rat surgical model of OA, which is described below. This model has several advantages that proved attractive to us: rapid and reproducible disease kinetics, the ability to examine histopathology of the entire affected joint, along with well-characterized and validated methods to measure hind limb pain.

3.1.1 Animals

Eight-week-old male Lewis rats were purchased from Charles River Canada (Saint-Constant, QC) and housed under standard conditions. All procedures were approved by the Sainte-Justine Hospital Research Centre animal ethics committee and conformed to Canadian Council on Animal Care guidelines [160].

3.1.2 Study design

The study was conducted as a fractional factorial experiment, which is defined as a judicious selection of a subset of the treatment combinations required for the complete factorial experiment [7]. That is, a fractional factorial experiment only tests some carefully selected treatment combinations, as opposed to every possible combination. These experimental designs are usually employed to exclude superfluous factor-level combinations, thereby maximizing limited resources, when the interaction terms in the statistical model are assumed to be negligible as compared to the main effects terms [154].

Animals were randomly assigned to one of three surgery conditions: anterior cruciate ligament transection (ACLT), sham surgery, or no surgery (negative control). Subsequently, animals were assigned to one of four treatment groups, as detailed below (Table 3.I). Sample size was $n = 4$ per group. This small sample size was mandated by the Sainte-Justine Hospital Research Centre animal ethics committee due to the pilot nature of the study, since we had no previous data whatsoever with regard to this animal model.

Table 3.I: Experimental groups. Six experimental groups were designated in the fractional factorial study, with 4 subjects per group.

Group Number	Surgery	Treatment
1	None	Saline
2	Sham	Saline
3	ACLT	Saline
4	ACLT	BQ-123
5	ACLT	R-954
6	ACLT	BQ-123+R-954

3.1.3 Surgical technique

OA was induced by surgical transection of the right anterior cruciate ligament. The procedure was modified from previously published reports [9, 92, 202, 222]. Animals were anaesthetized with inhaled isoflurane (3% / L O_2 induction in chamber, 2% / L O_2 maintenance with face-mask), and prepared for surgery by clipping the hair over the ventral and medial aspects of the right leg from hindpaw to hip. The skin was disinfected with povidone-iodine, and a 3-cm incision was made medial to the patellar tendon (Figure 3.1A). The subcutaneous tissue and muscle were then incised and the patella laterally sublaxed; the joint capsule was opened with the limb hyperextended (Figure 3.1B). With the limb in full flexion, the anterior cruciate ligament was visualized by blunt dissection, and sectioned by a latero-medial cut parallel to the tibial plateau, using a #11 scalpel blade (Figure 3.1C-D). Transection was confirmed with the anterior drawer test (Figure 3.1E-F: E depicts the knee before, and F shows an anterior drawer). The patella was then replaced, and the limb extended (Figure 3.1G). The joint capsule (Figure 3.1H) and muscle layers (Figure 3.1I) were closed with 4-0 polygalactin absorbable suture (horizontal mattress stitch, Figure 3.1J). 50 μL of lidocaine was then injected into the joint capsule to provide local analgesia. Skin was closed with steel surgical staples (Figure 3.1K). Post-operative hydration (6 mL/kg saline) and systemic analgesia (0.1 mg/kg buprenorphine HCl) were provided by subcutaneous injection. Surgical staples were removed 14 days post-operatively (Figure 3.1L). Sham surgery consisted of all of the above except ligament transection.

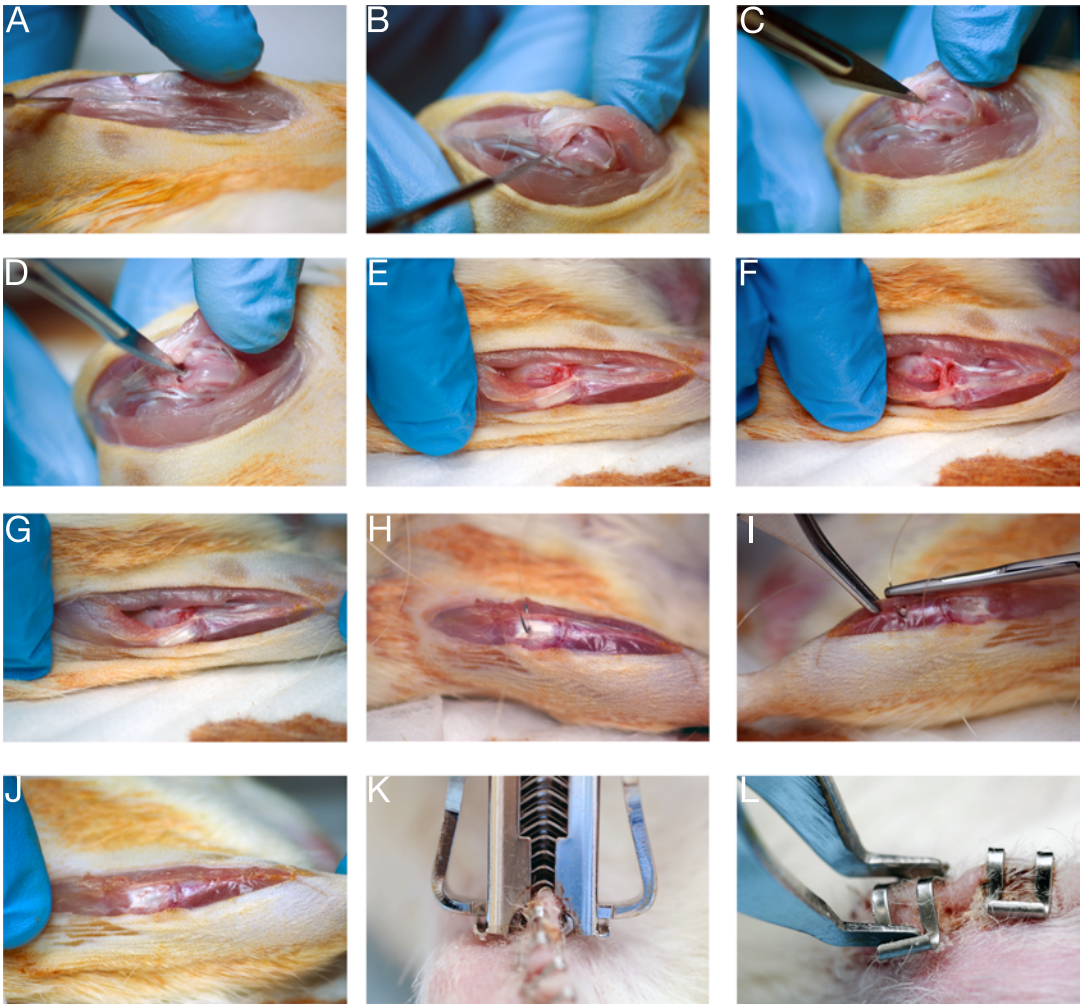

Figure 3.1: Rat ACLT surgical steps. Photos were taken with a 300-mm macro lens (approximate magnification 2×).

3.2 Drug treatment

Over the course of two months post-operatively, animals were treated by weekly intra-articular injections of ETA and/or BKB1 specific peptide antagonists: BQ-123 (ETA antagonist; Sigma-Aldrich, Oakville, ON) [98, 99], R-954 (BKB1 antagonist; kind gift from Pierre Sirois, IPS Thérapeutique, Sherbrooke, QC) [70, 156], both, or saline vehicle, was injected into the right knee at a dose of 30 nmol in a volume of 50 μL. Injections were performed under isoflurane anaesthesia, using a 28G needle (Figure 3.2). Chemical structures are depicted in Figure

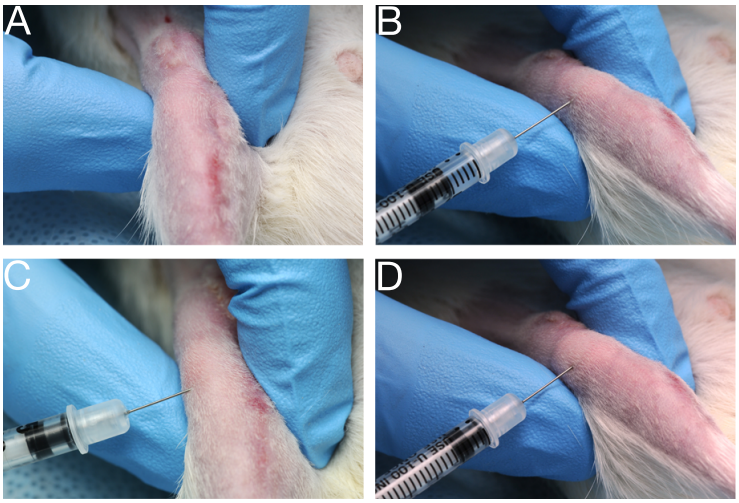

Figure 3.2: Intra-articular injection into the rat knee. A, the shaved knee is maintained in extension. B, the needle is inserted under the patellar tendon into the joint space. C, the syringe plunger is depressed slowly. D, successful injection is detected by a momentary swelling of the articular space. Photos were taken with a 300-mm macro lens (approximate magnification 2×).

3.3. Doses were based upon previously published reports [52, 206] of the same dosages, by intra-articular injection, in studies of acute ET-1- and BK-mediated pain in the rat knee joint.

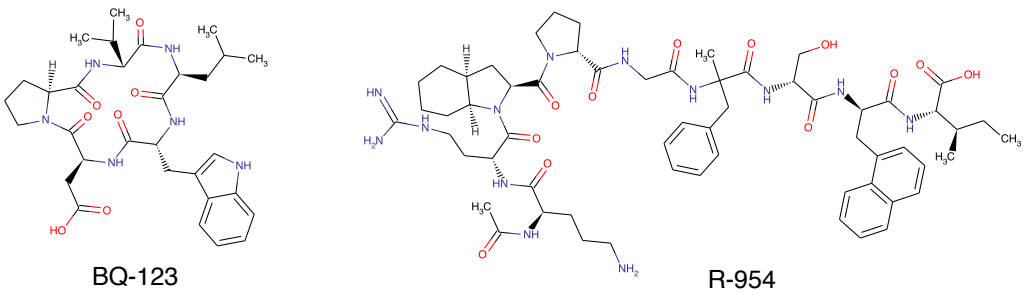

Figure 3.3: Receptor antagonist chemical structures. Left, BQ-123 (ETA antagonist); right, R-954 (BKB1 antagonist).

3.3 Static weight bearing

3.3.1 Reverse-engineering and design

A static weight bearing apparatus was reverse-engineered from previously published reports [31, 32, 213] as described below. We undertook this process because commercially available apparatuses are not very precise and restrict measurement paradigms to a few pre-programmed routines. Furthermore, they are prohibitively costly. Due to our selection of a more precise measurement strategy, our apparatus is roughly three times as precise as those on the market. It is also cheaper, costing about half as much as apparatus currently sold. Finally, the software allows for tremendous flexibility in designing test programs.

3.3.1.1 General features

The basic principle of the static weight bearing test is that a healthy animal will distribute its weight roughly equally over its hind limbs, and that any shift in this equilibrium, due to a traumatic intervention, is considered a pain response.

Rescue due to treatment will result in a return to an even weight distribution pattern [213]. A static weight bearing apparatus must therefore detect and record the applied force (weight) on both hind limbs of a rat standing in the apparatus. As such, the four main components of any static weight bearing apparatus are a pair of load cells or force transducers, to detect the vertical component of applied force on each hind limb of the animal; a support base or system for the apparatus and electronics; a restraint system for the animal with an inclined plane, to ensure that it stands on its hind limbs; and a computer interface for data recording.

3.3.1.2 Design process

The restraining box was designed using previously published photographs of commercially available apparatuses to sketch a prototype. Measurements of appropriate inclination angle, height, and width for the restraining box were conducted on 4-month-old rats (approximate weight 500 g), since our study protocol called for static weight bearing tests up to 16 weeks of age.

The Futek LSB200 (250 gram) load cell with universal serial bus (USB) 210 interface was selected as the force transducer of choice, due to its easy configurability, plug-and-play USB operability, and preprogrammed software. Appropriate capacity was estimated from the published growth curves for male Lewis rats from Charles River Canada [41], which indicate that a four-month-old rat should weigh between 375-425 grams. We therefore chose sensors with 250-gram capacity for each hind limb, which is a bit more than half the maximal weight of a four-month-old Lewis rat: this gives our apparatus an effective maximal capacity of 500 grams.

This also permits the apparatus to be used with slightly older rats and/or animals from other strains that have higher average body weights than Lewis rats. (These sensors are rated to protect against overload at 1000% of maximal calibrated load, which provides a very large margin of safety.) We then engineered the support system around it and the restraining box, with a base plate, force platforms for the feet of the animal, and the restraining box on top. Fully dimensioned scaled technical drawings (Figure 3.4) for all components were auto-drafted using CATIA (Computer Aided Three-dimensional Interactive Application) V5R19. Machining of the base plate, force platforms, and restraining box was performed by Usinage FB (Le Gardeur, QC). The apparatus was assembled in our laboratory (Figure 3.5) following the technical drawings.

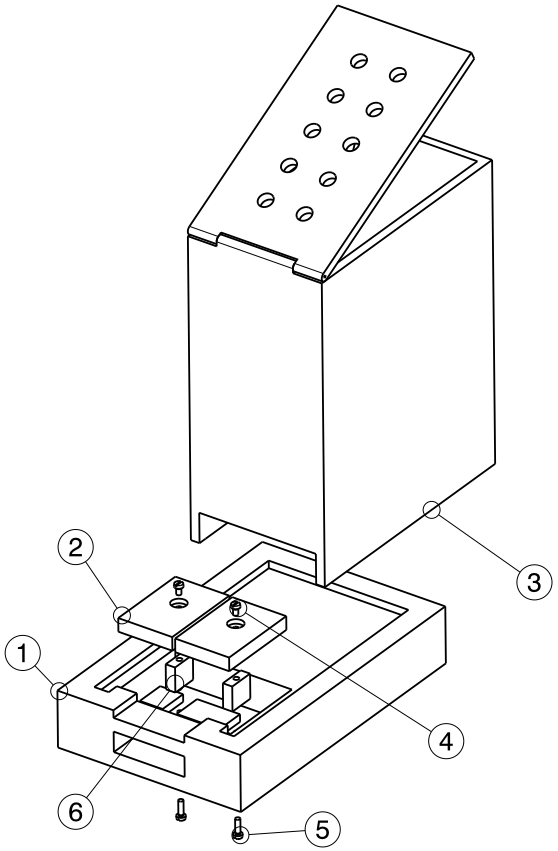

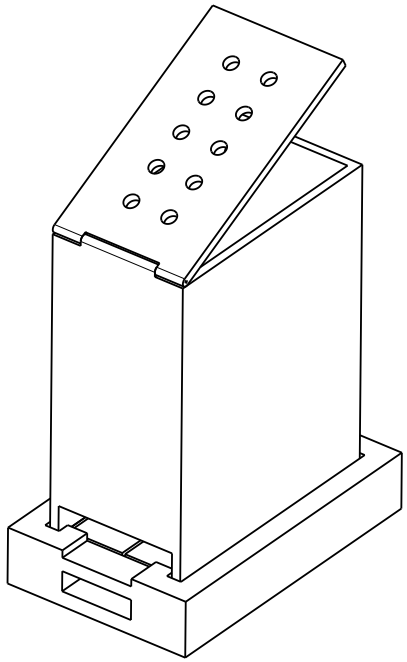

No.	No. Dessin	Nom du composant	Quantité
6	NON USINÉ	Cellules de charge (FUTEK MODEL LSB200 - 250g)	2
5	STANDARD	Spaenaur 382-079 : M3 x 10 mm	2
4	STANDARD	Spaenaur 382-078 : M3 x 6 mm	2
3	LBMO-003	Boîte de contention	1
2	LBMO-002	Plaque support	2
1	LBMO-001	Plateforme support	1

Centre de recherche (STE JUSTINE)

LABORATOIRE DE BIOLOGIE MOLÉCULAIRE ORTHOPÉDIQUE

...	...	...	...	...
...	...	...	...	...
No. Révision	Description	Révisé	Approuvé	Date

RÉVISIONS

NOTE

TITRE
Assemblage - Appareil d'incapacitance statique

No. DESSIN	MATÉRIAU	DIMENSIONS
LBMO-000	---	---

CONTACT
Gabriel KAUFMAN

DESSINATEUR	DATE
Barthélémy VALTEAU	23/07/09

APPROUVÉ	ÉCHELLE
F. MOLDOVAN	---

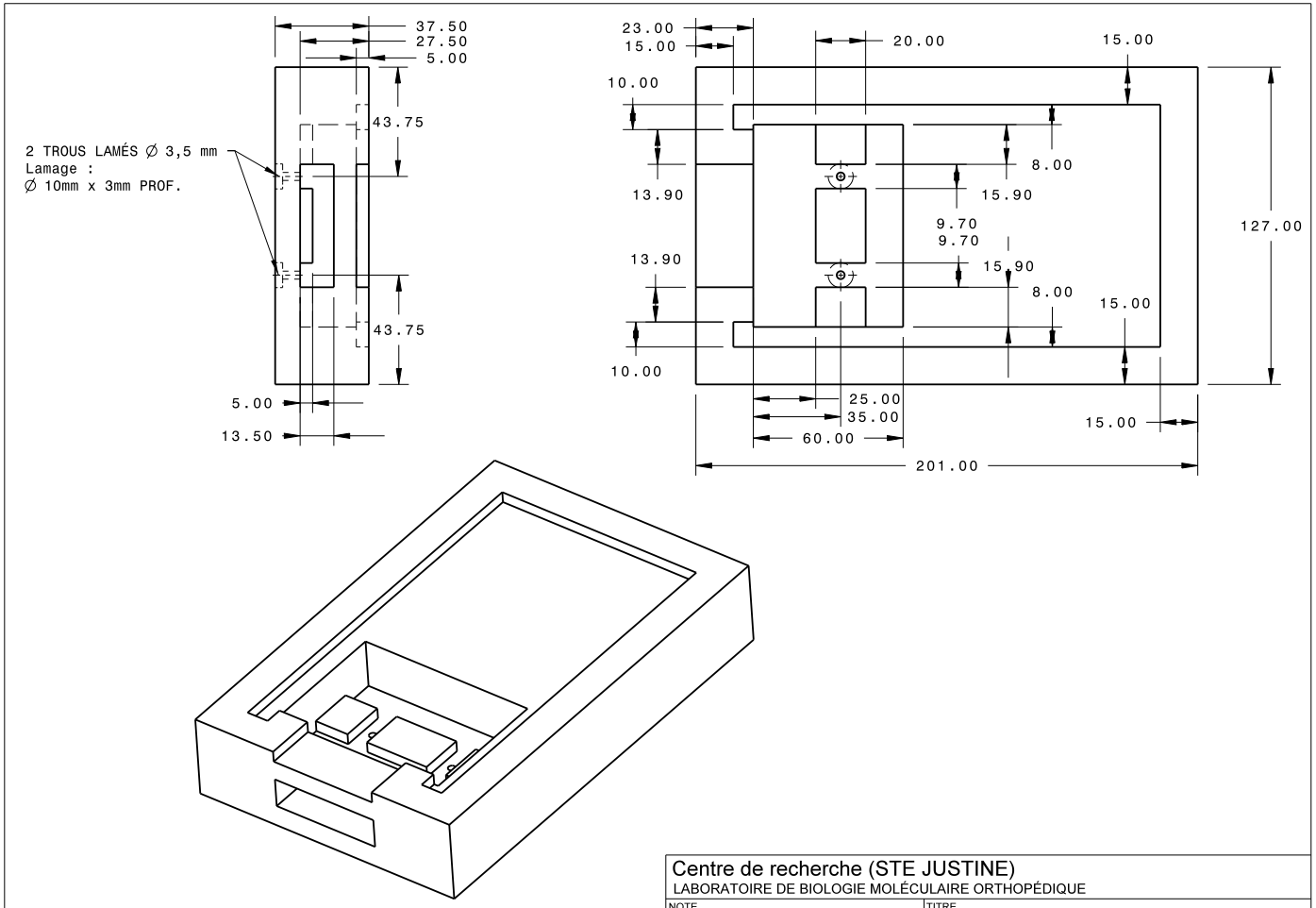

...	...	...	...	...
...	...	...	...	...
No. Révision	Description	Révisé	Approuvé	Date

RÉVISIONS

Centre de recherche (STE JUSTINE)

LABORATOIRE DE BIOLOGIE MOLÉCULAIRE ORTHOPÉDIQUE

NOTE ...	TITRE Plateforme support		
	No. DESSIN LBMO-001	MATÉRIAU UHMWPE Noir	DIMENSIONS mm
CONTACT Gabriel KAUFMAN	DESSINATEUR Barthélémy VALTEAU	DATE 23/07/09	TOLÉRANCES GÉNÉRALES X.XX ± 0.07mm Angle ± 0.5°
	APPROUVÉ F. MOLDOVAN	ÉCHELLE 1:2	

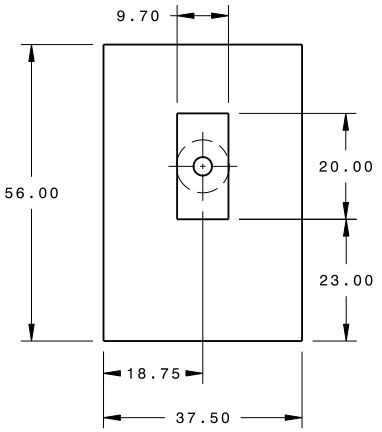

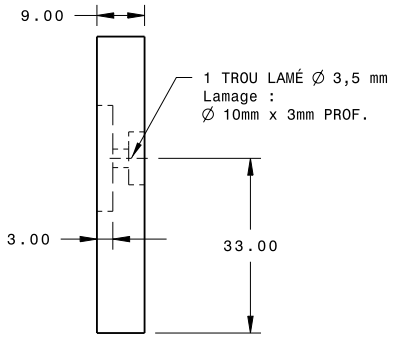

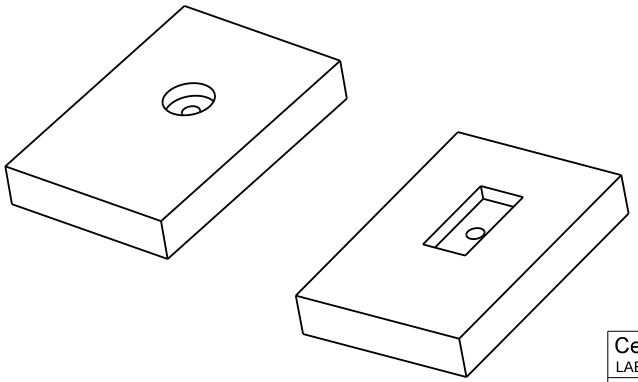

...	...	...	...	...
...	...	...	...	...
No. Révision	Description	Révisé	Approuvé	Date

RÉVISIONS

Centre de recherche (STE JUSTINE)

LABORATOIRE DE BIOLOGIE MOLÉCULAIRE ORTHOPÉDIQUE

NOTE
...

CONTACT
Gabriel KAUFMAN

TITRE
Plaque support

No. DESSIN	MATÉRIAU	DIMENSIONS
LBMO-002	UHMWPE Noir	mm

DESSINATEUR	DATE	TOLÉRANCES GÉNÉRALES
Barthélémy VALTEAU	23/07/09	X.XX ± 0.07mm Angle ± 0.5°

APPROUVÉ	ÉCHELLE
F. MOLDOVAN	1:1

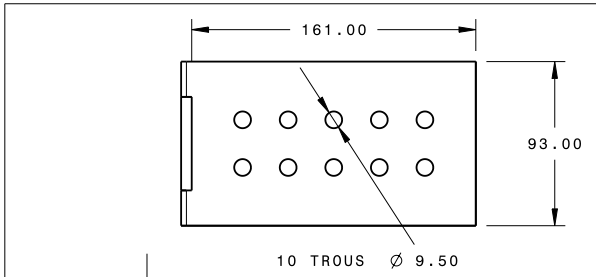

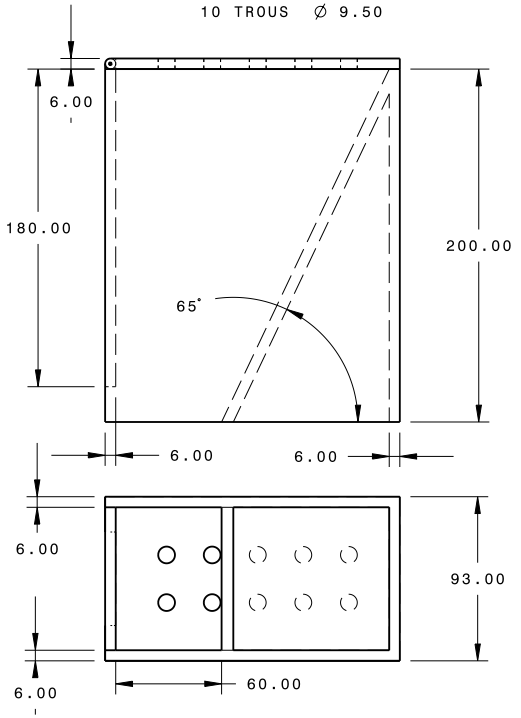

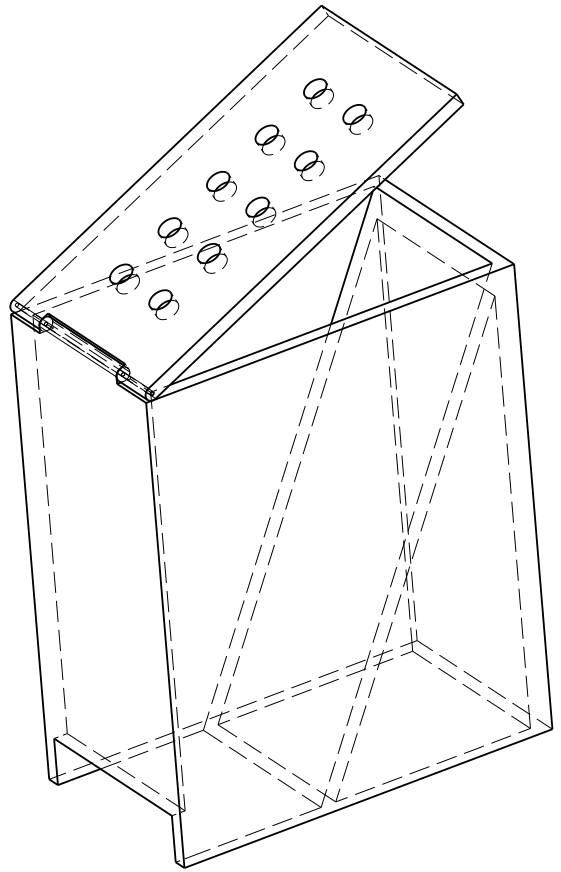

No. Révision	Description	Révisé	Approuvé	Date
...	...	...	...	...
...	...	...	...	...

RÉVISIONS

Centre de recherche (STE JUSTINE)

LABORATOIRE DE BIOLOGIE MOLÉCULAIRE ORTHOPÉDIQUE

NOTE ---	TITRE Boîte de contention		
	No. DESSIN LBMO-003	MATÉRIAU Plexiglass	DIMENSIONS mm
CONTACT Gabriel KAUFMAN	DESSINATEUR Barthélémy VALTEAU	DATE 23/07/09	TOLÉRANCES GÉNÉRALES X.XX ± 1mm Angle ± 0.5°
	APPROUVÉ F. MOLDOVAN	ÉCHELLE 1:3	

3.3.2 Software setup

Futek USB software (version 1.1.0.0) was used to set test parameters for the *in vivo* pain measurement (subsection 3.3.3) as follows: 4 samples recorded per second, read-out unit in grams, precision at 3 decimal places, test duration of 30 seconds (Figure 3.6). Test results were automatically saved into comma-separated variable files.

3.3.3 *In vivo* pain measurement

Over the course of the study, knee joint pain was evaluated biweekly by the static weight bearing test [31, 32], which evaluates the hind limb weight distribution: shifts from the operated limb towards the contralateral limb (a weight-bearing deficit) are taken as a pain measure [213]. After conditioning, animals were introduced to the apparatus and restrained in a plexiglass chamber with an angled base, such that each hind paw rested on a separate force plate connected to a load cell (Figure 3.7). The weight in grams distributed on each hind limb was recorded by a computer software interface as described above in subsection 3.3.2. Data were transferred off-line to a personal computer, and the weight bearing on the right hind limb as a percentage of total weight bearing on both hind limbs was calculated by the following equation [167]:

$$\% \text{ weight on right leg} = \frac{\text{weight on right leg}}{\text{weight on right leg} + \text{weight on left leg}} \times 100$$

Figure 3.5: Static weight bearing apparatus assembly. (A) assembled base plate; (B) force platform underside; (C) rat restraining box (angle view); (D) load cell placement inside force platform; (E) force platform installation; (F) complete apparatus assembled.

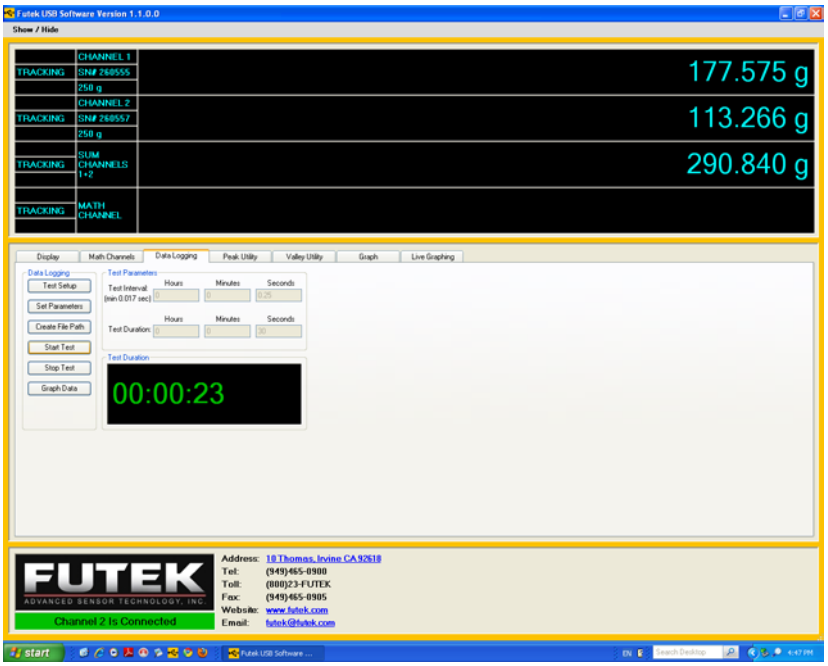

Figure 3.6: Futek USB software (version 1.1.0.0) screenshot. Parameters were set as described in subsection 3.3.2. Test depicted is from an ACLT animal: a significant difference can be seen between the applied weight on the left and right channels.

Measurements were averaged over three 30-second test periods. All values are given as mean ± s.e.m.

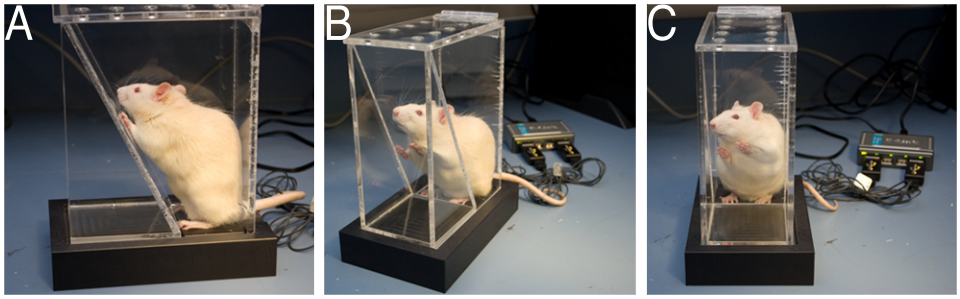

Figure 3.7: Static weight bearing apparatus with rat positioned for measurements. A, side view; B, angle view; C, front view.

3.3.4 Statistics

Static weight bearing data were analyzed by repeated measures analysis of variance (ANOVA), which compares the global differences between groups of response profiles measured on the same subjects repeatedly during the study [126, 218]. Test values were taken as the dependent variable and treatment group as the independent variable, with the animal as the grouping factor. Sphericity was confirmed with Mauchly's W test. Tukey multiple comparisons testing was used to establish significance in between groups, with directionality taken from the sign of the mean difference. P-values less than 0.05 were considered statistically significant. Analyses were conducted using R (version 2.11.0) [171].

3.4 Euthanasia and sample preparation

At four or eight weeks post-surgery, animals were sacrificed by cardiac puncture under deep isoflurane anaesthesia. The right knee was dissected and 40-mm-long samples were cut using a Stryker 810 oscillating bone saw. Rat knees were stored in phosphate-buffered saline until scanned by digital micro-X-ray (DX) and/or micro-magnetic resonance (MR) imaging. Samples were dissected the same day as the radiological scans.

3.5 Digital micro-X-ray

3.5.1 Image acquisition

All knee samples were X-rayed using a Faxitron MX-20 specimen X-ray system (Faxitron X-Ray Corporation, Lincolnshire, IL). Anteroposterior and lateral views were acquired at 5× magnification (10 × 10 μm pixel size) using a dose of 26 kV for 6 seconds (Figure 3.8). Images were acquired in DICOM format [56].

Figure 3.8: DX software screenshot (Faxitron SR v1.4.3).

3.5.2 Image analysis and scoring

After acquisition, images were transferred off-line to a Macintosh computer, and analyzed using OsiriX software (version 3.7.1) [184]. Radiological evidence of joint degradation was scored by two blinded examiners using an OA radiological score modified from Clark *et al.* [45] and Esser *et al.* [62]. Bone demineralization,

subchondral bone erosion, and heterotopic ossification were all scored on a scale from 0 (normal) to 3 (marked degenerative changes), using the criteria presented below in Table 3.II. Total scores were calculated by summing the individual scores for each index, with a maximum possible score of 9. Radiological scores were statistically analyzed by one-way analysis of variance, with total scores taken as the dependent variable and treatment group as the independent variable. Pairwise post-hoc testing with Holm correction was used to establish significance in between treatment groups. P-values less than 0.05 were considered statistically significant. Analyses were conducted using R (version 2.11.0) [171].

Table 3.II: Rubric for radiological scoring of OA joint degradation on DX views. Modified from Clark *et al.* [45] and Esser *et al.* [62].

Index	Score	Criteria
Bone demineralization		
	0	Normal bone mineralization
	1	Slight demineralization at joint margins
	2	Increasing bone loss
	3	Severe osteoporosis and loss of trabecular structure
Subchondral bone erosion		
	0	Normal appearance
	1	Small irregularities at joint margins
	2	Substantial subchondral bone remodelling
	3	Multiple severe disruptions of subchondral surface
Heterotopic ossification		
	0	None
	1	Early marginal osteophytes
	2	Increasing sclerosis and bony proliferation
	3	Multiple severe osteophytes

3.6 Micro-magnetic resonance imaging

3.6.1 Image acquisition

A subset of animals were sacrificed four weeks post-operatively and their right knees were imaged by micro-MR. Imaging was performed using a Bruker PharmaScan (Ettlingen, Germany) 7 Tesla MR scanner at the McGill University Small Animal Imaging Lab (Montreal, QC). Knee samples were placed in a custom-made support inside a 15-mL centrifuge tube (Figure 3.9), which was then filled with the MR-inert buffer FC-770 (3M Fluorinert Electronic Liquid). Samples were

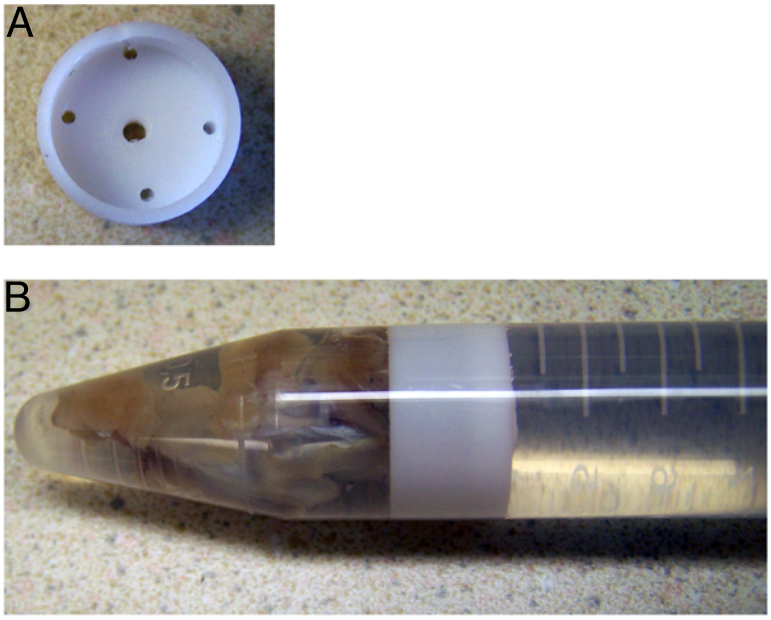

Figure 3.9: MR sample support. Teflon sample support plug (A). Dissected knee fixed in place with the sample support, inserted in tube, and filled with the MR-inert buffer FC-770 (B).

introduced into a ^{1}H mouse brain radio frequency (RF) coil (inner diameter 22 mm), and centred in the magnet. The RF coil was tuned and matched to the sample, and the magnet was then shimmed. The system was controlled via Bruker ParaVision software (version 5.0).

Positioning was confirmed with a tri-pilot rapid scan (Figure 3.10), which was then used to place 14 coronal slices (Figure 3.11) for two-dimensional anatomical scanning of the joint (Figure 3.12) using a rapid acquisition with relaxation enhancement (RARE) multiecho spin echo pulse sequence (TurboRARE). Scan parameters were as follows: repetition time (TR) = 3500 ms, echo time (TE) = 36 ms, echo train length (ETL) = 8, slice thickness = 500 μm, acquisition matrix = 384 $\times$ 384, and number of averages = 4. Voxel size was $104.1\overline{6} \times 104.1\overline{6} \times 500$ μm. These scans were then repeated in the sagittal projection (Figure 3.13).

Once these scans were acquired, one 1-mm-thick axial slice was placed in the centre of the knee joint (Figure 3.14) in order to scan the articular cartilage with a series of multislice multiecho (MSME) T_2-weighted pulse sequences. Scan parameters were TR = 3500 ms, ETL = 1, acquisition matrix = 192 $\times$ 256, with voxel size of 156.25 $\times$ 156.25 $\times$ 1000 μm. 16 different TE were used: 10, 20, 30, 40, 50, 60, 70, 80, 90, 100, 110, 120, 130, 140, 150, and 160 ms (Figure 3.15).

Total scan time was roughly 1 hour per sample. Scan sequences were based on previously published reports [43].

3.6.2 Image processing and analysis

After acquisition, images were converted to DICOM format [56], transferred off-line to a Macintosh computer, and analyzed using OsiriX software (version 3.7.1) [184]. Anatomical TurboRARE images were examined for correct depiction of anatomical features of the knee joint, and to confirm ACLT where applicable. As well, images were analyzed for signs of cartilage decay, indicated by lower

Figure 3.10: Tri-pilot scans. The sample was scanned in three planes (axial, sagittal, and coronal), and cross-hairs, representing the centre of the RF coil, were digitally superimposed in order to check sample positioning within the magnet. If adjustment was required, the distance was measured in the control software console and the sample was then physically moved to the correct position; the tri-pilot scan was then repeated. Scans depicted are from a negative control sample. Montage produced using NIH ImageJ (version 1.43t) [173].

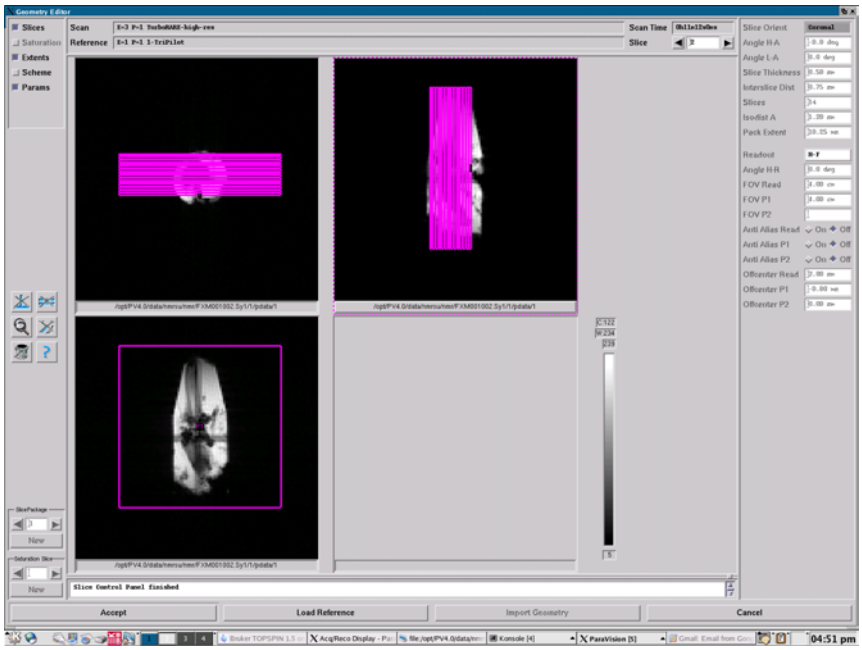

Figure 3.11: TurboRARE scan geometry. Geometry for the anatomical TurboRARE (rapid acquisition with relaxation enhancement multiecho spin echo pulse sequence) scans were specified using the tri-pilot scans as a reference frame. Fourteen 500-μm sliced were overlaid on the knee joint space, and were positioned to obtain complete coverage of the joint space. Screenshot from the MR control software (Bruker ParaVision 5.0).

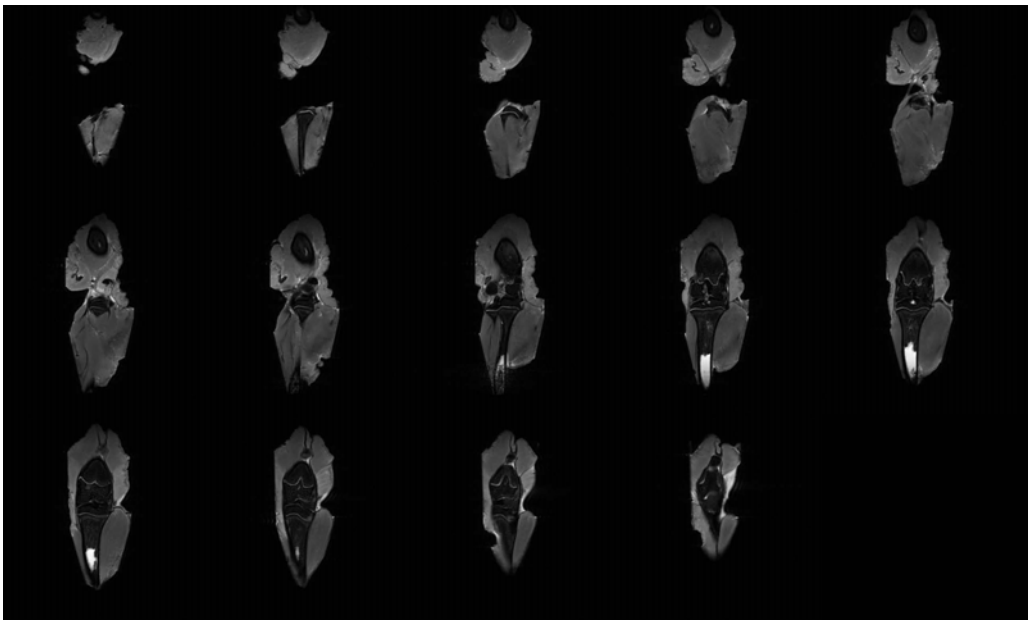

Figure 3.12: Image montage of the 14 slices obtained in the coronal projection. Images are displayed in anteroposterior order. Scans depicted are from a negative control sample. Montage produced using NIH ImageJ (version 1.43t) [173].

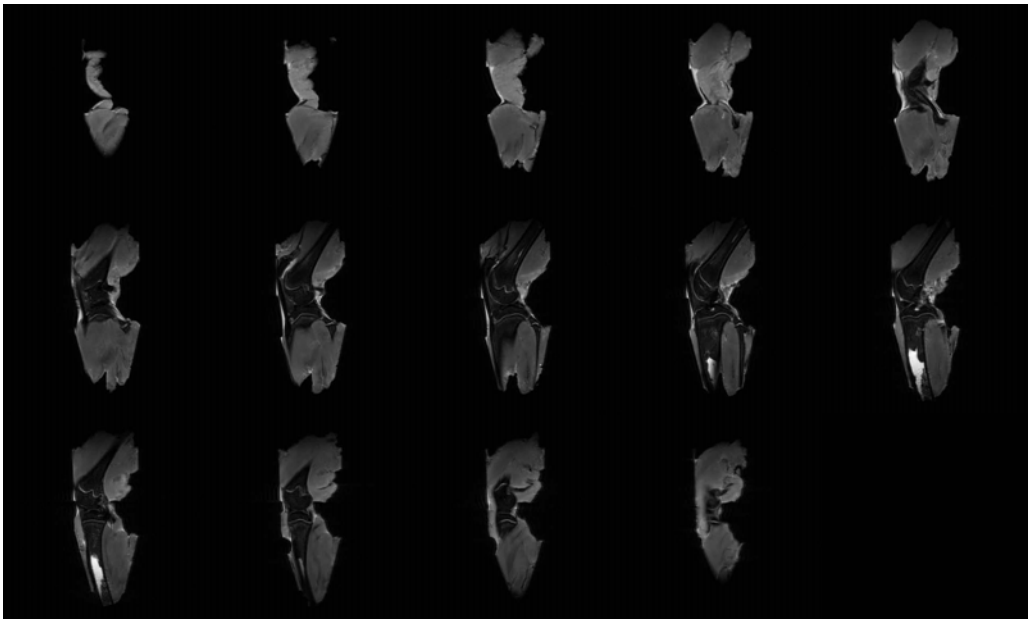

Figure 3.13: TurboRARE scans were repeated in the sagittal projection. Images are displayed in lateromedial order. Scans depicted are from a negative control sample. Montage produced using NIH ImageJ (version 1.43t) [173].

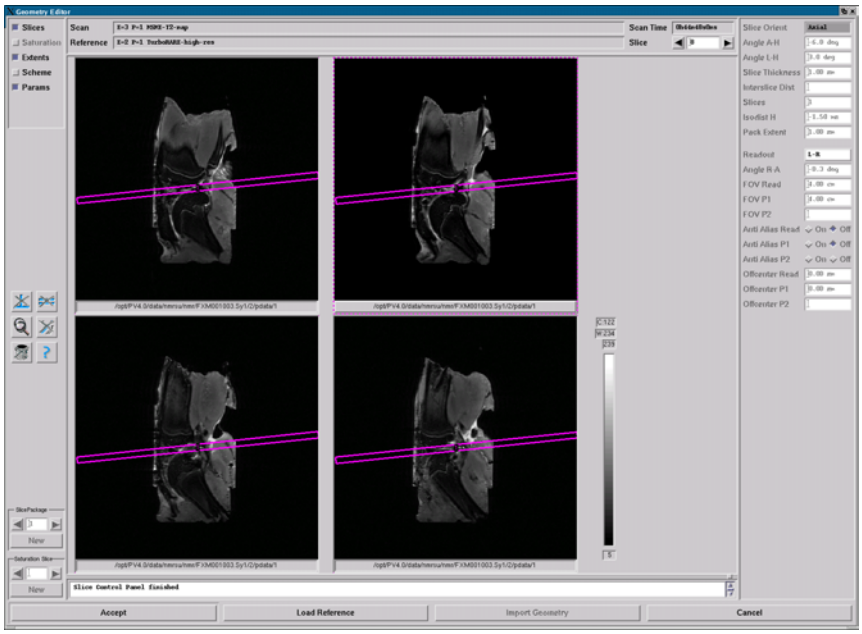

Figure 3.14: MSME-T_2 scan geometry. One 1-mm thick axial slice was placed in the centre of the knee joint using the sagittal TurboRARE scans as a reference frame. Slice placement and angle were adjusted in order to scan the maximum possible amount of articular cartilage. Sixteen multislice multiecho (MSME) T_2-weighted scans with varying echo time were then specified. Screenshot from the MR control software (Bruker ParaVision 5.0).

signal intensity of the articular surfaces. The MSME-T_2 images were aligned into an image stack, and regions of interest (ROI), corresponding to the articular cartilage, were manually drawn and propagated throughout the stack (Figure 3.16A). A mean T_2 fit map was then automatically generated by fitting the signal intensity to the spin-spin relaxation signal decay equation

$$S(TE) = M_0 \exp -\left(\frac{TE}{T_2}\right)$$

where signal intensity S is defined as a function of echo time TE, and is related to the spin density M_0 and the transverse relaxation time T_2. The equation was solved for the mean T_2 value over the 16-image stack by using least-squares single-

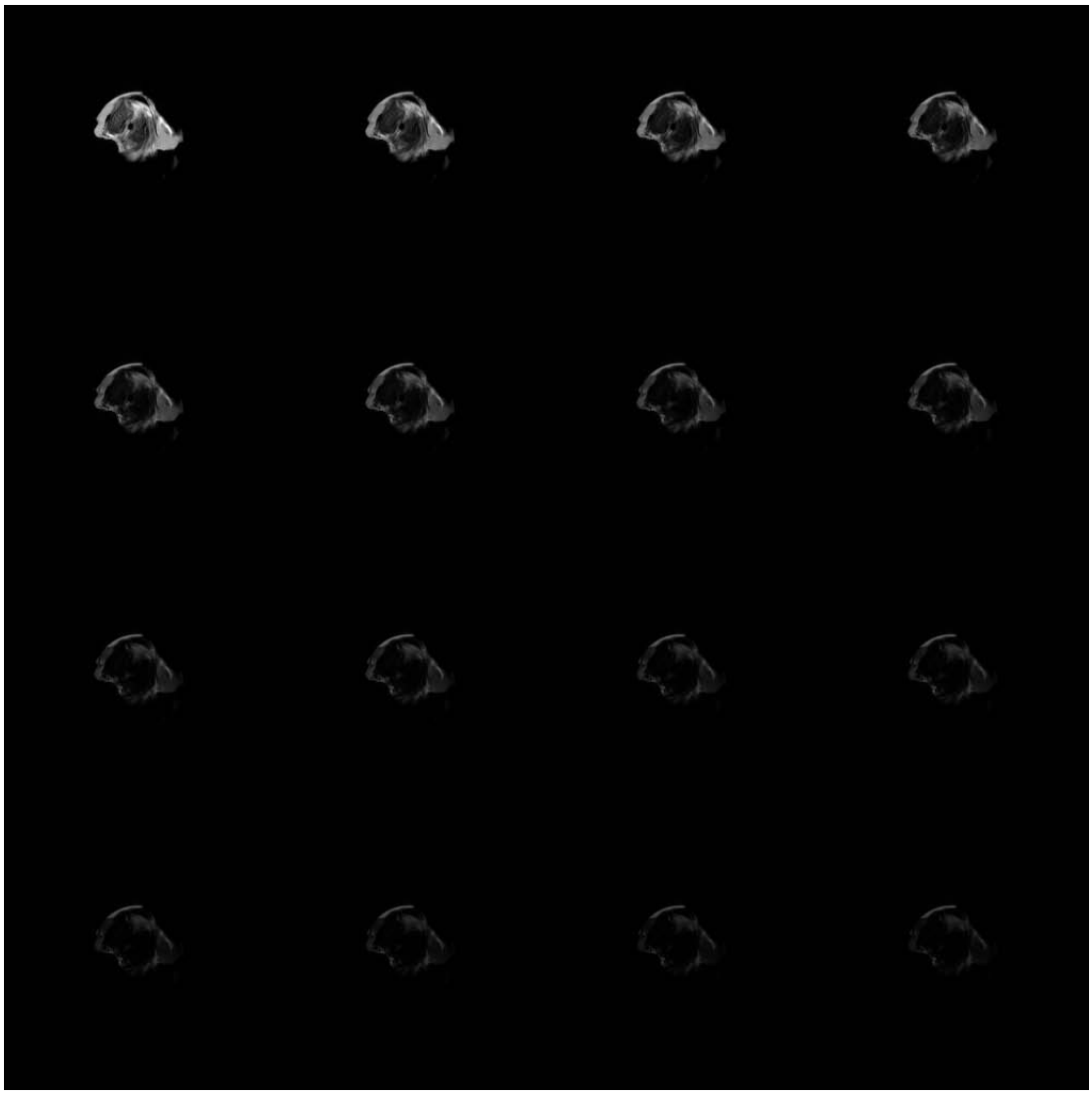

Figure 3.15: Image montage of the 16 different MSME-T_2 scans with TE (echo time) ranging from 10-160 ms. Images are displayed in order of increasing echo time. Scans depicted are from a negative control sample. Montage produced using NIH ImageJ (version 1.43t) [173].

exponential curve-fitting, with initial guesses of M_0 = signal intensity at 10 ms and T_2 = 30 ms, in order to guarantee rapid convergence [43]. OsiriX then generated a T_2 fit map graph with regression line and values for T_2 and M_0 (Figure 3.16B).

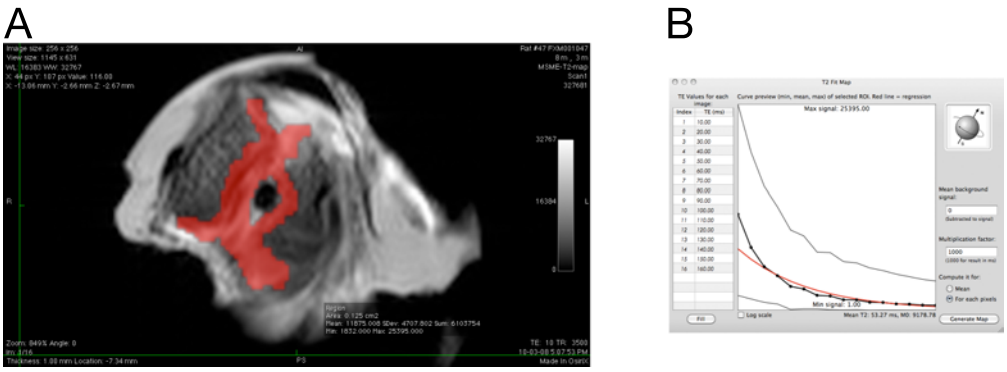

Figure 3.16: T_2 mapping. Using OsiriX, a ROI was drawn on the axial slice (A), propagated through the image stack, and signal intensity was calculated. This was then fit to the spin-spin relaxation signal decay equation and solved to yield a mean T_2 value (B). Data depicted is from a negative control sample.

3.7 Cartilage and bone histomorphology

3.7.1 Decalcified tissue

After radiological examination, half the knee samples were fixed in 10% neutral buffered formalin for two weeks and then decalcified with RDO Rapid Decalcifier (Apex Engineering Products, Aurora, Illinois) for three days (3 changes, 24 hours each). Decalcification was confirmed by the absence of radio-opaque bone signal on DX (Figure 3.17). Samples were then circulated (70% ethanol, 95% ethanol, 3 baths of 100% ethanol, 3 baths of xylene, and 3 baths of paraffin, 35 hours total) using a Leica TP 1020 automatic tissue processor (Nußloch, Germany) and embedded in paraffin. Five-micron sagittal sections were acquired from the middle of the knee joint using a Leica RM 2145 rotary microtome (Nußloch, Germany).

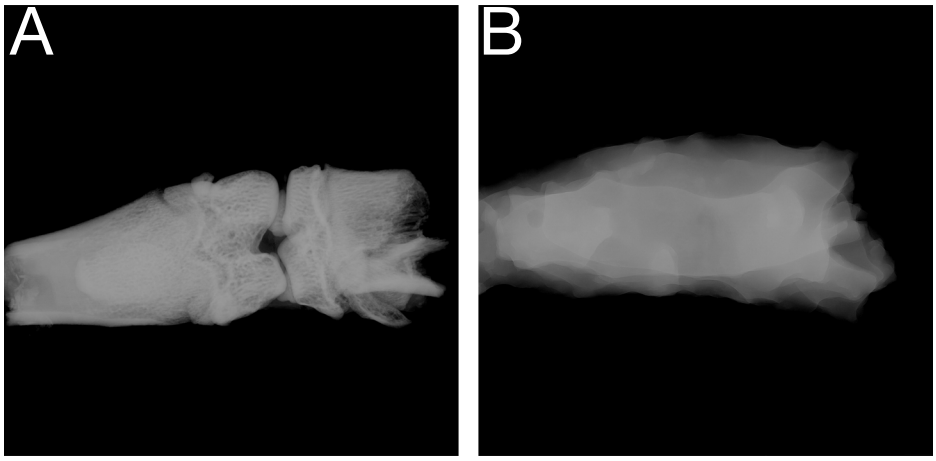

Figure 3.17: Decalcification confirmation. Decalcification was verified by DX; images were acquired as above in section 3.5. A, pre-decalcification; B, post-decalcification (anteroposterior views). Images are from a negative control sample. There is no radio-opaque signal from bone in B, indicating complete decalcification.

Histomorphological staining was performed using standard protocols [182]: slides were deparrafinized in xylene (2 baths), rehydrated in decreasing concentrations of ethanol (two baths of 100%, 90%, 70%, 50%), brought to water, stained with Fast Green FCF for 2 minutes (which colours collagens green) and Safranin O for 5 minutes (which colours proteoglycans red), counterstained with hematoxylin for 4 minutes, dehydrated with increasing concentrations of ethanol (70%, 90%, 2 baths of 100%), cleared in xylene (2 baths), and mounted in Permount. Representative digital photomicrographs were acquired with a Leica DM R microscope (Wetzlar, Germany) fitted with a QImaging Retiga 1300 B camera (Surrey, BC), controlled by QCapture software (version 2.95.0). All images were captured at 50× magnification and subsequently colour-matched and balanced using Adobe Photoshop CS3.

3.7.2 Undecalcified tissue

After radiological examination, half the knee samples were fixed in 10% neutral buffered formalin for two weeks and subsequently processed for undecalcified hard-tissue histology. Samples were hand-circulated in increasing concentrations of ethanol (70%, 90%, 2 changes of 100%, 24 hours each), cleared in xylene (3 changes over the course of 8 hours), and infiltrated with progressively increasing concentrations of benzoyl peroxide in methyl methacrylate (MMA) solution (0%, 1%, 2 changes of 4.5%, 48 hours each). Samples were exposed to vacuum for 2 hours at room temperature, in approximately 30 mL of MMA-4.5% benzoyl peroxide per sample, to aid polymerization. Subsequently, samples were stored in the dark at room temperature for two weeks, until polymerization was complete. This was done in order to have sample blocks that could be used for hard-tissue histology–sectioned using a sledge microtome–but we ultimately did not pursue this assay due to time constraints and (ultimately) successful histomorphological staining of paraffin sections, as described above in subsection 3.7.1. The blocks remain in the lab for future use.

3.7.3 Histopathological scoring

Four slides from each condition were scored by two blinded examiners using the Osteoarthritis Research Society International (OARSI) histopathology assessment system [168], which assigns numeric values to grade, or depth progression into cartilage (0-6), and stage, or extent of joint involvement (0-4); multiplying grade and stage yields a total OA score with a maximum value of 24. Slides were

examined at 25× magnification and the two indices of joint pathology were rated using the criteria presented below (Tables 3.III and 3.IV). Scores were averaged in between the two examiners; inter-examiner variation was within ±5%.

Table 3.III: Grade, or depth progression into cartilage, OARSI histopathology assessment system. Adapted from Prizker *et al.* [168].

Grade (key feature)	Associated criteria (tissue reaction)
Grade 0: cartilage morphology intact	Matrix: normal architecture Cells: intact, appropriate orientation
Grade 1: surface intact	Matrix: superficial zone intact, oedema and/or superficial fibrillation (abrasion), focal superficial matrix condensation Cells: death, proliferation (clusters), superficial zone hypertrophy Reaction must be more than superficial fibrillation only
Grade 2: surface discontinuity	As above Matrix discontinuity at superficial zone (deep fibrillation) ± Matrix depletion, as detected by loss of Safranin O staining, in upper 1/3 of cartilage ± Focal perichondronal increased stain (mid zone) ± Disorientation of chondron columns Cells: death, proliferation (clusters), hypertrophy
Grade 3: vertical fissures (clefts)	As above Matrix vertical fissures into mid zone, branched fissures ± Loss of Safranin O staining into lower 2/3 of cartilage (deep zone) Cells: death, regeneration (clusters), hypertrophy, cartilage domains adjacent to fissures
Grade 4: erosion	Cartilage matrix loss: delamination of superficial layer, mid layer cyst formation Excavation: matrix loss in superficial layer and mid zone
Grade 5: denudation	Surface: sclerotic bone or reparative tissue including fibrocartilage within denuded surface Microfracture with repair limited to bone surface
Grade 6: deformation	Bone remodelling (more than osteophyte formation only) Includes: microfracture with fibrocartilaginous and osseous repair extending above the previous surface

Table 3.IV: Stage, or extent of joint involvement, OARSI histopathology assessment system. Adapted from Prizker *et al*. [168].

Stage	% Involvement (surface, area, volume)
Stage 0	No OA activity seen
Stage 1	$< 10\%$
Stage 2	$10 - 25\%$
Stage 3	$25 - 50\%$
Stage 4	$> 50\%$

CHAPTER 4

ARTICLE MANUSCRIPT: DUAL ANTAGONISM OF ENDOTHELIN TYPE A AND BRADYKININ B1 RECEPTORS IMPROVES PAIN TOLERANCE AND PROTECTS JOINT MORPHOLOGY IN A SURGICAL MODEL OF OSTEOARTHRITIS

Gabriel N Kaufman[1], Charlotte Zaouter[1], Barthélémy Valteau[2], Pierre Sirois[3] and Florina Moldovan[1,4]

(1) Orthopaedic Molecular Biology Laboratory, Sainte-Justine Hospital Research Centre, 3175 Côte Sainte-Catherine, Montreal, Quebec, Canada H3T 1C5

(2) Paediatric Mechanobiology Laboratory, Sainte-Justine Hospital Research Centre, 3175 Côte Sainte-Catherine, Montreal, Quebec, Canada H3T 1C5

(3) IPS Thérapeutique, 3201 Jean-Mignault, Sherbrooke, Quebec, Canada J1E 4K8

(4) Faculty of Dentistry, Université de Montréal, PO Box 6128 Stn CV, Montreal, Quebec, Canada H3C 3J7

4.1 Abstract

Introduction: Endothelin-1, the vasocontrictor peptide, influences cartilage metabolism mainly via endothelin receptor type A (ETA). Along with the inflammatory nonapeptide vasodilator bradykinin (BK), which acts via bradykinin receptor

B1 (BKB1) in chronic inflammatory conditions, these vasoactive factors potentiate joint pain and inflammation. We describe a preclinical study of the efficacy of treatment of surgically induced osteoarthritis with ETA and/or BKB1 specific peptide antagonists. We hypothesize that antagonism of both receptors will diminish osteoarthritis progress and articular pain in a synergistic manner.

Methods: Osteoarthritis was surgically induced in rats by transection of the right anterior cruciate ligament. Animals were subsequently treated with weekly intra-articular injections of specific peptide antagonists of ETA and/or BKB1. Hind limb pain was measured by static weight bearing for two months post-operatively. Post-mortem, right knee joints were analyzed radiologically by X-ray and magnetic resonance, and histologically by the OARSI histopathology assessment system.

Results: Single and dual local antagonist treatment diminished overall limb pain, and accelerated post-operative recovery, after disease induction. Treatments also protected joint radiomorphology and histomorphology. Dual ETA/BKB1 antagonism was slightly more protective, as measured by radiology and histology.

Conclusions: ETA and BKB1 dual antagonism improves chronic pain and prevents joint cartilage degradation in a surgical model of osteoarthritis. Therefore, they represent a novel therapeutic strategy: specific receptor dual antagonism may prove beneficial in disease management.

4.2 Introduction

Osteoarthritis (OA) is characterized by a progressive destruction of articular cartilage accompanied by subchondral bone remodelling, osteophyte formation, and

synovial membrane inflammation [79]. Clinically, this disease progresses slowly and principally affects the hands and large weight-bearing joints. Pain is the primary complaint of patients with OA. Its aetiology is multifactorial: subchondral bone can have microfractures, osteophytes can cause stretching of periosteal nerve endings, ligaments may be stretched, the joint capsule can be inflamed or distended, the synovium may be inflamed, and muscles may spasm [137]. Furthermore, neo-innervation of joint tissue concurrent with angiogenesis [13, 28] may contribute to deep joint pain. Further understanding of the molecular mechanisms behind these effects should provide avenues towards targeted disease-modifying or -slowing treatments [3, 133].

We have previously shown that endothelin-1 (ET-1), a 21-amino-acid potent vasoconstrictor peptide, plays a major role in OA pathogenesis. It reduces cartilage anabolism by inhibiting collagen and proteoglycan synthesis [109]. It causes matrix metalloproteinases 1 and 13 to be synthesized and activated in OA cartilage [187]. ET-1 also causes excessive production of nitric oxide, which is generated as the result of an increase in inducible nitric oxide synthase levels [132]. These effects occur mainly via endothelin receptor type A (ETA) [110]: it is expressed in articular tissue by chondrocytes, synoviocytes, and endothelial cells, where it plays a significant role in cartilage and bone metabolism [124, 144]; ETA also potentiates inflammatory joint pain induced by ET-1 [52, 111].

ET-1 affects vascular homeostasis via the renin-angiotensin-aldosterone system [185]. Through cross-talk with the kallikrein-kinin system [196], it can also mediate kinin-induced pain and inflammation. Bradykinin (BK), the inflammatory

nonapeptide vasodilator, has also been implicated in OA pain and inflammation. It is generated in OA synovium, as in all inflamed tissue; it also is released due to the increased vascular pressure in subchondral bone [142]. BK ligates two receptors, bradykinin receptor B1 (BKB1) and bradykinin receptor B2 (BKB2). The effects of BK in OA occur largely via BKB1, a receptor implicated in articular nociception [189, 206] and pro-inflammatory reactions [23]. BKB1 also potentiates the effects of other pro-inflammatory mediators such as cytokines and prostaglandins. BKB2, though it has been implicated in nociceptor sensitization in OA [142, 206], may be less relevant as a therapeutic target in the context of a chronic inflammatory response. It is constitutively expressed to a large extent, and is primarily involved in the acute phase of inflammation [85, 149]. In contrast, BKB1 is up-regulated in chronic inflammatory conditions, its expression often induced secondary to inflammatory mediator release [34, 35, 85].

Antagonism of ETA and/or BKB1 may represent a novel therapeutic option to alleviate, and perhaps prevent or reverse, the pain, inflammation, and tissue damage that occur as OA progresses from an acute to a chronic state. We hypothesize that ETA and BKB1 antagonism will diminish OA progress in a synergistic manner. In the present work, we describe a preclinical study of the efficacy of treatment of surgically induced OA with ETA and/or BKB1 peptide antagonists, using an established rat model of the disease. We found that antagonist treatment diminished hind limb pain and protected joint radiomorphology and histomorphology. This demonstrates that ETA and BKB1 dual receptor expression is involved in OA pathogenesis, and that dual receptor antagonism may prove beneficial in OA

disease management.

4.3 Materials and methods

4.3.1 Rat model of osteoarthritis

4.3.1.1 Animals

Eight-week-old male Lewis rats were purchased from Charles River Canada (Saint-Constant, QC) and housed under standard conditions. All procedures were approved by the Sainte-Justine Hospital Research Centre animal ethics committee and conformed to Canadian Council on Animal Care guidelines [160].

4.3.1.2 Study design

The study was conducted as a fractional factorial experiment. Animals were randomly assigned to one of three surgery conditions: anterior cruciate ligament transection (ACLT), sham surgery, or no surgery (negative control). Subsequently, animals were assigned to one of four treatment groups, as detailed below (Table 4.I). Sample size was $n = 4$ per group.

Table 4.I: Experimental groups. Six experimental groups were designated in the fractional factorial study, with 4 subjects per group.

Group Number	Surgery	Treatment
1	None	Saline
2	Sham	Saline
3	ACLT	Saline
4	ACLT	BQ-123
5	ACLT	R-954
6	ACLT	BQ-123+R-954

4.3.1.3 Surgical technique

OA was induced by surgical transection of the right anterior cruciate ligament. The procedure was modified from previously published reports [9, 92, 202, 222]. Animals were anaesthetized with inhaled isoflurane (3% / L O_2 induction in chamber, 2% / L O_2 maintenance with face-mask), and prepared for surgery by clipping the hair over the ventral and medial aspects of the right leg from hindpaw to hip. The skin was disinfected with povidone-iodine, and a 3-cm incision was made medial to the patellar tendon (Figure 4.1A). The subcutaneous tissue and muscle were then incised and the patella laterally sublaxed; the joint capsule was opened with the limb hyperextended (Figure 4.1B). With the limb in full flexion, the anterior cruciate ligament was visualized by blunt dissection, and sectioned by a latero-medial cut parallel to the tibial plateau, using a #11 scalpel blade (Figure 4.1C). Transection was confirmed with the anterior drawer test (Figure 4.1D). The patella was then replaced, and the limb extended. The joint capsule and muscle layers were closed with 4-0 polygalactin absorbable suture (horizontal mattress stitch) (Figure 4.1E). 50 μL of lidocaine was then injected into the joint capsule to provide local analgesia. Skin was closed with steel surgical staples (Figure 4.1F). Post-operative hydration (6 mL/kg saline) and systemic analgesia (0.1 mg/kg buprenorphine HCl) were provided by subcutaneous injection. Surgical staples were removed 14 days post-operatively (Figure 4.1G). Sham surgery consisted of all of the above except ligament transection.

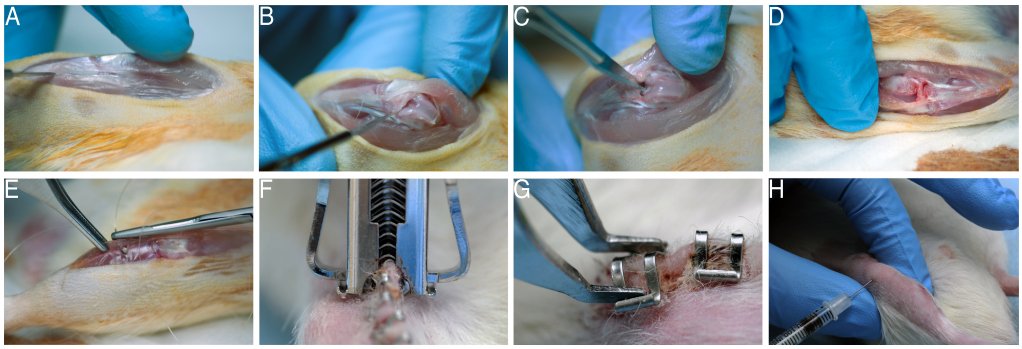

Figure 4.1: Rat anterior cruciate transection and intra-articular injection. Rat ACLT surgical steps (A-G) and intra-articular injection (H). Photos were taken with a 300-mm macro lens (approximate magnification 2×).

4.3.2 Drug treatment

Over the course of two months post-operatively, animals were treated by weekly intra-articular injections of ETA and/or BKB1 specific peptide antagonists: BQ-123 (ETA antagonist; Sigma-Aldrich, Oakville, ON) [98, 99], R-954 (BKB1 antagonist; kind gift from Pierre Sirois, IPS Thérapeutique, Sherbrooke, QC) [70, 156], both, or saline vehicle, was injected into the right knee at a dose of 30 nmol in a volume of 50 μL. Injections were performed under isoflurane anaesthesia, using a 28G needle (Figure 4.1H). Chemical structures are depicted in Additional File 4.11.1. Doses were based upon previously published reports [52, 206].

4.3.3 Static weight bearing

Over the course of the study, knee joint pain was evaluated biweekly by the static weight bearing test. A static weight bearing apparatus was reverse-engineered from previously published reports [31, 32, 213], designed, and machined by Usinage FB (Le Gardeur, Quebec). Technical drawings and photos are appended in

Additional Files 4.11.2 and 4.11.3.

After conditioning, animals were introduced to the apparatus and restrained in a plexiglass chamber with an angled base, such that each hind paw rested on a separate force plate connected to a load cell. The weight in grams distributed on each hind limb was recorded by a computer software interface (Futek USB software interface version 2.10). Data were transferred off-line to a personal computer, and the weight bearing on the right hind limb as a percentage of total weight bearing on both hind limbs was calculated by the following equation[167]:

$$\%\ \text{weight on right leg} = \frac{\text{weight on right leg}}{\text{weight on right leg} + \text{weight on left leg}} \times 100$$

Measurements were averaged over three 30-second test periods. All values are given as mean ± s.e.m.

4.3.3.1 Statistics

Static weight bearing data were analyzed by repeated measures analysis of variance (ANOVA) [126, 218]. Test values were taken as the dependent variable and treatment group as the independent variable, with the animal as the grouping factor. Sphericity was confirmed with Mauchly's W test. Tukey multiple comparisons testing was used to establish significance in between groups, with directionality taken from the sign of the mean difference. P-values less than 0.05 were considered statistically significant. Analyses were conducted using R (version 2.11.0) [171].

4.3.4 Euthanasia and sample preparation

At four or eight weeks post-surgery, animals were sacrificed by cardiac puncture under deep isoflurane anaesthesia. The right knee was dissected, and 40-mm-long samples were cut and stored in phosphate-buffered saline until scanned by digital micro-X-ray (DX) and/or micro-magnetic resonance (MR) imaging. Samples were dissected the same day as the radiological scans.

4.3.5 Digital micro-X-ray

All knee samples were X-rayed using a Faxitron MX-20 specimen X-ray system (Faxitron X-Ray Corporation, Lincolnshire, IL). Anteroposterior and lateral views were acquired at 5× magnification (10 × 10 μm pixel size) using a dose of 26 kV for 6 seconds. Images were analyzed using OsiriX software (version 3.7.1) [184]. Radiological evidence of joint degradation was scored by two blinded examiners using an an OA radiological score modified from Clark *et al.* [45] and Esser *et al.* [62]. Bone demineralization, subchondral bone erosion, and heterotopic ossification were all scored on a scale from 0 (normal) to 3 (marked degenerative changes). Total scores were calculated by summing the individual scores for each index, with a maximum possible score of 9.

OA radiological scores were statistically analyzed by one-way analysis of variance, with total scores taken as the dependent variable and treatment group as the independent variable. Pairwise post-hoc testing with Holm correction was used to establish significance in between treatment groups. P-values less than 0.05 were considered statistically significant. Analyses were conducted using R (version

2.11.0) [171].

4.3.6 Micro-magnetic resonance imaging

4.3.6.1 Image acquisition

A subset of animals were sacrificed four weeks post-operatively and their right knees were imaged by micro-MR. Imaging was performed using a Bruker PharmaScan (Ettlingen, Germany) 7 Tesla MR scanner at the McGill University Small Animal Imaging Lab (Montreal, QC). Knee samples were placed in a custom-made support inside a 15-mL centrifuge tube, which was then filled with the MR-inert buffer FC-770 (3M Fluorinert Electronic Liquid). Samples were introduced into a ^{1}H mouse brain radio frequency (RF) coil (inner diameter 22 mm), and centred in the magnet. The RF coil was tuned and matched to the sample, and the magnet was then shimmed. The system was controlled via Bruker ParaVision software (version 5.0).

Positioning was confirmed with a tri-pilot rapid scan, which was then used to place 14 coronal slices for two-dimensional anatomical scanning of the joint using a rapid acquisition with relaxation enhancement (RARE) multiecho spin echo pulse sequence (TurboRARE). Scan parameters were as follows: repetition time (TR) = 3500 ms, echo time (TE) = 36 ms, echo train length (ETL) = 8, slice thickness = 500 μm, acquisition matrix = 384 $\times$ 384, and number of averages = 4. Voxel size was $104.1\overline{6} \times 104.1\overline{6} \times 500$ μm. These scans were then repeated in the sagittal projection.

Once these scans were acquired, one 1-mm-thick axial slice was placed in the

centre of the knee joint in order to scan the articular cartilage with a series of multislice multiecho (MSME) T_2-weighted pulse sequences. Scan parameters were TR = 3500 ms, ETL = 1, acquisition matrix = 192 × 256, with voxel size of 156.25 × 156.25 × 1000 μm. 16 different TE were used: 10, 20, 30, 40, 50, 60, 70, 80, 90, 100, 110, 120, 130, 140, 150, and 160 ms.

Total scan time was roughly 1 hour per sample. Scan sequences were based on previously published reports [43].

4.3.6.2 Image processing and analysis

After acquisition, images were analyzed using OsiriX software (version 3.7.1) [184]. Anatomical TurboRARE images were examined for correct depiction of anatomical features of the knee joint, and to confirm ACLT where applicable. As well, images were analyzed for signs of cartilage decay, indicated by lower signal intensity of the articular surfaces. The MSME-T_2 images were aligned into an image stack, and regions of interest, corresponding to the articular cartilage, were manually drawn and propagated throughout the stack. A mean T_2 fit map was then automatically generated by fitting the signal intensity to the spin-spin relaxation signal decay equation

$$S(TE) = M_0 \exp -\left(\frac{TE}{T_2}\right)$$

where signal intensity S is defined as a function of echo time TE, and is related to the spin density M_0 and the transverse relaxation time T_2. The equation was solved for the mean T_2 value over the 16-image stack by using least-squares

single-exponential curve-fitting, with initial guesses of M_0 = signal intensity at 10 ms and T_2 = 30 ms, in order to guarantee rapid convergence [43]. OsiriX then generated a T_2 fit map graph with regression line and values for T_2 and M_0.

4.3.7 Cartilage and bone histomorphology

After radiological examination, knee samples were fixed in 10% neutral buffered formalin for two weeks, decalcified with RDO Rapid Decalcifier (Apex Engineering Products, Aurora, Illinois) for three days, circulated, and embedded in paraffin. Five-micron sagittal sections were acquired from the middle of the knee joint. Histomorphological staining was performed as previously described [182]: slides were deparrafinized, rehydrated, stained with Safranin O (which colours proteoglycans red) and Fast Green FCF (which colours collagens green), counterstained with hematoxylin, dehydrated, cleared, and mounted in Permount. Representative digital photomicrographs were acquired with a Leica DM R microscope (Wetzlar, Germany) fitted with a QImaging Retiga 1300 B camera (Surrey, BC), controlled by QCapture software (version 2.95.0). All images were captured at 50× magnification and subsequently colour-matched and balanced using Adobe Photoshop CS3.

4.3.7.1 Histopathological scoring

Four slides from each condition were scored by two blinded examiners using the Osteoarthritis Research Society International (OARSI) histopathology assessment system [168], which assigns numeric values to grade, or depth progression into

cartilage (0-6), and stage, or extent of joint involvement (0-4); multiplying grade and stage yields a total score with a maximum value of 24. Scores were averaged in between the two examiners; inter-examiner variation was within ±5%.

4.4 Results

4.4.1 Dual antagonism ameliorates OA pain tolerance

To determine the effects of ETA and/or BKB1 local antagonist treatment on nociception in a surgical OA model, the static weight bearing asymmetry of the animals was measured repeatedly over the course of the study (Figure 4.2). Pre-operative baseline values for all groups indicated hind limb weight bearing symmetry ($49.89 \pm 0.42\%$). Unoperated vehicle-treated animals showed no important changes in hind limb weight bearing from baseline pre-operative values over the course of the study, staying roughly within ±4% of even weight distribution. Sham-operated vehicle-treated animals displayed an initial weight bearing imbalance 14 days post-operatively ($36.47 \pm 1.12\%$), but recovered weight bearing symmetry quickly thereafter ($44.84 \pm 0.33\%$ by day 26 post-operatively). ACLT vehicle-treated animals showed significant weight bearing imbalance two weeks post-operatively, down to $33.66 \pm 2.05\%$ weight on the right leg, suggesting severe nociception. All animals had similar nociceptive tolerance at the last measured time-point (day 50 post-operatively), indicating nociceptive adaptation, but drug-treated animals were able to recover faster than saline-treated animals (up to $40.54 \pm 3.36\%$ weight on right leg by day 33 post-operatively).

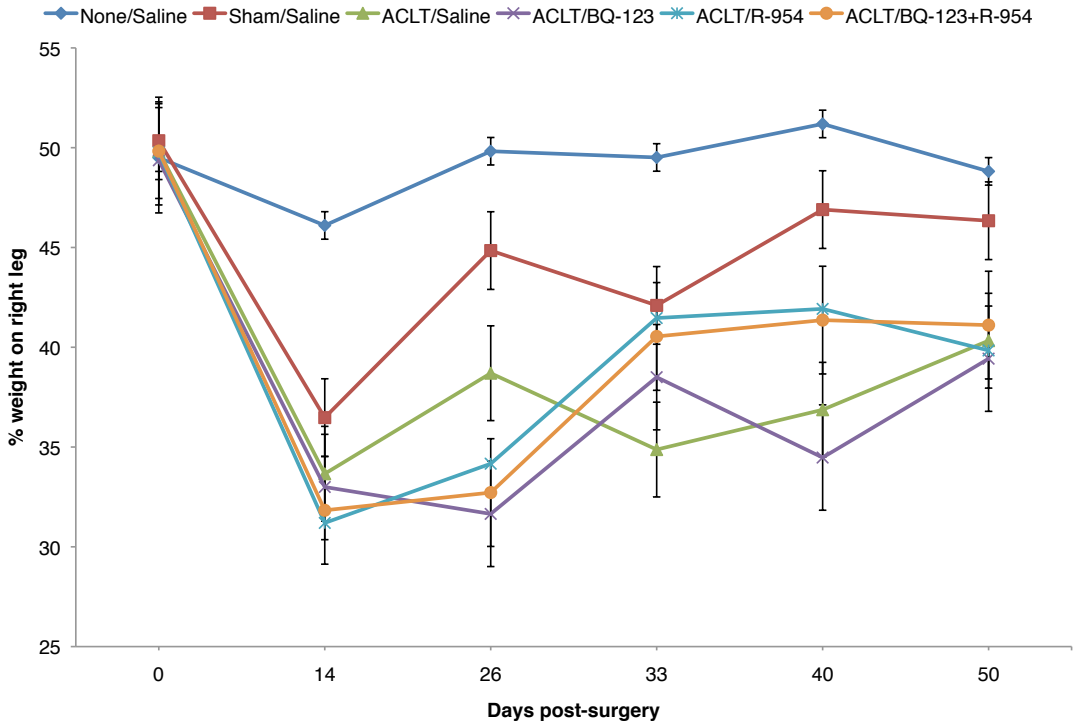

Figure 4.2: Antagonist treatment improves static weight bearing tolerance. Static weight bearing was measured repeatedly at defined time points over the course of the study. Data are presented as mean $\pm$ s.e.m, per experimental group ($n = 4$), of weight on the right leg as a percentage of total weight on both hind limbs. Day 0, baseline pre-operative values. Repeated measures ANOVA with Tukey post-hoc (Table 4.II) indicated that antagonist treatment significantly ameliorated pain tolerance in ACLT animals over the study period, as compared to saline-treated positive controls.

Repeated measures analysis of variance of the static weight bearing data, followed by Tukey post-hoc hypothesis tests (Table 4.II), demonstrated that treatment with BQ-123, R-954, or both, significantly ameliorated pain tolerance in ACLT animals over the study period, as compared to saline-treated positive controls ($0.00192 \leq P \leq 0.00713$). Sham surgery was found to be slightly less painful than ACL transection ($P = 0.03115$), confirming that ACLT is necessary for a maximal nociceptive response. Furthermore, nociception in the sham-operated animals was comparable to unoperated animals, with no statistically significant difference calculated ($P = 0.99313$).

Table 4.II: Tukey post-hoc tests were conducted following repeated measures ANOVA of the static weight bearing data using R (version 2.11.0) [171]. From left to right, the table columns present the contrast of interest, the parameter estimate from the linear matrix model, the standard error of that estimate, the standard *z*-score, and the associated *P*-value.

Contrast	Estimate	Standard Error	z score	$P(>\|z\|)$
None/Saline vs Sham/Saline	6.56489	1.84612	3.556	0.99313
Sham/Saline vs ACLT/Saline	5.78468	1.86531	3.101	0.03115
ACLT/BQ-123 vs ACLT/Saline	-1.23127	1.77364	-0.694	0.00713
ACLT/R-954 vs ACLT/Saline	1.00281	1.83227	0.547	0.00192
ACLT/BQ-123+R-954 vs ACLT/Saline	0.97373	1.74878	0.557	0.00211

4.4.2 Dual antagonist treatment improves radiological indices of OA

Right knee joints were dissected at the end of the study period and imaged by DX (Figure 4.3) and MR (Figure 4.4) to examine the radiological effects of antagonist treatments. ACLT rapidly induced radiological evidence of OA: knee

joints showed signs of degradation such as subchondral bone remodelling, osteophyte formation (Figure 4.3c and Table 4.III), cartilage layer thinning (Figure 4.4c), and lengthened cartilage T_2 (Table 4.IV). Neither sham surgery nor intra-articular injection affected joint radiomorphology (Figure 4.3a-b and Figure 4.4a-b). DX analysis of antagonist-treated knee joints showed less subchondral bone remodelling and heterotopic ossification than saline-treated animals (Figure 4.3d-f and Table 4.III). Dual ETA/BKB1 antagonism appeared to be slightly more protective than single antagonism: less subchondral bone remodelling and greater trabecular integrity was observed in the dual-antagonist-treated animals than in the single-antagonist-treated animals. Radiological scoring of the DX views for a panel of OA joint degenerative changes (Table 4.III) demonstrated that treatment with BQ-123, R-954, or both, significantly ameliorated radiological indices of disease progression in ACLT animals, as compared to saline-treated positive controls ($0.0020 \leq P \leq 0.0214$, one-way ANOVA with Holm post-hoc). MR analysis of knee joints revealed that antagonist-treated animals had greater cartilage thickness and fewer cartilage lesions (Figure 4.4d-f), as well as shorter cartilage T_2 (Table 4.IV, statistical significance not achieved) than saline-treated animals. These data suggest that antagonist treatment protected joint radiomorphology after ACLT.

4.4.3 Antagonism protects joint histomorphology

To investigate the effects of ETA and/or BKB1 antagonist treatment on histological indices of disease, rat knee joints were processed to assess cartilage proteogly-

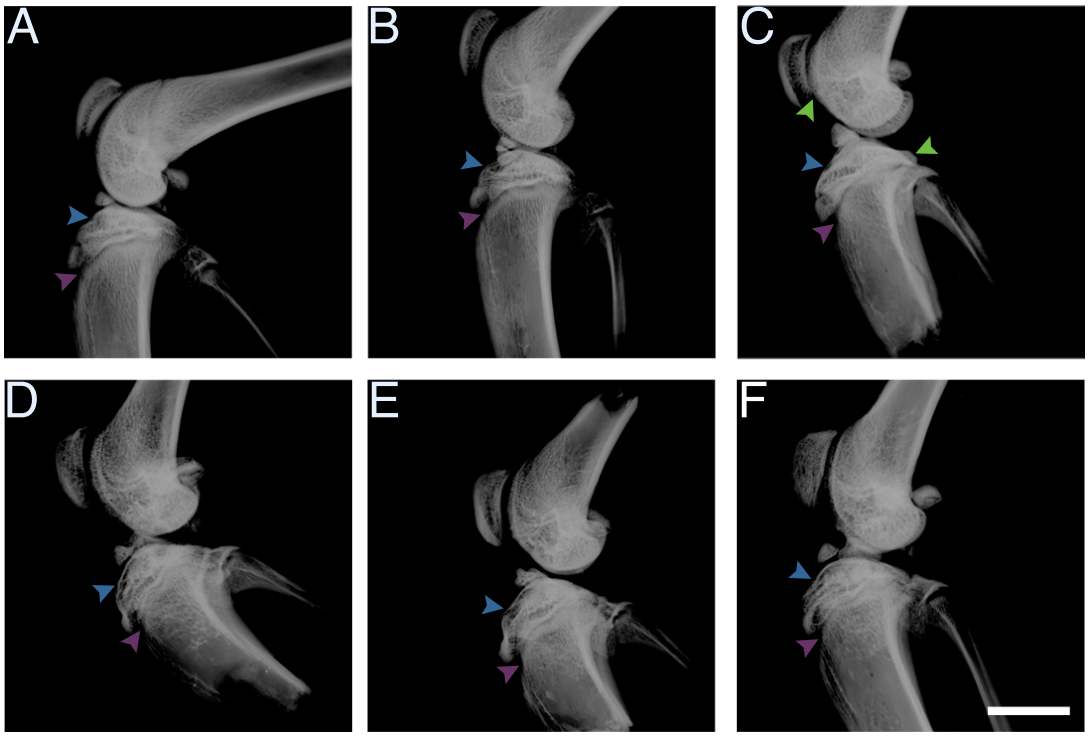

Figure 4.3: Dual antagonist treatment improves radiological indices of OA: X-ray results. A) no surgery and saline treatment; B) sham surgery and saline treatment; C) ACLT and saline treatment; D) ACLT and BQ-123 treatment; E) ACLT and R-954 treatment; F) ACLT and BQ-123+R-954 dual treatment. Blue arrows indicate tibial plateau, purple arrows indicate subchondral bone, and green arrows indicate osteophytes. Sagittal views. Scale bar, 1 cm.

Table 4.III: Radiological scoring of the DX views of the knee joints indicated that antagonist treatment protected joint radiomorphology after ACLT. One-way ANOVA with Holm post-hoc: †, $P = 0.0214$, ACLT/BQ-123 treatment versus ACLT/saline treatment; ‡, $P = 0.0020$, ACLT/R-954 treatment versus ACLT/saline treatment; §, $P = 0.0125$, ACLT/BQ-123+R-954 dual treatment versus ACLT/saline treatment.

Group Number	Surgery	Treatment	Mean total radiological score
1	None	Saline	0.25
2	Sham	Saline	1.16
3	ACLT	Saline	4.86
4	ACLT	BQ-123	2.83 †
5	ACLT	R-954	2.50 ‡
6	ACLT	BQ-123+R-954	2.67 §

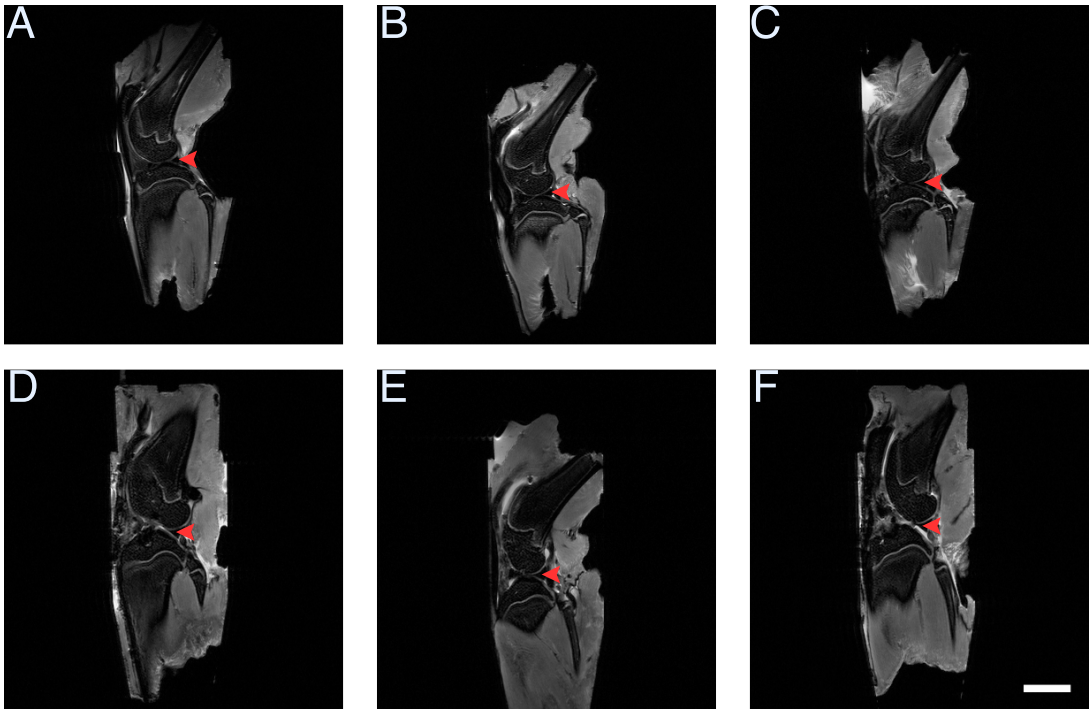

Figure 4.4: Dual antagonist treatment improves radiological indices of OA: MR results. A) no surgery and saline treatment; B) sham surgery and saline treatment; C) ACLT and saline treatment; D) ACLT and BQ-123 treatment; E) ACLT and R-954 treatment; F) ACLT and BQ-123+R-954 dual treatment. Red arrows indicate articular cartilage. Sagittal views. Scale bar, 1 cm.

Table 4.IV: Cartilage mean T_2 values in milliseconds were calculated for all conditions using OsiriX software (version 3.7.1) [184]. Statistical significance was not achieved.

Group Number	Surgery	Treatment	Mean T_2 value (ms)
1	None	Saline	51.60
2	Sham	Saline	52.12
3	ACLT	Saline	64.38
4	ACLT	BQ-123	63.23
5	ACLT	R-954	61.13
6	ACLT	BQ-123+R-954	56.57

can content and joint histomorphology (Figure 4.5). ACLT sham-treated animals lost most proteoglycan staining when examined at 8 weeks post-operatively, with severe articular surface disruptions and osteophyte formation (Figure 4.5c). In contrast, cartilage proteoglycans were detected in the knees of ETA and/or BKB1 antagonist-treated animals, indicating that treatment protects cartilage structural components. As well, articular surface integrity was preserved to a greater extent, with dual antagonism appearing to be most protective (Figure 4.5d-f). Neither sham surgery nor intra-articular injection affected joint histomorphology (Figure 4.5a-b). Mean OARSI scores (Table 4.V, statistical significance not achieved) indicate that antagonist treatment reduced the amount of affected joint tissue and the degree of histopathology.

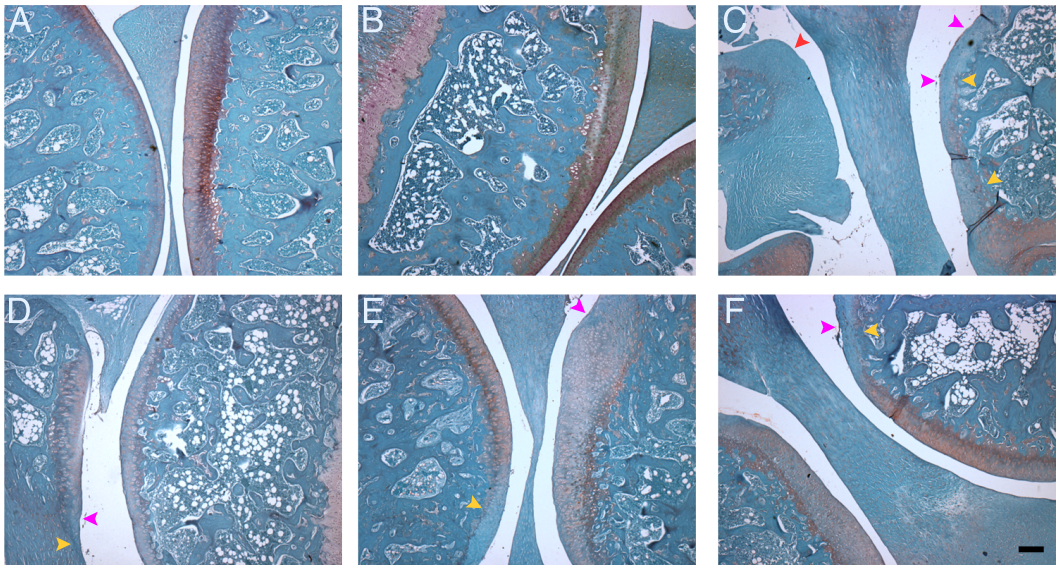

Figure 4.5: Antagonist treatment protects joint histomorphometry. A) no surgery and saline treatment; B) sham surgery and saline treatment; C) ACLT and saline treatment; D) ACLT and BQ-123 treatment; E) ACLT and R-954 treatment; F) ACLT and BQ-123+R-954 dual treatment. Yellow arrows indicate loss of Safranin O staining, purple arrows indicate cartilage notching, and red arrow indicates an osteophyte. Sagittal sections, Safranin O/Fast Green FCF staining. Scale bar, 200 μm. Original magnification 50×.

Table 4.V: OARSI histopathology scores. Four slides per condition were scored by two blinded examiners using the OARSI histopathology assessment system [168]. Results were averaged and are presented as mean scores per condition. Inter-examiner variation was within ±5%; statistical significance not achieved.

Group Number	Surgery	Treatment	OARSI score
1	None	Saline	0.43
2	Sham	Saline	0.00
3	ACLT	Saline	17.00
4	ACLT	BQ-123	10.25
5	ACLT	R-954	4.25
6	ACLT	BQ-123+R-954	3.50

4.5 Discussion

In the present study, we investigated whether antagonism of ETA and/or BKB1 could slow and/or prevent osteoarthritic cartilage degradation and joint pain in a rat surgical model of OA. We provide several lines of evidence that suggest protective effects of ETA and BKB1 dual antagonism *in vivo*: antagonist treatment improved hind limb pain tolerance, ameliorated radiological indices of disease, and protected cartilage biochemical integrity and articular cartilage and bone histomorphometry.

The most interesting finding of our study is that nociceptive tolerance was augmented in our model after ETA and/or BKB1 antagonist treatment, with faster post-operative recovery than vehicle-treated controls. These results are consistent with other reports where local treatment with ETA or BKB1 receptor antagonists reduced overt acute joint pain [52, 206]. We extend this finding to the dual antagonist treatment approach in a model of chronic pain, as well as relating it to measures of joint integrity by radiology and histology. Low-grade joint pain is the

most common reason for patient presentation, and is often the major debilitating factor in OA cases [60, 65]. Thus, the anti-nociceptive effects of ETA and/or BKB1 antagonism make this treatment strategy attractive.

We found that single and dual ETA/BKB1 antagonist treatments decreased radiological disease indices, in terms of osteophyte formation, cartilage thinning, and subchondral bone remodelling, with dual antagonism being most protective. As well, cartilage T_2, increased in ACLT animals, was decreased by antagonist treatment, which indicates a cartilage-preserving effect. Longer cartilage transverse relaxation times are an indicator of cartilage degradation; this MR parameter is indicative of cartilage composition and integrity [25, 27, 201]. Radiographic evidence is the main criterion for OA diagnosis and progression [1, 162]. The most common clinical diagnostic test is via X-ray of the affected joint: joint space narrowing as measured on X-ray is often used as a longitudinal marker of disease evolution. It is difficult to directly compare radiological parameters between human and rat knees due to the quadrupedal nature of the animal and the markedly different radiological anatomy that this entails [216]. However, we were able to detect radiological evidence of OA progression in ACLT animals, as has been described in similar studies [43, 217].

OA induction in rat knees led to a rapid decrease in cartilage proteoglycan staining, along with articular surface disruption and osteophyte formation [9, 92]. ETA/BKB1 antagonist treatment protected the proteoglycan content of the joint and preserved articular surface integrity. This allowed the joint cartilage to retain its normal biophysical properties, as cartilage proteoglycans are responsible,

along with collagen, for retaining water in the tissue, which provides spring and resilience [151, 186]. These findings likely suggest that the protection of cartilage proteoglycans and articular surface histomorphology may be one explanation for the increased pain tolerance observed in antagonist-treated animals; our results concur with those of other reports, which correlated the preservation of articular cartilage proteoglycan staining with pain tolerance behaviour [9].

The ET-1 and BK systems are involved in joint tissue inflammation and nociception, concomitant with pro-inflammatory mediators. However, exploration of potential therapeutic targets in these systems has been modest: the main classes of disease-modifying osteoarthritis drugs currently in development include cytokine and matrix metalloproteinase inhibitors, anti-resorptives, and growth factors [170]. To our knowledge, the only clinical trial of a drug targeting a vasoactive factor in OA is the bradykinin receptor B2 antagonist Icatibant, by Sanofi-Aventis [190]. This drug is no longer in clinical development [174], due to mixed results: while it provided local analgesia in knee OA, no anti-inflammatory effect could be detected [200]. Our results suggest that ETA and BKB1 represent novel therapeutic targets in OA. Specific receptor antagonists could be tested in clinical trials for OA pain and tissue damage.

4.6 Conclusions

Using a rat surgically induced model of OA, we demonstrated that local treatment with specific peptide antagonists of ETA and/or BKB1 may slow or stabilize the development of radiomorphological and histomorphological changes occurring

in OA pathogenesis. Furthermore, we showed that antagonist treatment accelerated recovery of, and improved longitudinally, pain tolerance in ACLT animals. Taken together, our results indicate that blocking ETA and BKB1 improves OA prognostic indices, which implies that defective signalling might play a role in chronic OA pain. Our results also raise the possibility of targeted dual receptor antagonism as a relevant therapeutic option. Further studies are required to understand the mechanisms underlying the exact nature of receptor cross-regulation and synergism.

4.7 List of abbreviations

ACLT, anterior cruciate ligament transection; ANOVA, analysis of variance; BK, bradykinin; BKB1, bradykinin receptor B1; BKB2, bradykinin receptor B2; DX, digital micro-X-ray; ET-1, endothelin-1; ETA, endothelin receptor type A; ETL, echo train length; MR, magnetic resonance; MSME, multislice multiecho; OA, osteoarthritis; OARSI, Osteoarthritis Research Society International; RARE, rapid acquisition with relaxation enhancement; RF, radio frequency; TE, echo time; TR, repetition time.

4.8 Competing interests

Intellectual property rights (GNK, PS, FM) of the dual-antagonist treatment strategy are protected through Univalor, the technology transfer corporation of Université de Montréal. CZ and BV declare that they have no competing interests.

4.9 Authors' contributions

GNK designed the *in vivo* study, performed the surgeries, injections, static weight bearing measurements, dissections, and radiological analyses, analyzed the data, and wrote the paper. CZ assisted with surgeries and dissections, performed histological studies, and revised the paper. BV reverse-engineered the static weight bearing apparatus and assisted with data analysis. PS contributed the BKB1 antagonist R-954. FM conceived the study and supervised the research group. GNK takes responsibility for the integrity of the work as a whole. All authors read and approved the final manuscript.

4.10 Acknowledgements

We thank Archana Sangole for valuable help with the static weight bearing apparatus design. We thank Saadallah Bouhanik of the Viscogliosi Laboratory for Molecular Genetics of Musculoskeletal Disorders (Montreal, QC) for providing access to and help with the Faxitron micro-X-ray system, as well as Jason Cakiroglu (MR engineer) and Barry J. Bedell (director) of the Small Animal Imaging Lab at McGill University (Montreal, QC) for providing access to their 7 Tesla micro-MRI scanner. We thank Stéphane Faubert and Serge Nadeau for their surgical instruction, as well as Denise Carrier (director) and the staff of the Sainte-Justine Hospital Research Centre animal facility for their technical assistance. Finally, we thank Kessen Patten for his writing and editing suggestions.

This work was supported by operating grants from the The Arthritis Society

(RG05/084) and the Canadian Institutes of Health Research (IMH-94011). GNK held a Sainte-Justine Hospital Foundation/Foundation of Stars bursary.

4.11 Additional Files

4.11.1 Additional file 1 — Chemical structures of BQ-123 and R-945

2D chemical structures of selective ETA peptide antagonist BQ-123 (left) and selective BKB1 peptide antagonist R-954 (right). PDF file named antagonist structures.pdf (1 page). [See Figure 3.3]

4.11.2 Additional file 2 — Design diagrams for static weight bearing apparatus

Original technical drawings for static weight bearing apparatus. Labels in French. Auto-drafted using CATIA V5 R19. PDF file named static weight bearing apparatus technical drawings.pdf (4 pages). [See Figure 3.4]

4.11.3 Additional file 3 — Static weight bearing apparatus in use

Static weight bearing apparatus with rat positioned for measurements. A, side view; B, angle view; C, front view. PDF file named static weight bearing apparatus photos.pdf (1 page). [See Figure 3.7]

CHAPTER 5

DISCUSSION

5.1 Main results of experimental study

In the article manuscript that makes up the previous chapter, we describe a preclinical study of the efficacy of ETA and BKB1 antagonism at reducing OA pathology and joint pain in an animal model of OA. We report that local treatment with specific peptide antagonists of ETA and/or BKB1 was able to slow and/or prevent early OA pathogenesis in the rat ACLT model of OA, as determined by pain behaviour assessment, radiological joint examination, and joint histopathology. We found that treatment diminished hind limb pain, improved radiological indices of disease, protected cartilage biochemical integrity, and preserved articular cartilage and bone histomorphometry.

As noted above, we found that antagonist treatment improved pain tolerance in ACLT animals. Apart from the operative trauma, it is well-documented that surgical destabilization of the rat knee joint causes chronic joint pain [32], which is concurrent with a rapid development of radiographic [217] and histological OA [9, 92]. Thus, examination of the pain tolerance behaviour in our model appears to be a valid measure of functional biomechanics. This observed pain reduction is perhaps the most important result in terms of its impact on clinical therapy: low-grade joint pain is the most common reason for initial patient complaints in OA cases [60, 65], and engenders severe functional limitations. De-Melo *et al.* [52]

have previously demonstrated that local treatment with ETA antagonists reduces overt acute joint pain, and similar work by Tonussi *et al.* [206] has demonstrated acute pain reduction with BKB1 antagonists. We extend this finding to the dual antagonist treatment approach in a model of chronic pain, as well as relating it to measures of joint integrity by radiology and histology. Thus, the anti-nociceptive effects of ETA and/or BKB1 antagonism make this treatment strategy attractive.

We determined that antagonist treatment decreased radiological indices of OA: treated animals had fewer osteophytes (if at all), thicker articular cartilage, and less subchondral bone remodelling. Dual antagonism appeared to be the most protective treatment strategy. As well, cartilage transverse relaxation time (T_2), which increases in ACLT animals [43], was decreased by antagonist treatment, which indicates a cartilage-preserving effect. Shorter cartilage transverse relaxation times are an indicator of intact articular cartilage and longer times indicate cartilage degradadion; this MR parameter is indicative of cartilage composition and integrity [25, 27, 201]. More generally, radiographic evidence is the main criterion for OA diagnosis and progression [1, 162], but is not without controversy as a prognostic measure (as discussed below). The most common clinical diagnostic test for OA is an X-ray of the affected joint: joint space narrowing as measured on X-ray is often used as a longitudinal marker of disease evolution, and osteophyte formation and/or subchondral bone remodelling can be detected. While it is difficult to directly compare radiological parameters between human and rat knees due to the quadrupedal nature of the animal and the markedly different radiological anatomy that this entails [216], we were able to detect radiological

evidence of OA progression in ACLT animals, as has been described in similar studies [43, 217].

In terms of joint histopathology, we ascertained that OA induction in rat knees by ACLT led to a rapid decrease in cartilage proteoglycan staining, along with articular cartilage surface disruption and osteophyte formation. This confirm previous reports [9, 92] of the histopathological findings in similar surgical OA models in the rat. ETA and/or BKB1 antagonist treatment protected the proteoglycan content of the joint cartilage to a large extent and preserved articular surface integrity, with less cartilage notching and almost no osteophytes detected upon histological examination. This most likely allowed the joint cartilage to retain its normal biophysical properties, as cartilage proteoglycans are responsible, along with collagen, for retaining water in the tissue, which provides spring and resilience [151, 186]. We speculate that the protection of cartilage proteoglycans and articular surface histomorphology may be one explanation for the increased pain tolerance observed in antagonist-treated animals; our results concur with those of other reports, which correlated the preservation of articular cartilage proteoglycan staining with pain tolerance behaviour [9].

5.2 Limitations of study and suggested experimental work

Our study has several limitations, which must colour the interpretation of our results. Our chosen animal model, rat ACLT, has been critiqued for producing pathology that is more aggressive than human OA, and thus not entirely representative of the disease phenotype as observed in human patients. We chose this

model because of its rapid and stereotypical disease kinetics, the established and validated pain measurement modalities available for it, as well as a favourable cost-benefit ratio. As we suggest below in subsection 6.2.1, large-animal studies would strengthen our conclusions. However, testing a hypothesis with little previous *in vitro* data in an *in vivo* context represents a high-risk/high-benefit approach to the problem. As such, potential pitfalls, especially time and financial constraints, must be carefully considered.

The treatment strategy for our study was selected based upon previously published reports, but we did not perform *in-vivo* dose-response or time-course analyses ourselves to determine the pharmacokinetics and pharmacodynamics in our system. While we feel our treatment strategy is robust, given the well-established disease kinetics of our animal model, a full examination of dose-response and time-course experiments would add to the study, lending more weight to the final treatment pattern. At the very least, low- and high-dose treatments would allow dose optimization. This limitation might be partially addressed by *in vitro* studies: our laboratory routinely isolates human chondrocytes and synoviocytes from tibial plateaus of OA patients undergoing total knee arthroplasty [132]. These cells could be cultured in the presence of the antagonists, and stimulated with ET-1 and/or BK. Downstream cellular responses, such as MAP kinase phosphorylation or pro-inflammatory gene transcription, could be examined following varying drug doses and time courses. However, this author would question the relevance of such an approach, since *in vitro* assays and *in vivo* pharmacological effects are due to two very different sets of phenomena, and it is difficult to extrapolate from one

to the other. Furthermore, a strict dose-response experiment would be indicated where the pain phenomenon or the pharmacological approach is completely unexplored, with no previous *in vivo* data. Our strategy is in contrast to such a case, since both of our drugs and the animal disease model have been extensively studied; our novel contributions were to extend the existing knowledge to the chronic joint degeneration condition, and to test the dual-antagonist combined treatment approach for potential synergistic or additive effects.

Some reviewers of our work had questioned the necessity of a local treatment strategy, noting (correctly) that patients much prefer oral treatment options, since they are easier to comply with, and do not necessitate regular physician intervention for injection. We had initially investigated a systemic treatment model, by implantation of an osmotic mini-pump to deliver drug constantly. However, this was abandoned for two main reasons. First, we feared that the administration of antagonists of vasoactive substances would negatively affect blood pressure regulation. Second, and perhaps more importantly, we wanted to ensure that our drugs would actually reach and affect the target tissues. Cartilage is avascular, nourished by diffusion; given the short circulating half-life of small peptides, we did not think that our drugs would arrive intact after peripheral circulation uptake, arterial distribution, and then diffusion to the joint cartilage. We preferred to inject the drugs directly next to the target tissues, in the synovial space. We did not perform radio-tracer studies, which are *de rigueur* with novel pharmacological agents. However, both our antagonists are well-characterized and have been used in a number of animal and human clinical studies: thus, a full phar-

macodynamic/pharmacokinetic study would have unnecessarily repeated previous work, and would have not added to our results, in the opinion of this author.

Our histological assessment was carried out on decalcified tissues, using standard histochemical protocols. Such examination of cartilage biopsies or serial sections of animal knee joints, followed by scoring using a validated assessment system, is the gold standard for articular histomorphology [138, 168]. Some reports have argued for immunohistochemical end-point targets in OA histopathology assessment, such as staining for proteoglycans, collagens, or aggrecans [15, 38], claiming that conventional histochemical approaches fail to convey a complete picture of the disease. This author would view such immunohistochemical assessments as interesting complementary information, but believes that the ease of use and standardized conditions of classical histochemical techniques make them a first choice for evaluating OA pathology in an animal model.

Any histological assessment system can be critiqued as follows: histological scoring of any phenomenon can be an imprecise approach that is often more art than science. Using well-described and validated systems obviates this concern somewhat. In this author's view, the most important features of a histopathology assessment system are that it assigns numerical indices to at least two different histological features of a given disease, and that it has detailed criteria to allow for reproducible scoring. Such systems are robust and can form the basis for quantitative statistical analysis, if sampling size is large enough. It must be noted that our system of choice, the OARSI histopathology assessment, has been validated and meets these criteria.

Pain tolerance in our study was measured by static weight bearing, a cost-effective and rapid method of assessing hind limb pain in laboratory animals. However, this is an artificial modality in many senses, since the animal adopts an unnatural posture and is confined in a stationary restraint for the duration of the test. There is a considerable amount of controversy in the pain research field as to the best evaluation for joint pain in animal models [8, 30, 155]. This investigator had considered von Frey filaments, a modified Randall-Selito test, pressure application measurements, and direct joint compression, but decided on static weight bearing following expert recommendations (Geoffrey Bove DC PhD and Stéphane Faubert DVM, personal communications). Furthermore, in the human patient population, improvements in physical function correlate well with pain relief [16], making biomechanical assessment a priority for our research.

While informative, static weight bearing is generally being phased out in favour of dynamic weight bearing, an assay where the animal is free-moving in a cage with a force sensor array on the bottom and a synchronized video camera capture to score individual limb use and match it to applied force. This allows the animal to be observed with a natural posture as it moves, giving a more complete picture of joint pain as it affects behaviour. We had investigated the possibility of reverse-engineering a dynamic weight bearing apparatus, but it was deemed too costly and time-consuming. While it is impossible to directly question lab rats as to their perceived functional impairment, classical behavioural assays such as open-field activity monitoring [83, 84] might shed light on the behavioural correlates of pain in our model. Collaboration with pain researchers may be helpful to realize these

studies; the author has therefore initiated contact with the Alan Edwards Centre for Research on Pain at McGill University.

Our data indicated that the animals became tolerant of a painful knee joint by the end of the study period, with values clustering towards a common mean for all conditions. This author interprets that result as a tolerance phenomenon, whereby the nociceptive stimulus is perceived less and less over time due to habituation. Thus, the length of our study, while selected to allow the maximal radio- and histo-pathogenesis in our chosen model, may be less ideal for nociceptive studies, due to the potential for the confounding effects of tolerance behaviour.

Radiological examinations of the rat knee joints were only undertaken post-mortem *ex vivo* in our study. This allowed us to examine samples at the highest possible resolution (10×10 μm pixel size for DX, $104.1\overline{6} \times 104.1\overline{6} \times 500$ μm voxel size for MR) with very high signal-to-noise ratio, since the samples were scanned in isolation after dissection. However, this strategy only allows for retrospective evaluation of joint radiomorphology, and does not permit longitudinal monitoring and evaluation of disease phenotype and/or treatment effects. Thus, it would be intriguing to perform *in vivo* longitudinal MR and/or CT studies, imaging knee joints at several time-points over the course of the experiment. Moreover, it has long been established that there is a *poor* correlation between radiological evidence of joint degradation and human pain perception [18, 57, 82, 113], which raises the question: precisely what is being examined via radiological imaging in animal models of OA?

A complementary project would be to investigate the neurological correlates

of joint pain by imaging the brain and central nervous system components by MR (Pascal Vachon DVM, personal communication) to examine central nervous system changes concurrent with peripheral chronic pain. This line of investigation is relevant because we and others [67] have demonstrated pain tolerance behaviour over time in chronic surgical models of OA. The musculoskeletal research axis at Sainte-Justine Hospital Research Centre has just acquired a SkyScan whole-body micro-CT machine for rodents, and the author has set up a study protocol with the McGill Small Animal Imaging Lab for longitudinal MR: it will be interesting to see the results of these experiments.

CHAPTER 6

CONCLUSIONS AND FUTURE WORK

6.1 Conclusions

Using a rat surgically induced model of OA, we demonstrated that local treatment with specific peptide antagonists of ETA and/or BKB1 may slow or stabilize the development of radiomorphological and histomorphological changes occurring in OA pathogenesis. Furthermore, we showed that antagonist treatment accelerated recovery of, and improved longitudinally, pain tolerance in ACLT animals. Taken together, our results indicate that blocking ETA and BKB1 improves OA prognostic indices, which implies that defective signalling might play a role in chronic OA pain. Our results also raise the possibility of targeted dual receptor antagonism as a relevant therapeutic option. Further studies are required to understand the mechanisms underlying the exact nature of receptor cross-regulation and synergism.

6.2 Future research questions

6.2.1 Preclinical *in vivo* trials

This study opens several potential avenues of investigation. First, the rat ACLT model of OA and the static weight bearing apparatus represent important research tools. The robustness and rapid kinetics of the surgical OA model make it an attractive option for preclinical studies [9, 92]. The static weight bearing

apparatus is an accepted modality to measure hind limb and joint pain in laboratory rodents [31, 32, 213]. They may be used to test other disease-modifying OA drugs [170] for pain-lowering efficacy and joint morphology protection in an accepted preclinical disease model. *A priori*, this author would suggest the evaluation of other endothelial factor blockers (such as receptor antagonists, signalling inhibitors, or direct inhibitors), or anti-angiogenic factors, as drugs targeting these OA disease processes are currently under-represented in Phase II/III clinical trials [170, 221]. As OA is a multifactorial disease, drugs that target other molecular processes in OA pathogenesis could also be tested in the same paradigm.

In a similar vein, large-animal studies could be undertaken with our compounds, or with other ETA and/or BKB1 antagonists: surgically induced OA in the dog [75] is the model of choice for demonstrating efficacy in OA drug development. Another approach would be to use ETA and/or BKB1 antagonists to treat OA as it develops in one or more of the spontaneously occurring animal models. As the aetiology is usually well-understood in this class of models [231], delaying or preventing joint disease from developing would add to our understanding of how ETA and BKB1 antagonism interferes with the molecular pathogenesis of OA. To discuss a model that the author had initially considered using: if ETA and BKB1 antagonism protects against the onset of joint disease in male STR/ort mice, we would be able to suggest that it promotes the increased expression of protective cytokines TGF-β1 and IL-4 in the articular microenvironment, since female STR/ort mice develop less OA than males due to increased local expression of these cytokines in joint tissues at 2 months of age [130].

6.2.2 *In vitro* mechanistic studies

The identification of molecular targets for OA treatment is a rapidly expanding discipline [3]. By taking a reductionist approach, we can investigate the signalling pathways involved in ETA and/or BKB1 receptor antagonism, thereby elucidating the molecular mechanisms and downstream effectors responsible for the observed reduction in disease severity in the rat model. That is to say, we would examine the effects of ETA and/or BKB1 receptor antagonism on a cellular and molecular level. We have outlined studies to examine the common PI3-K and NF-κB signalling pathways engaged by both ET-1 and BK, via ETA and BKB1 (see subsections 2.2.5 and 2.2.8), in human chondrocytes and synoviocytes, building on preliminary data that shows receptor co-localization in OA synovial tissue. As well, we intend to examine downstream effector molecule gene expression by RT-qPCR, and protein production by ELISA, following ET-1 and/or BK stimulation, with or without single and/or dual antagonist pre-treatment. Targets of interest include: gelatinases (MMP-2, MMP-9); collagenases (MMP-1, MMP-13); stromelysin (MMP-3); aggrecanases (ADAMTS4, ADAMTS5); and pro-inflammatory cytokines (IL-1β, TNF-α). Finally, by examining ETA and BKB1 receptor gene and protein expression under these conditions, we hope to determine the precise nature of receptor cross-up-regulation, to allow a more tailored pharmacological approach based on the ratio of relative expression. This will also inform the development of second-generation drugs, including single-molecule approaches.

BIBLIOGRAPHY

[1] E. Abadie, D. Ethgen, B. Avouac, G. Bouvenot, J. Branco, O. Bruyere, G. Calvo, J. P. Devogelaer, R. L. Dreiser, G. Herrero-Beaumont, A. Kahan, G. Kreutz, A. Laslop, E. M. Lemmel, G. Nuki, L. Van De Putte, L. Vanhaelst, and J. Y. Reginster. Recommendations for the use of new methods to assess the efficacy of disease-modifying drugs in the treatment of osteoarthritis. *Osteoarthr Cartil*, 12:263–268, Apr 2004.

[2] Steven B Abramson and Mukundan Attur. Developments in the scientific understanding of osteoarthritis. *Arthritis Res Ther*, 11(3):227, 2009.

[3] Maria José Alcaraz, Javier Megías, Isabel García-Arnandis, Victoria Clérigues, and Maria Isabel Guillén. New molecular targets for the treatment of osteoarthritis. *Biochemical Pharmacology*, 80(1):13–21, Jul 2010.

[4] RD Altman. Early management of osteoarthritis. *Am J Manag Care*, 16 (Suppl Management):S41–7, Mar 2010.

[5] R.D. Altman, E. Asch, D. Bloch, G. Bole, D. Borenstein, K. Brandt, W. Christy, T. D. Cooke, R. Greenwald, and M. Hochberg. Development of criteria for the classification and reporting of osteoarthritis. Classification of osteoarthritis of the knee. Diagnostic and Therapeutic Criteria Committee of the American Rheumatism Association. *Arthritis Rheum*, 29:1039–1049, Aug 1986.

[6] American College of Rheumatology Subcommittee on Osteoarthritis Guidelines. Recommendations for the medical management of osteoarthritis of the hip and knee: 2000 update. *Arthritis Rheum*, 43(9):1905–15, Sep 2000.

[7] American Society for Quality Statistics Division. *Glossary and Tables for Statistical Quality Control*. ASQ Quality Press, 4th edition, 2004.

[8] Laurent G Ameye and Marian F Young. Animal models of osteoarthritis: lessons learned while seeking the "Holy Grail". *Current opinion in rheumatology*, 18(5):537–47, Sep 2006.

[9] C Thomas G Appleton, David D McErlain, Vasek Pitelka, Neil Schwartz, Suzanne M Bernier, James L Henry, David W Holdsworth, and Frank Beier. Forced mobilization accelerates pathogenesis: characterization of a preclinical surgical model of osteoarthritis. *Arthritis Res Ther*, 9(1):R13, Jan 2007.

[10] Nigel Arden and Michael C Nevitt. Osteoarthritis: epidemiology. *Best Pract Res Clin Rheumatol*, 20(1):3–25, Feb 2006.

[11] D Armstrong, J B Jepson, C A Keele, and J W Stewart. Pain-producing substance in human inflammatory exudates and plasma. *J Physiol*, 135(2): 350–70, Feb 1957.

[12] Elizabeth C Arner. Aggrecanase-mediated cartilage degradation. *Curr Opin Pharmacol*, 2(3):322–9, Jun 2002.

[13] Sadaf Ashraf and David Andrew Walsh. Angiogenesis in osteoarthritis. *Current opinion in rheumatology*, 20(5):573–80, Sep 2008.

[14] Mukundan Attur, Jonathan Samuels, Svetlana Krasnokutsky, and Steven B Abramson. Targeting the synovial tissue for treating osteoarthritis (OA): where is the evidence? *Best Practice & Research Clinical Rheumatology*, 24 (1):71–9, Feb 2010.

[15] R D C Barley, K M Bagnall, and N M Jomha. Histological scoring of articular cartilage alone provides an incomplete picture of osteoarthritic disease progression. *Histol Histopathol*, 25(3):291–7, Mar 2010.

[16] H Richard Barthel, John H Peniston, Michael B Clark, Morris S Gold, and Roy D Altman. Correlation of pain relief with physical function in hand osteoarthritis: randomized controlled trial post hoc analysis. *Arthritis Res Ther*, 12(1):R7, Jan 2010.

[17] Gregory M Barton. A calculated response: control of inflammation by the innate immune system. *J Clin Invest*, 118(2):413–20, Feb 2008.

[18] John Bedson and Peter R Croft. The discordance between clinical and radiographic knee osteoarthritis: a systematic search and summary of the literature. *BMC Musculoskelet Disord*, 9:116, Jan 2008.

[19] Nicholas Bellamy. WOMAC: a 20-year experiential review of a patient-centered self-reported health status questionnaire. *J Rheumatol*, 29(12): 2473–6, Dec 2002.

[20] L Benaroyo. [How do we define inflammation?]. *Praxis (Bern)*, 83(48): 1343–7, Nov 1994.

[21] A. M. Bendele and S. L. White. Early histopathologic and ultrastructural alterations in femorotibial joints of partial medial meniscectomized guinea pigs. *Vet. Pathol.*, 24:436–443, Sep 1987.

[22] M J Benito, D J Veale, O FitzGerald, W B van den Berg, and B Bresnihan. Synovial tissue inflammation in early and late osteoarthritis. *Ann Rheum Dis*, 64(9):1263–7, Sep 2005.

[23] H P Benton, T R Jackson, and M R Hanley. Identification of a novel inflammatory stimulant of chondrocytes. early events in cell activation by bradykinin receptors on pig articular chondrocytes. *Biochem J*, 258(3):861–7, Mar 1989.

[24] R. C. Billinghurst, L. Dahlberg, M. Ionescu, A. Reiner, R. Bourne, C. Rorabeck, P. Mitchell, J. Hambor, O. Diekmann, H. Tschesche, J. Chen, H. Van Wart, and A. R. Poole. Enhanced cleavage of type II collagen by collagenases in osteoarthritic articular cartilage. *J. Clin. Invest.*, 99:1534–1545, Apr 1997.

[25] G Blumenkrantz and S Majumdar. Quantitative magnetic resonance imaging of articular cartilage in osteoarthritis. *European cells & materials*, 13: 76–86, Jan 2007.

[26] Felix Böhm, John Pernow, Jonas Lindström, and Gunvor Ahlborg. ETA receptors mediate vasoconstriction, whereas ETB receptors clear endothelin-

1 in the splanchnic and renal circulation of healthy men. *Clin Sci (Lond)*, 104(2):143–51, Feb 2003.

[27] R I Bolbos, Jin Zuo, Suchandrima Banerjee, Thomas M Link, C Benjamin Ma, Xiaojuan Li, and Sharmila Majumdar. Relationship between trabecular bone structure and articular cartilage morphology and relaxation times in early OA of the knee joint using parallel MRI at 3 T. *Osteoarthr Cartil*, 16 (10):1150–9, Oct 2008.

[28] C S Bonnet and D A Walsh. Osteoarthritis, angiogenesis and inflammation. *Rheumatology (Oxford)*, 44(1):7–16, Jan 2005.

[29] Ali Bouallegue, Grace Bou Daou, and Ashok K Srivastava. Endothelin-1-induced signaling pathways in vascular smooth muscle cells. *Curr Vasc Pharmacol*, 5(1):45–52, Jan 2007.

[30] Geoffrey Bove. Mechanical sensory threshold testing using nylon monofilaments: the pain field's "tin standard". *Pain*, 124(1-2):13–7, Sep 2006.

[31] S E Bove, S L Calcaterra, R M Brooker, C M Huber, R E Guzman, P L Juneau, D J Schrier, and K S Kilgore. Weight bearing as a measure of disease progression and efficacy of anti-inflammatory compounds in a model of monosodium iodoacetate-induced osteoarthritis. *Osteoarthr Cartil*, 11 (11):821–30, Nov 2003.

[32] S E Bove, K D Laemont, R M Brooker, M N Osborn, B M Sanchez, R E Guzman, K E Hook, P L Juneau, J R Connor, and K S Kilgore. Surgi-

cally induced osteoarthritis in the rat results in the development of both osteoarthritis-like joint pain and secondary hyperalgesia. *Osteoarthr Cartil*, 14(10):1041–8, Oct 2006.

[33] Kenneth D Brandt. Animal models of osteoarthritis. *Biorheology*, 39(1-2): 221–35, Jan 2002.

[34] J B Calixto, D A Cabrini, J Ferreira, and M M Campos. Inflammatory pain: kinins and antagonists. *Current opinion in anaesthesiology*, 14(5):519–26, Oct 2001.

[35] João B Calixto, Rodrigo Medeiros, Elizabeth S Fernandes, Juliano Ferreira, Daniela A Cabrini, and Maria M Campos. Kinin B1 receptors: key G-protein-coupled receptors and their role in inflammatory and painful processes. *Br J Pharmacol*, 143(7):803–18, Dec 2004.

[36] H Cambridge and S D Brain. Mechanism of bradykinin-induced plasma extravasation in the rat knee joint. *Br J Pharmacol*, 115(4):641–7, Jun 1995.

[37] D J Campbell. The kallikrein-kinin system in humans. *Clin Exp Pharmacol Physiol*, 28(12):1060–5, Dec 2001.

[38] KL Camplejohn and SA Allard. Limitations of safranin 'O' staining in proteoglycan-depleted cartilage demonstrated with monoclonal antibodies. *Histochemistry and Cell Biology*, 89(2):185–188, 1988.

[39] Canadian Arthritis Network. Arthritis facts and figures, 2010. URL `http://www.arthritisnetwork.ca/home/Facts_and_Figures_2010.pdf`.

[40] L O Cardell, R Uddman, and L Edvinsson. Endothelins: a role in cerebrovascular disease? *Cephalalgia*, 14(4):259–65, Aug 1994.

[41] Charles River Canada. Lewis Rats: Canadian strain origin and pricing, 2010. URL `http://www.criver.com/SiteCollectionDocuments/ca_rm_c_Lewis_Rats_en.pdf`.

[42] Qing-wen Chen, Lars Edvinsson, and Cang-Bao Xu. Role of ERK/MAPK in endothelin receptor signaling in human aortic smooth muscle cells. *BMC Cell Biol*, 10:52, 2009.

[43] M-C Chou, P-H Tsai, G-S Huang, H-S Lee, C-H Lee, M-H Lin, C-Y Lin, and H-W Chung. Correlation between the MR T2 value at 4.7 T and relative water content in articular cartilage in experimental osteoarthritis induced by ACL transection. *Osteoarthr Cartil*, 17(4):441–7, Apr 2009.

[44] S. Christgau, P. Garnero, C. Fledelius, C. Moniz, M. Ensig, E. Gineyts, C. Rosenquist, and P. Qvist. Collagen type II C-telopeptide fragments as an index of cartilage degradation. *Bone*, 29:209–215, Sep 2001.

[45] R L Clark, J T Cuttino, Jr, S K Anderle, W J Cromartie, and J H Schwab. Radiologic analysis of arthritis in rats after systemic injection of streptococcal cell walls. *Arthritis Rheum*, 22(1):25–35, Jan 1979.

[46] K A Clarke, S A Heitmeyer, A G Smith, and Y O Taiwo. Gait analysis in a rat model of osteoarthrosis. *Physiol Behav*, 62(5):951–4, Nov 1997.

[47] Janet D Conway, Michael A Mont, and Hari P Bezwada. Arthrodesis of the knee. *J Bone Joint Surg Am*, 86-A(4):835–48, Apr 2004.

[48] M. B. Coventry. Osteotomy of the upper portion of the tibia for degenerative arthritis of the knee. A preliminary report. *J Bone Joint Surg Am*, 47:984–90, Jul 1965.

[49] H Cramer, K Schmenger, K Heinrich, A Horstmeyer, H Böning, A Breit, A Piiper, K Lundstrom, W Müller-Esterl, and C Schroeder. Coupling of endothelin receptors to the ERK/MAP kinase pathway. Roles of palmitoylation and G(alpha)q. *Eur J Biochem*, 268(20):5449–59, Oct 2001.

[50] Pierre Dagenais and Alicia Framarin. La viscosuppléance pour le traitement de la gonarthrose. *ETMIS*, 3(6), Jul 2007.

[51] J Damas. The brown Norway rats and the kinin system. *Peptides*, 17(5): 859–72, 1996.

[52] J D De-Melo, C R Tonussi, P D'Orléans-Juste, and G A Rae. Articular nociception induced by endothelin-1, carrageenan and LPS in naive and previously inflamed knee-joints in the rat: inhibition by endothelin receptor antagonists. *Pain*, 77(3):261–9, Sep 1998.

[53] G de Nucci, R Thomas, P D'Orleans-Juste, E Antunes, C Walder, T D Warner, and J R Vane. Pressor effects of circulating endothelin are limited

by its removal in the pulmonary circulation and by the release of prostacyclin and endothelium-derived relaxing factor. *Proc Natl Acad Sci U S A*, 85(24): 9797–800, Dec 1988.

[54] D. D. Dean, J. Martel-Pelletier, J. P. Pelletier, D. S. Howell, and J. F. Woessner. Evidence for metalloproteinase and metalloproteinase inhibitor imbalance in human osteoarthritic cartilage. *J. Clin. Invest.*, 84:678–685, Aug 1989.

[55] P A Dearnley. A review of metallic, ceramic and surface-treated metals used for bearing surfaces in human joint replacements. *Proc Inst Mech Eng H*, 213(2):107–35, 1999.

[56] DICOM Standards Committee. *Digital Imaging and Communications in Medicine (DICOM)*. Number PS 3.1-2009. National Electrical Manufacturers Association, Rosslyn, Virginia, 2009.

[57] Paul A Dieppe and L Stefan Lohmander. Pathogenesis and management of pain in osteoarthritis. *Lancet*, 365(9463):965–73, Jan 2005.

[58] John H Dirckx, editor. *Stedman's medical dictionary for the health professions and nursing: illustrated*. Wolters Kluwer Health/Lippincott Williams & Wilkins, Philadelphia, 6th edition, 2008.

[59] Vishva Dixit and Tak W Mak. NF-kappaB signaling. Many roads lead to Madrid. *Cell*, 111(5):615–9, Nov 2002.

[60] Andy Dray and Simon J Read. Arthritis and pain. Future targets to control osteoarthritis pain. *Arthritis Res Ther*, 9(3):212, Jan 2007.

[61] Danielle L Drayton, Shan Liao, Rawad H Mounzer, and Nancy H Ruddle. Lymphoid organ development: from ontogeny to neogenesis. *Nat Immunol*, 7(4):344–53, Apr 2006.

[62] R E Esser, A R Hildebrand, R A Angelo, L M Watts, M D Murphey, and L E Baugh. Measurement of radiographic changes in adjuvant-induced arthritis in rats by quantitative image analysis. *Arthritis Rheum*, 38(1):129–38, Jan 1995.

[63] W H Ettinger, Jr, R Burns, S P Messier, W Applegate, W J Rejeski, T Morgan, S Shumaker, M J Berry, M O'Toole, J Monu, and T Craven. A randomized trial comparing aerobic exercise and resistance exercise with a health education program in older adults with knee osteoarthritis. The Fitness Arthritis and Seniors Trial (FAST). *JAMA*, 277(1):25–31, Jan 1997.

[64] D A Ewald, I H Pang, P C Sternweis, and R J Miller. Differential G protein-mediated coupling of neurotransmitter receptors to Ca2+ channels in rat dorsal root ganglion neurons in vitro. *Neuron*, 2(2):1185–93, Feb 1989.

[65] David T Felson. The sources of pain in knee osteoarthritis. *Current opinion in rheumatology*, 17(5):624–8, Sep 2005.

[66] David T Felson, Sara McLaughlin, Joyce Goggins, Michael P LaValley, M Elon Gale, Saara Totterman, Wei Li, Catherine Hill, and Daniel Gale.

Bone marrow edema and its relation to progression of knee osteoarthritis. *Ann Intern Med*, 139(5 Pt 1):330–6, Sep 2003.

[67] Janet Fernihough, Clive Gentry, Marzia Malcangio, Alyson Fox, John Rediske, Theodore Pellas, Bruce Kidd, Stuart Bevan, and Janet Winter. Pain related behaviour in two models of osteoarthritis in the rat knee. *Pain*, 112 (1-2):83–93, Nov 2004.

[68] Juliano Ferreira, Alessandra Beirith, Marcelo A S Mori, Ronaldo C Araújo, Michael Bader, João B Pesquero, and João B Calixto. Reduced nerve injury-induced neuropathic pain in kinin B1 receptor knock-out mice. *J Neurosci*, 25(9):2405–12, Mar 2005.

[69] S H Ferreira, M Romitelli, and G de Nucci. Endothelin-1 participation in overt and inflammatory pain. *J Cardiovasc Pharmacol*, 13 Suppl 5:S220–2, 1989.

[70] Bichoy H Gabra, Ouhida Benrezzak, Leng-Hong Pheng, Dana Duta, Philippe Daull, Pierre Sirois, François Nantel, and Bruno Battistini. Inhibition of type 1 diabetic hyperalgesia in streptozotocin-induced Wistar versus spontaneous gene-prone BB/Worchester rats: efficacy of a selective bradykinin B1 receptor antagonist. *J Neuropathol Exp Neurol*, 64(9):782–9, Sep 2005.

[71] P. Garnero, E. Gineyts, S. Christgau, B. Finck, and P. D. Delmas. Association of baseline levels of urinary glucosyl-galactosyl-pyridinoline and type II

collagen C-telopeptide with progression of joint destruction in patients with early rheumatoid arthritis. *Arthritis Rheum.*, 46:21–30, Jan 2002.

[72] S Garofalo, E Vuorio, M Metsaranta, R Rosati, D Toman, J Vaughan, G Lozano, R Mayne, J Ellard, and W Horton. Reduced amounts of cartilage collagen fibrils and growth plate anomalies in transgenic mice harboring a glycine-to-cysteine mutation in the mouse type II procollagen alpha 1-chain gene. *Proc Natl Acad Sci U S A*, 88(21):9648–52, Nov 1991.

[73] Stephan D Gauldie, Daniel S McQueen, Christopher J Clarke, and Iain P Chessell. A robust model of adjuvant-induced chronic unilateral arthritis in two mouse strains. *J Neurosci Methods*, 139(2):281–91, Oct 2004.

[74] P Gegout-Pottie, L Philippe, M A Simonin, C Guingamp, P Gillet, P Netter, and B Terlain. Biotelemetry: an original approach to experimental models of inflammation. *Inflamm Res*, 48(8):417–24, Aug 1999.

[75] E M Gilbertson. Development of periarticular osteophytes in experimentally induced osteoarthritis in the dog. A study using microradiographic, microangiographic, and fluorescent bone-labelling techniques. *Ann Rheum Dis*, 34(1):12–25, Feb 1975.

[76] Sonya S Glasson, Roger Askew, Barbara Sheppard, Brenda Carito, Tracey Blanchet, Hak-Ling Ma, Carl R Flannery, Diane Peluso, Kim Kanki, Zhiyong Yang, Manas K Majumdar, and Elisabeth A Morris. Deletion of active

ADAMTS5 prevents cartilage degradation in a murine model of osteoarthritis. *Nature*, 434(7033):644–8, Mar 2005.

[77] A Gohla, G Schultz, and S Offermanns. Role for G(12)/G(13) in agonist-induced vascular smooth muscle cell contraction. *Circ Res*, 87(3):221–7, Aug 2000.

[78] Haydar Gök, Süreyya Ergin, and Günes Yavuzer. Kinetic and kinematic characteristics of gait in patients with medial knee arthrosis. *Acta Orthop Scand*, 73(6):647–52, Dec 2002.

[79] Mary B Goldring and Steven R Goldring. Osteoarthritis. *J Cell Physiol*, 213(3):626–34, Dec 2007.

[80] Rachael Gooberman-Hill, Gillian Woolhead, Fiona Mackichan, Salma Ayis, Susan Williams, and Paul Dieppe. Assessing chronic joint pain: lessons from a focus group study. *Arthritis Rheum*, 57(4):666–71, May 2007.

[81] S Gutowski, A Smrcka, L Nowak, D G Wu, M Simon, and P C Sternweis. Antibodies to the alpha q subfamily of guanine nucleotide-binding regulatory protein alpha subunits attenuate activation of phosphatidylinositol 4,5-bisphosphate hydrolysis by hormones. *J Biol Chem*, 266(30):20519–24, Oct 1991.

[82] S E Gwilym, T C B Pollard, and A J Carr. Understanding pain in osteoarthritis. *J Bone Joint Surg Br*, 90(3):280–7, Mar 2008.

[83] C.S. Hall. Emotional behavior in the rat. I. Defecation and urination as measures of individual differences in emotionality. *Journal of Comparative Psychology (1921)*, 18(3):385 – 403, 1934.

[84] C.S. Hall. Emotional behavior in the rat. III. The relationship between emotionality and ambulatory activity. *Journal of Comparative Psychology (1921)*, 22(3):345 – 352, 1936.

[85] J M Hall. Bradykinin receptors. *Gen Pharmacol*, 28(1):1–6, Jan 1997.

[86] M C Hall. Articular changes in the knee of the adult rat after prolonged immobilization in extension. *Clin Orthop Relat Res*, 34:184–95, 1964.

[87] Jeong S Han, Gary C Bird, Weidong Li, Justina Jones, and Volker Neugebauer. Computerized analysis of audible and ultrasonic vocalizations of rats as a standardized measure of pain-related behavior. *J Neurosci Methods*, 141(2):261–9, Feb 2005.

[88] Jeong Seok Han and Volker Neugebauer. mGluR1 and mGluR5 antagonists in the amygdala inhibit different components of audible and ultrasonic vocalizations in a model of arthritic pain. *Pain*, 113(1-2):211–22, Jan 2005.

[89] Guy Hans, Kristof Deseure, Dominique Robert, and Stefan De Hert. Neurosensory changes in a human model of endothelin-1 induced pain: a behavioral study. *Neurosci Lett*, 418(2):117–21, May 2007.

[90] Guy Hans, Kristof Deseure, and Hugo Adriaensen. Endothelin-1-induced

pain and hyperalgesia: a review of pathophysiology, clinical manifestations and future therapeutic options. *Neuropeptides*, 42(2):119–32, Apr 2008.

[91] Victoria Harvey and Anthony Dickenson. Behavioural and electrophysiological characterisation of experimentally induced osteoarthritis and neuropathy in C57Bl/6 mice. *Molecular Pain*, 5(1):18, 2009.

[92] Tadashi Hayami, Maureen Pickarski, Ya Zhuo, Gregg A Wesolowski, Gideon A Rodan, and Le T Duong. Characterization of articular cartilage and subchondral bone changes in the rat anterior cruciate ligament transection and meniscectomized models of osteoarthritis. *Bone*, 38(2):234–43, Feb 2006.

[93] J Amir Hendiani, Karin N Westlund, Nada Lawand, Niti Goel, Jeffrey Lisse, and Terry McNearney. Mechanical sensation and pain thresholds in patients with chronic arthropathies. *J Pain*, 4(4):203–11, May 2003.

[94] Y Hirota, T Tsukazaki, A Yonekura, Y Miyazaki, M Osaki, H Shindo, and S Yamashita. Activation of specific MEK-ERK cascade is necessary for TGFbeta signaling and crosstalk with PKA and PKC pathways in cultured rat articular chondrocytes. *Osteoarthritis Cartilage*, 8(4):241–7, Jul 2000.

[95] Aaron A Hofmann, Scott M Heithoff, and Marcelo Camargo. Cementless total knee arthroplasty in patients 50 years or younger. *Clin Orthop Relat Res*, (404):102–7, Nov 2002.

[96] Yanguo Hong, Haiming Ji, and Hua Wei. Topical ketanserin attenuates

hyperalgesia and inflammation in arthritis in rats. *Pain*, 124(1-2):27–33, Sep 2006.

[97] D. J Hunter. Focusing osteoarthritis management on modifiable risk factors and future therapeutic prospects. *Therapeutic Advances in Musculoskeletal Diseases*, 1(1):35–47, Oct 2009.

[98] M Ihara, K Ishikawa, T Fukuroda, T Saeki, K Funabashi, T Fukami, H Suda, and M Yano. In vitro biological profile of a highly potent novel endothelin (ET) antagonist BQ-123 selective for the ETA receptor. *J Cardiovasc Pharmacol*, 20 Suppl 12:S11–4, Jan 1992.

[99] M Ihara, K Noguchi, T Saeki, T Fukuroda, S Tsuchida, S Kimura, T Fukami, K Ishikawa, M Nishikibe, and M Yano. Biological profiles of highly potent novel endothelin antagonists selective for the ETA receptor. *Life Sci*, 50(4): 247–55, Jan 1992.

[100] J P Jackson and W Waugh. Tibial osteotomy for osteoarthritis of the knee. *J Bone Joint Surg Br*, 43-B:746–51, Nov 1961.

[101] Dianhua Jiang, Jiurong Liang, Juan Fan, Shuang Yu, Suping Chen, Yi Luo, Glenn D Prestwich, Marcella M Mascarenhas, Hari G Garg, Deborah A Quinn, Robert J Homer, Daniel R Goldstein, Richard Bucala, Patty J Lee, Ruslan Medzhitov, and Paul W Noble. Regulation of lung injury and repair by Toll-like receptors and hyaluronan. *Nat Med*, 11(11):1173–9, Nov 2005.

[102] Dianhua Jiang, Jiurong Liang, and Paul W Noble. Hyaluronan in tissue injury and repair. *Annu Rev Cell Dev Biol*, 23:435–61, 2007.

[103] Sindhu R Johnson, Alison Archibald, Aileen M Davis, Elizabeth Badley, James G Wright, and Gillian A Hawker. Is self-reported improvement in osteoarthritis pain and disability reflected in objective measures? *J Rheumatol*, 34(1):159–64, Jan 2007.

[104] K. M. Jordan, S. Sawyer, P. Coakley, H. E. Smith, C. Cooper, and N. K. Arden. The use of conventional and complementary treatments for knee osteoarthritis in the community. *Rheumatology (Oxford)*, 43:381–384, Mar 2004.

[105] Michael Karin and Florian R Greten. NF-kappaB: linking inflammation and immunity to cancer development and progression. *Nat Rev Immunol*, 5(10): 749–59, Oct 2005.

[106] Michael Karin, Yumi Yamamoto, and Q May Wang. The IKK NF-kappa B system: a treasure trove for drug development. *Nat Rev Drug Discov*, 3(1): 17–26, Jan 2004.

[107] M Katori and M Majima. Pivotal role of renal kallikrein-kinin system in the development of hypertension and approaches to new drugs based on this relationship. *Jpn J Pharmacol*, 70(2):95–128, Feb 1996.

[108] M A Kessler, H Behrend, S Henz, G Stutz, A Rukavina, and M S Kuster. Function, osteoarthritis and activity after ACL-rupture: 11 years follow-up

results of conservative versus reconstructive treatment. *Knee Surg Sports Traumatol Arthrosc*, 16(5):442–8, May 2008.

[109] A-M Khatib, G Siegfried, H Messai, F Moldovan, and D R Mitrovic. Mechanism of inhibition of endothelin-1-stimulated proteoglycan and collagen synthesis in rat articular chondrocytes. *Cytokine*, 17(5):254–61, Mar 2002.

[110] A M Khatib, A Lomri, R D Mitrovic, and F Moldovan. Articular chondrocyte aging and endothelin-1. *Cytokine*, 37(1):6–13, Jan 2007.

[111] Alla Khodorova, Jean-Pierre Montmayeur, and Gary Strichartz. Endothelin receptors and pain. *J Pain*, 10(1):4–28, Jan 2009.

[112] B L Kidd and L A Urban. Mechanisms of inflammatory pain. *Br J Anaesth*, 87(1):3–11, Jul 2001.

[113] Bruce L Kidd. Osteoarthritis and joint pain. *Pain*, 123(1-2):6–9, Jul 2006.

[114] H. Kotlarz, C. L. Gunnarsson, H. Fang, and J. A. Rizzo. Insurer and out-of-pocket costs of osteoarthritis in the US: evidence from national survey data. *Arthritis Rheum.*, 60:3546–3553, Dec 2009.

[115] U M Kujala, J Kaprio, and S Sarna. Osteoarthritis of weight bearing joints of lower limbs in former élite male athletes. *BMJ*, 308(6923):231–4, Jan 1994.

[116] Evren Kul-Panza and Nadire Berker. Pedobarographic findings in patients with knee osteoarthritis. *Am J Phys Med Rehabil*, 85(3):228–33, Mar 2006.

[117] V Kumar, RS Cotran, and SL Robbins. *Robbin's Basic Pathology*. Saunders Elsevier, 2003.

[118] V J LaMorte, A T Harootunian, A M Spiegel, R Y Tsien, and J R Feramisco. Mediation of growth factor induced DNA synthesis and calcium mobilization by Gq and Gi2. *J Cell Biol*, 121(1):91–9, Apr 1993.

[119] Edward R LaVallie, Priya S Chockalingam, Lisa A Collins-Racie, Bethany A Freeman, Cristin C Keohan, Michael Leitges, Andrew J Dorner, Elisabeth A Morris, Manas K Majumdar, and Maya Arai. Protein kinase Cζ is up-regulated in osteoarthritic cartilage and is required for activation of NF-κB by tumor necrosis factor and interleukin-1 in articular chondrocytes. *J Biol Chem*, 281(34):24124–37, Aug 2006.

[120] Chap T. Le. *Health and Numbers: A Problems-Based Introduction to Biostatistics*. Wiley-Blackwell, 3rd edition, Feb 2009.

[121] J I Lee and G J Burckart. Nuclear factor kappa B: important transcription factor and therapeutic target. *J Clin Pharmacol*, 38(11):981–93, Nov 1998.

[122] C Liebmann, A Graness, B Ludwig, A Adomeit, A Boehmer, F D Boehmer, B Nürnberg, and R Wetzker. Dual bradykinin B2 receptor signalling in A431 human epidermoid carcinoma cells: activation of protein kinase C is counteracted by a GS-mediated stimulation of the cyclic AMP pathway. *Biochem J*, 313 (Pt 1):109–18, Jan 1996.

[123] John E Linley, Kirstin Rose, Lezanne Ooi, and Nikita Gamper. Under-

standing inflammatory pain: ion channels contributing to acute and chronic nociception. *Pflügers Arch*, 459(5):657–69, Apr 2010.

[124] K M Lodhi, H Sakaguchi, S Hirose, S Shibabe, and H Hagiwara. Perichondrial localization of ETA receptor in rat tracheal and xiphoid cartilage and in fetal rat epiphysis. *Am J Physiol*, 268(2 Pt 1):C496–502, Feb 1995.

[125] John Loughlin, Barbara Dowling, Zehra Mustafa, and Kay Chapman. Association of the interleukin-1 gene cluster on chromosome 2q13 with knee osteoarthritis. *Arthritis Rheum*, 46(6):1519–27, Jun 2002.

[126] T A Louis. General methods for analysing repeated measures. *Stat Med*, 7 (1-2):29–45, 1988.

[127] Oliva Erendira Luis-Delgado, Michel Barrot, Jean-Luc Rodeau, Grégory Schott, Malika Benbouzid, Pierrick Poisbeau, Marie-José Freund-Mercier, and François Lasbennes. Calibrated forceps: a sensitive and reliable tool for pain and analgesia studies. *J Pain*, 7(1):32–9, Jan 2006.

[128] Jörg Lützner, Philip Kasten, Klaus-Peter Günther, and Stephan Kirschner. Surgical options for patients with osteoarthritis of the knee. *Nat Rev Rheumatol*, 5(6):309–16, Jun 2009.

[129] A Machner, G Pap, H Schwarzberg, R Eberhardt, A Roessner, and W Neumann. [Deterioration of sensory joint innervation as an enabling factor for development of arthrosis. An animal experiment study of the rat model]. *Z Rheumatol*, 58(3):148–54, Jun 1999.

[130] S Mahr, J Menard, V Krenn, and B Müller. Sexual dimorphism in the osteoarthritis of STR/ort mice may be linked to articular cytokines. *Ann Rheum Dis*, 62(12):1234–7, Dec 2003.

[131] G Majno and I Joris. *Cells, Tissues and Disease*. Oxford University Press, 2004.

[132] Christina Alexandra Manacu, Johanne Martel-Pelletier, Marjolaine Roy-Beaudry, Jean-Pierre Pelletier, Julio C Fernandes, Fazool S Shipkolye, Dragoslav R Mitrovic, and Florina Moldovan. Endothelin-1 in osteoarthritic chondrocytes triggers nitric oxide production and upregulates collagenase production. *Arthritis Res Ther*, 7(2):R324–32, Jan 2005.

[133] B Mandelbaum and D Waddell. Etiology and pathophysiology of osteoarthritis. *Orthopedics*, 28:S207–214, Feb 2005.

[134] Flora Linda Marasciulo, Monica Montagnani, and Maria Assunta Potenza. Endothelin-1: the yin and yang on vascular function. *Curr Med Chem*, 13 (14):1655–65, 2006.

[135] J. Martel-Pelletier, N. Alaaeddine, and J. P. Pelletier. Cytokines and their role in the pathophysiology of osteoarthritis. *Front. Biosci.*, 4:694–703, Oct 1999.

[136] Johanne Martel-Pelletier and Jean-Pierre Pelletier. *Mechanisms in Rheumatology. H Tannenbaum and AS Russell, editors*, chapter 13: Osteoarthritis. CORE Health Services, 2001.

[137] Johanne Martel-Pelletier, Daniel Lajeunesse, and Jean-Pierre Pelletier. *Arthritis and Allied Conditions: A Textbook of Rheumatology. WJ Koopman and LW Moreland, editors*, chapter 109: Etiopathogenesis of osteoarthritis, pages 2199–2226. Williams & Wilkins, 15th edition, 2005.

[138] R M Mason, M G Chambers, J Flannelly, J D Gaffen, J Dudhia, and M T Bayliss. The STR/ort mouse and its use as a model of osteoarthritis. *Osteoarthr Cartil*, 9(2):85–91, Feb 2001.

[139] S McConnell, P Kolopack, and A M Davis. The Western Ontario and McMaster Universities Osteoarthritis Index (WOMAC): a review of its utility and measurement properties. *Arthritis Rheum*, 45(5):453–61, Oct 2001.

[140] I D McDermott and A A Amis. The consequences of meniscectomy. *J Bone Joint Surg Br*, 88(12):1549–56, Dec 2006.

[141] Ruslan Medzhitov. Origin and physiological roles of inflammation. *Nature*, 454(7203):428–35, Jul 2008.

[142] S Meini and C A Maggi. Knee osteoarthritis: a role for bradykinin? *Inflamm Res*, 57(8):351–61, Aug 2008.

[143] R Melzack. The McGill Pain Questionnaire: major properties and scoring methods. *Pain*, 1(3):277–99, Sep 1975.

[144] H Messai, A Panasyuk, A Khatib, A Barbara, and D R Mitrovic. Endothelin-1 receptors on cultured rat articular chondrocytes: regulation

by age, growth factors, and cytokines, and effect on cAMP production. *Mech Ageing Dev*, 122(6):519–31, May 2001.

[145] R J Mier, D Holderbaum, R Ferguson, and R Moskowitz. Osteoarthritis in children associated with a mutation in the type II procollagen gene (COL2A1). *Mol Genet Metab*, 74(3):338–41, Nov 2001.

[146] N Miyasaka, Y Hirata, K Ando, K Sato, H Morita, M Shichiri, K Kanno, K Tomita, and F Marumo. Increased production of endothelin-1 in patients with inflammatory arthritides. *Arthritis Rheum*, 35(4):397–400, Apr 1992.

[147] Kazue Mizumura, Takeshi Sugiura, Kimiaki Katanosaka, Ratan K Banik, and Yasuko Kozaki. Excitation and sensitization of nociceptors by bradykinin: what do we know? *Exp Brain Res*, 196(1):53–65, Jun 2009.

[148] F Moldovan, J P Pelletier, F Mineau, M Dupuis, J M Cloutier, and J Martel-Pelletier. Modulation of collagenase 3 in human osteoarthritic cartilage by activation of extracellular transforming growth factor beta: role of furin convertase. *Arthritis Rheum*, 43(9):2100–9, Sep 2000.

[149] Marie Eve Moreau, Nancy Garbacki, Giuseppe Molinaro, Nancy J Brown, François Marceau, and Albert Adam. The kallikrein-kinin system: current and future pharmacological targets. *J Pharmacol Sci*, 99(1):6–38, Sep 2005.

[150] Roland W Moskowitz. The burden of osteoarthritis: clinical and quality-of-life issues. *Am J Manag Care*, 15(8 Suppl):S223–9, Sep 2009.

[151] H Muir. Proteoglycans of cartilage. *J Clin Pathol Suppl (R Coll Pathol)*, 12:67–81, Jan 1978.

[152] A M Nahir, A Hoffman, M Lorber, and H R Keiser. Presence of immunoreactive endothelin in synovial fluid: analysis of 22 cases. *J Rheumatol*, 18(5): 678–80, May 1991.

[153] K Nakata, K Ono, J Miyazaki, B R Olsen, Y Muragaki, E Adachi, K Yamamura, and T Kimura. Osteoarthritis associated with mild chondrodysplasia in transgenic mice expressing alpha 1(IX) collagen chains with a central deletion. *Proc Natl Acad Sci U S A*, 90(7):2870–4, Apr 1993.

[154] National Institute of Standards and Technology. NIST/SEMATECH e-Handbook of Statistical Methods, Sep 2010. URL `http://www.itl.nist.gov/div898/handbook/`.

[155] Volker Neugebauer, Jeong S Han, Hita Adwanikar, Yu Fu, and Guangchen Ji. Techniques for assessing knee joint pain in arthritis. *Molecular pain*, 3: 8, Jan 2007.

[156] Witold Neugebauer, Paul A Blais, Stephanie Hallé, Catherine Filteau, Domenico Regoli, and Fernand Gobeil. Kinin B1 receptor antagonists with multi-enzymatic resistance properties. *Can J Physiol Pharmacol*, 80(4):287–92, Apr 2002.

[157] M C Nevitt, D T Felson, E N Williams, and D Grady. The effect of estrogen plus progestin on knee symptoms and related disability in postmenopausal

women: The Heart and Estrogen/Progestin Replacement Study, a randomized, double-blind, placebo-controlled trial. *Arthritis Rheum*, 44(4):811–8, Apr 2001.

[158] NIH Consensus Panel. NIH Consensus Statement on total knee replacement. December 8-10, 2003. *J Bone Joint Surg Am*, 86-A(6):1328–35, Jun 2004.

[159] K. Notoya, D. V. Jovanovic, P. Reboul, J. Martel-Pelletier, F. Mineau, and J. P. Pelletier. The induction of cell death in human osteoarthritis chondrocytes by nitric oxide is related to the production of prostaglandin E2 via the induction of cyclooxygenase-2. *J. Immunol.*, 165:3402–3410, Sep 2000.

[160] Ernest D Olfert, Brenda M Cross, and A Ann McWilliam, editors. *Guide to the care and use of experimental animals*. Canadian Council on Animal Care, Ottawa, Ontario, 1993.

[161] S. A. Oliveria, D. T. Felson, J. I. Reed, P. A. Cirillo, and A. M. Walker. Incidence of symptomatic hand, hip, and knee osteoarthritis among patients in a health maintenance organization. *Arthritis Rheum.*, 38:1134–1141, Aug 1995.

[162] P. Ornetti, K. Brandt, M. P. Hellio-Le Graverand, M. Hochberg, D. J. Hunter, M. Kloppenburg, N. Lane, J. F. Maillefert, S. A. Mazzuca, T. Spector, G. Utard-Wlerick, E. Vignon, and M. Dougados. OARSI-OMERACT definition of relevant radiological progression in hip/knee osteoarthritis. *Osteoarthr Cartil*, 17:856–863, Jul 2009.

[163] T Otsuki, H Nakahama, H Niizuma, and J Suzuki. Evaluation of the analgesic effects of capsaicin using a new rat model for tonic pain. *Brain Res*, 365(2):235–40, Feb 1986.

[164] Vincent D Pelligrini Jr. *Netter's Orthopaedics, Walter B Greene, ed*, chapter 4: Arthritic Disorders. Saunders Elsevier, 2006.

[165] J B Pesquero, R C Araujo, P A Heppenstall, C L Stucky, J A Silva, Jr, T Walther, S M Oliveira, J L Pesquero, A C Paiva, J B Calixto, G R Lewin, and M Bader. Hypoalgesia and altered inflammatory responses in mice lacking kinin B1 receptors. *Proc Natl Acad Sci U S A*, 97(14):8140–5, Jul 2000.

[166] Theodore Pincus and Tuulikki Sokka. Quantitative measures and indices to assess rheumatoid arthritis in clinical trials and clinical care. *Rheum Dis Clin North Am*, 30(4):725–51, vi, Nov 2004.

[167] James D Pomonis, Jamie M Boulet, Susan L Gottshall, Steve Phillips, Rani Sellers, Tracie Bunton, and Katharine Walker. Development and pharmacological characterization of a rat model of osteoarthritis pain. *Pain*, 114 (3):339–46, Apr 2005.

[168] K P H Pritzker, S Gay, S A Jimenez, K Ostergaard, J-P Pelletier, P A Revell, D Salter, and W B van den Berg. Osteoarthritis cartilage histopathology: grading and staging. *Osteoarthr Cartil*, 14(1):13–29, Jan 2006.

[169] Qiagen. GeneGlobe Pathway Atlas, 2010. URL `https://www.qiagen.com/geneglobe/pathways.aspx`.

[170] Per Qvist, Anne-Christine Bay-Jensen, Claus Christiansen, Erik B Dam, Philippe Pastoureau, and Morten A Karsdal. The disease modifying osteoarthritis drug (DMOAD): Is it in the horizon? *Pharmacol Res*, 58(1): 1–7, Jul 2008.

[171] R Development Core Team. *R: A Language and Environment for Statistical Computing*. R Foundation for Statistical Computing, Vienna, Austria, 2010.

[172] LO Randall and JJ Selitto. A method for measurement of analgesic activity on inflamed tissue. *Arch Int Pharmacodyn Ther*, 111(4):409–19, Sep 1957.

[173] Wayne S Rasband. ImageJ. U.S. National Institutes of Health, Bethesda, Maryland, U.S.A., 1997-2010. URL `http://rsb.info.nih.gov/ij/`.

[174] Simon J Read and Andy Dray. Osteoarthritic pain: a review of current, theoretical and emerging therapeutics. *Expert Opin Investig Drugs*, 17(5): 619–40, May 2008.

[175] P. Reboul, J. P. Pelletier, G. Tardif, J. M. Cloutier, and J. Martel-Pelletier. The new collagenase, collagenase-3, is expressed and synthesized by human chondrocytes but not by synoviocytes. A role in osteoarthritis. *J. Clin. Invest.*, 97:2011–2019, May 1996.

[176] Anthony M Reginato and Bjorn R Olsen. The role of structural genes in the pathogenesis of osteoarthritic disorders. *Arthritis Res*, 4(6):337–45, 2002.

[177] D Regoli and J Barabé. Pharmacology of bradykinin and related kinins. *Pharmacol Rev*, 32(1):1–46, Mar 1980.

[178] R S Richmond, C S Carlson, T C Register, G Shanker, and R F Loeser. Functional estrogen receptors in adult articular cartilage: estrogen replacement therapy increases chondrocyte synthesis of proteoglycans and insulin-like growth factor binding protein 2. *Arthritis Rheum*, 43(9):2081–90, Sep 2000.

[179] M Rocha e Silva. A brief survey of the history of inflammation. *Agents Actions*, 8(1-2):45–9, Jan 1978.

[180] M Rocha e Silva, W T Beraldo, and G Rosenfeld. Bradykinin, a hypotensive and smooth muscle stimulating factor released from plasma globulin by snake venoms and by trypsin. *Am J Physiol*, 156(2):261–73, Feb 1949.

[181] R Rollín, F Marco, J A Jover, J A García-Asenjo, L Rodríguez, L López-Durán, and B Fernández-Gutiérrez. Early lymphocyte activation in the synovial microenvironment in patients with osteoarthritis: comparison with rheumatoid arthritis patients and healthy controls. *Rheumatol Int*, 28(8): 757–64, Jun 2008.

[182] L Rosenberg. Chemical basis for the histological use of safranin O in the study of articular cartilage. *J Bone Joint Surg Am*, 53(1):69–82, Jan 1971.

[183] Amy K Roshak, James F Callahan, and Simon M Blake. Small-molecule

inhibitors of NF-kappaB for the treatment of inflammatory joint disease. *Curr Opin Pharmacol*, 2(3):316–21, Jun 2002.

[184] Antoine Rosset, Luca Spadola, and Osman Ratib. OsiriX: an open-source software for navigating in multidimensional DICOM images. *Journal of digital imaging : the official journal of the Society for Computer Applications in Radiology*, 17(3):205–16, Sep 2004.

[185] G P Rossi, A Sacchetto, M Cesari, and A C Pessina. Interactions between endothelin-1 and the renin-angiotensin-aldosterone system. *Cardiovasc Res*, 43(2):300–7, Aug 1999.

[186] P J Roughley. The structure and function of cartilage proteoglycans. *European cells & materials*, 12:92–101, Jan 2006.

[187] Marjolaine Roy-Beaudry, Johanne Martel-Pelletier, Jean-Pierre Pelletier, Khatija Nait M'Barek, Stephan Christgau, Fazool Shipkolye, and Florina Moldovan. Endothelin 1 promotes osteoarthritic cartilage degradation via matrix metalloprotease 1 and matrix metalloprotease 13 induction. *Arthritis Rheum*, 48(10):2855–64, Oct 2003.

[188] N M Rupniak, S Boyce, J K Webb, A R Williams, E J Carlson, R G Hill, J A Borkowski, and J F Hess. Effects of the bradykinin B1 receptor antagonist des-Arg9[Leu8]bradykinin and genetic disruption of the B2 receptor on nociception in rats and mice. *Pain*, 71(1):89–97, May 1997.

[189] I M Sainz, A B Uknis, I Isordia-Salas, R A Dela Cadena, R A Pixley,

and R W Colman. Interactions between bradykinin (BK) and cell adhesion molecule (CAM) expression in peptidoglycan-polysaccharide (PG-PS)-induced arthritis. *FASEB J*, 18(7):887–9, May 2004.

[190] Sanofi-Aventis. Efficacy and safety study of intra-articular multiple doses of icatibant in patients with painful knee osteoarthritis. 2006-2007. Clinicaltrials.gov identifier: NCT00303056., Apr 2007. URL `http://clinicaltrials.gov/show/NCT00303056`.

[191] Markus P Schneider, Erika I Boesen, and David M Pollock. Contrasting actions of endothelin ET(A) and ET(B) receptors in cardiovascular disease. *Annu Rev Pharmacol Toxicol*, 47:731–59, 2007.

[192] A Scott, K M Khan, J L Cook, and V Duronio. What is "inflammation"? Are we ready to move beyond Celsus? *Br J Sports Med*, 38(3):248–9, Jun 2004.

[193] Daisuke Seino, Atsushi Tokunaga, Toshiya Tachibana, Shinichi Yoshiya, Yi Dai, Koichi Obata, Hiroki Yamanaka, Kimiko Kobayashi, and Koichi Noguchi. The role of ERK signaling and the P2X receptor on mechanical pain evoked by movement of inflamed knee joint. *Pain*, 123(1-2):193–203, Jul 2006.

[194] Charles N Serhan. Resolution phase of inflammation: novel endogenous anti-inflammatory and proresolving lipid mediators and pathways. *Annu Rev Immunol*, 25:101–37, 2007.

[195] Charles N Serhan and John Savill. Resolution of inflammation: the beginning programs the end. *Nat Immunol*, 6(12):1191–7, Dec 2005.

[196] Bing Shen and Samir S El-Dahr. Cross-talk of the renin-angiotensin and kallikrein-kinin systems. *Biol Chem*, 387(2):145–50, Feb 2006.

[197] David A Skyba, Rajan Radhakrishnan, and Kathleen A Sluka. Characterization of a method for measuring primary hyperalgesia of deep somatic tissue. *J Pain*, 6(1):41–7, Jan 2005.

[198] K A Sluka and K N Westlund. Behavioral and immunohistochemical changes in an experimental arthritis model in rats. *Pain*, 55(3):367–77, Dec 1993.

[199] K A Sluka, M A Milton, W D Willis, and K N Westlund. Differential roles of neurokinin 1 and neurokinin 2 receptors in the development and maintenance of heat hyperalgesia induced by acute inflammation. *Br J Pharmacol*, 120(7):1263–73, Apr 1997.

[200] I H Song, C E Althoff, K G Hermann, A K Scheel, T Knetsch, G R Burmester, and M Backhaus. Contrast-enhanced ultrasound in monitoring the efficacy of a bradykinin receptor 2 antagonist in painful knee osteoarthritis compared with MRI. *Annals of the Rheumatic Diseases*, 68(1): 75–83, Jan 2009.

[201] Robert Stahl, Anthony Luke, Xiaojuan Li, Julio Carballido-Gamio, C Benjamin Ma, Sharmila Majumdar, and Thomas M Link. T1rho, T2 and focal

knee cartilage abnormalities in physically active and sedentary healthy subjects versus early OA patients–a 3.0-Tesla MRI study. *Eur Radiol*, 19(1): 132–43, Jan 2009.

[202] R Stoop, P Buma, P M van der Kraan, A P Hollander, R C Billinghurst, T H Meijers, A R Poole, and W B van den Berg. Type II collagen degradation in articular cartilage fibrillation after anterior cruciate ligament transection in rats. *Osteoarthr Cartil*, 9(4):308–15, May 2001.

[203] B L Tang. ADAMTS: a novel family of extracellular matrix proteases. *Int J Biochem Cell Biol*, 33(1):33–44, Jan 2001.

[204] The NCBI handbook [Internet]. Entrez Gene - BDKRB1 bradykinin receptor B1 [Homo sapiens]. Gene ID: 623, 27 Jul 2010. URL `http://www.ncbi.nlm.nih.gov/sites/entrez?db=gene&cmd=retrieve&list_uids=623`.

[205] Edward C Thornborrow, Sejal Patel, Anthony E Mastropietro, Elissa M Schwartzfarb, and James J Manfredi. A conserved intronic response element mediates direct p53-dependent transcriptional activation of both the human and murine bax genes. *Oncogene*, 21(7):990–9, Feb 2002.

[206] C R Tonussi and S H Ferreira. Bradykinin-induced knee joint incapacitation involves bradykinin B2 receptor mediated hyperalgesia and bradykinin B1 receptor-mediated nociception. *Eur J Pharmacol*, 326(1):61–5, May 1997.

[207] M Uchino, T Izumi, T Tominaga, R Wakita, H Minehara, M Sekiguchi, and M Itoman. Growth factor expression in the osteophytes of the human

femoral head in osteoarthritis. *Clin Orthop Relat Res*, (377):119–25, Aug 2000.

[208] Veronica Ulici, Claudine G James, Katie D Hoenselaar, and Frank Beier. Regulation of gene expression by PI3K in mouse growth plate chondrocytes. *PLoS One*, 5(1):e8866, 2010.

[209] A M Valdes, M Doherty, and T D Spector. The additive effect of individual genes in predicting risk of knee osteoarthritis. *Ann Rheum Dis*, 67(1):124–7, Jan 2008.

[210] Ana M Valdes, John Loughlin, Kirsten M Timms, Joyce J B van Meurs, Lorraine Southam, Scott G Wilson, Sally Doherty, Rik J Lories, Frank P Luyten, Alexander Gutin, Victor Abkevich, Dongliang Ge, Albert Hofman, André G Uitterlinden, Deborah J Hart, Feng Zhang, Guangju Zhai, Rainer J Egli, Michael Doherty, Jerry Lanchbury, and Tim D Spector. Genome-wide association scan identifies a prostaglandin-endoperoxide synthase 2 variant involved in risk of knee osteoarthritis. *Am J Hum Genet*, 82(6):1231–40, Jun 2008.

[211] Maria S Valle, Antonino Casabona, Rosaria Sgarlata, Rosaria Garozzo, Maria Vinci, and Matteo Cioni. The pendulum test as a tool to evaluate passive knee stiffness and viscosity of patients with rheumatoid arthritis. *BMC Musculoskelet Disord*, 7:89, 2006.

[212] Wim B van den Berg. Lessons from animal models of osteoarthritis. *Current rheumatology reports*, 10(1):26–9, Jan 2008.

[213] Hilde Vermeirsch, Ria Biermans, Philip L Salmon, and Theo F Meert. Evaluation of pain behavior and bone destruction in two arthritic models in guinea pig and rat. *Pharmacol Biochem Behav*, 87(3):349–59, Jan 2007.

[214] Matthew P Vincenti and Constance E Brinckerhoff. Transcriptional regulation of collagenase (MMP-1, MMP-13) genes in arthritis: integration of complex signaling pathways for the recruitment of gene-specific transcription factors. *Arthritis Res*, 4(3):157–64, 2002.

[215] Simon Wandel, Peter Jüni, Britta Tendal, Eveline Nüesch, Peter M Villiger, Nicky J Welton, Stephan Reichenbach, and Sven Trelle. Effects of glucosamine, chondroitin, or placebo in patients with osteoarthritis of hip or knee: network meta-analysis. *BMJ (Clinical research ed)*, 341:c4675, Jan 2010.

[216] Y-X J Wang, D P Bradley, H Kuribayashi, and F R Westwood. Some aspects of rat femorotibial joint microanatomy as demonstrated by high-resolution magnetic resonance imaging. *Lab Anim*, 40(3):288–95, Jul 2006.

[217] Yi-Xiang Wang. In vivo magnetic resonance imaging of animal models of knee osteoarthritis. *Lab Anim*, 42(3):246–64, Jul 2008.

[218] James H Ware. Linear models for the analysis of longitudinal studies. *The American Statistician*, 39(2):95–101, 1985.

[219] L. Wei, A. Hjerpe, B. H. Brismar, and O. Svensson. Effect of load on articular cartilage matrix and the development of guinea-pig osteoarthritis. *Osteoarthr. Cartil.*, 9:447–453, Jul 2001.

[220] M Weinberger, W M Tierney, P A Cowper, B P Katz, and P A Booher. Cost-effectiveness of increased telephone contact for patients with osteoarthritis. A randomized, controlled trial. *Arthritis Rheum*, 36(2):243–6, Feb 1993.

[221] Heike A Wieland, Martin Michaelis, Bernhard J Kirschbaum, and Karl A Rudolphi. Osteoarthritis - an untreatable disease? *Nature reviews Drug discovery*, 4(4):331–44, Apr 2005.

[222] J M Williams, D L Felten, R G Peterson, and B L O'Connor. Effects of surgically induced instability on rat knee articular cartilage. *J Anat*, 134(Pt 1):103–9, Jan 1982.

[223] A E Wluka, F M Cicuttini, and T D Spector. Menopause, oestrogens and arthritis. *Maturitas*, 35(3):183–99, Jun 2000.

[224] Jiake Xu, Hua Fei Wu, Estabelle S M Ang, Kirk Yip, Magdalene Woloszyn, Ming H Zheng, and Ren Xiang Tan. NF-κB modulators in osteolytic bone diseases. *Cytokine Growth Factor Rev*, 20(1):7–17, Feb 2009.

[225] Yuji Yamanishi, David L Boyle, Melody Clark, Rich A Maki, Micky D Tortorella, Elizabeth C Arner, and Gary S Firestein. Expression and regulation of aggrecanase in arthritis: the role of TGF-beta. *J Immunol*, 168(3):1405–12, Feb 2002.

[226] F Yanaga, M Hirata, and T Koga. Evidence for coupling of bradykinin receptors to a guanine-nucleotide binding protein to stimulate arachidonate liberation in the osteoblast-like cell line, MC3T3-E1. *Biochim Biophys Acta*, 1094(2):139–46, Sep 1991.

[227] M Yanagisawa, H Kurihara, S Kimura, Y Tomobe, M Kobayashi, Y Mitsui, Y Yazaki, K Goto, and T Masaki. A novel potent vasoconstrictor peptide produced by vascular endothelial cells. *Nature*, 332(6163):411–5, Mar 1988.

[228] X P Yang, Y H Liu, G M Scicli, C R Webb, and O A Carretero. Role of kinins in the cardioprotective effect of preconditioning: study of myocardial ischemia/reperfusion injury in B2 kinin receptor knockout mice and kininogen-deficient rats. *Hypertension*, 30(3 Pt 2):735–40, Sep 1997.

[229] Joo-Byoung Yoon, Song-Ja Kim, Sang-Gu Hwang, Sunghoe Chang, Shin-Sung Kang, and Jang-Soo Chun. Non-steroidal anti-inflammatory drugs inhibit nitric oxide-induced apoptosis and dedifferentiation of articular chondrocytes independent of cyclooxygenase activity. *J Biol Chem*, 278(17): 15319–25, Apr 2003.

[230] H Yoshida, Y Imafuku, M Ohhara, M Miyata, R Kasukawa, K Ohsumi, and J Horiuchi. Endothelin-1 production by human synoviocytes. *Ann Clin Biochem*, 35 (Pt 2):290–4, Mar 1998.

[231] Marian F Young. Mouse models of osteoarthritis provide new research tools. *Trends Pharmacol Sci*, 26(7):333–5, Jul 2005.

[232] Yun Cho Yu, Sung Tae Koo, Chang Hoon Kim, Yeoungsu Lyu, James J Grady, and Jin Mo Chung. Two variables that can be used as pain indices in experimental animal models of arthritis. *J Neurosci Methods*, 115(1): 107–13, Mar 2002.

[233] G Zhai, D J Hart, B S Kato, A MacGregor, and T D Spector. Genetic influence on the progression of radiographic knee osteoarthritis: a longitudinal twin study. *Osteoarthritis Cartilage*, 15(2):222–5, Feb 2007.

[234] W Zhang, R W Moskowitz, G Nuki, S Abramson, R D Altman, N Arden, S Bierma-Zeinstra, K D Brandt, P Croft, M Doherty, M Dougados, M Hochberg, D J Hunter, K Kwoh, L S Lohmander, and P Tugwell. OARSI recommendations for the management of hip and knee osteoarthritis, Part II: OARSI evidence-based, expert consensus guidelines. *Osteoarthr Cartil*, 16(2):137–62, Feb 2008.

[235] W Zhang, M Doherty, G Peat, M A Bierma-Zeinstra, N K Arden, B Bresnihan, G Herrero-Beaumont, S Kirschner, B F Leeb, L S Lohmander, B Mazières, K Pavelka, L Punzi, A K So, T Tuncer, I Watt, and J W Bijlsma. EULAR evidence-based recommendations for the diagnosis of knee osteoarthritis. *Ann Rheum Dis*, 69(3):483–9, Mar 2010.